



**Promoters:** Prof. Dr. Ir. Paul Van der Meeren  
Particle and Interfacial Technology Group (PaInT)  
Department of Green Chemistry and Technology  
Ghent University  
Dr. Sayed Amir Hossein Goli  
Department of Food Science and Technology  
Faculty of Agriculture  
Isfahan University of Technology (IUT)

**Dean:** Prof. Dr. Ir. Marc Van Meirvenne

**Rector:** Prof. Dr. Ir. Rik Van de Walle

**Maryam Nikbakht Nasrabadi**

**Fabrication and physicochemical investigation of plant-based flaxseed oil-in-water Pickering emulsions stabilized by flaxseed protein-mucilage complex particles**

For citation:

Nikbakht Nasrabadi, M. (2019), Fabrication and physicochemical investigation of plant based flaxseed oil-in-water Pickering emulsion stabilized by flaxseed protein-mucilage complex particles.

**ISBN – Number: 978-94-6357-258-3**

Thesis submitted in fulfillment of the requirements for the joint degree of Doctor (PhD) in Bioscience Engineering

The author and promoter give the authorisation to consult and to copy parts of this work for personal use only. Every other use is subjected to copyright laws. Permission to reproduce any material contained in this work should be obtained from the author.

## ACKNOWLEDGMENTS

Without the support and help of various individuals, the completion of this thesis would not have been possible. I would like first express my deepest tons of gratitude to my promotors Prof. Dr. Ir. Paul Van der Meeren and Dr. Sayed Amir Hossein Goli for their invaluable support. Their wide knowledge, creative research ideas, and insightful thought have been inspiring to me. In one word, I really feel proud of myself and great honoured to be their student. My PhD study in the Particle & Interfacial Technology Group at Gent university has been an unforgettable period in my life. I feel really lucky to have this great opportunity and meet all my kind lab mates thanks to the supports of Prof. Paul Van der Meeren. Among them, I am really grateful to Ali Sedaghat Doost one of my supportive colleagues for imparting his knowledge and skills to me and training me for the use of equipment and helping me by offering a lot of useful suggestions. His help and guidance have been pivotal in shaping this work. Warm thanks go to Quenten, Eric, Saskia who helped me with their supports. The last but not least, I owe my deepest gratitude to my dearest dad, mum, sis and bro, for their unconditional support, love and encouragement.

Nov. 2019, Gent

Maryam Nikbakht Nasrabadi



## Samenvetting

Het doel van deze studie was de productie van stabiele lijnzaadolie (FO)-in-water Pickering-emulsies gestabiliseerd door complexe en plantaardige lijnzaad proteïne (FP) en de oplosbare fractie van lijnzaadsljm (SFM) als een afleversysteem voor voedselproducten. FO is een lipofiele functionele verbinding die een beperkte toepassing heeft in de voedingsmiddelenindustrie vanwege zijn slechte oplosbaarheid in water en zijn gevoeligheid voor oxidatie. Het effect van pH, totale concentratie (TC) en FP tot SFM-verhouding op de vorming van complexen werd onderzocht door lichtverstrooiing, oppervlaktelading en optische dichtheitsmetingen. De geselecteerde complexe deeltjes bij pH = 3, FP tot SFM-verhouding van 50:50 en TC = 0,45 wt% waren negatief geladen met een zetapotentialwaarde van -22,3 mV en de grootte van 369 nm met de polydispersiteitsindex (PDI) van 0,31, die goede fysische stabiliteit heeft en verzekert een bijna neutrale bevochtigbaarheid (67 °). Deze nanocomplexen werden gebruikt voor het vervaardigen van Pickering-emulsies met verschillend FO-gehalte (1, 2,5 en 5 w / v%) en TC = 0,45 wt%. En de druppelgrootte gedurende 28 dagen opslag en versnelde roomstabiliteit van de emulsies werd onderzocht. 2,5 wt% FO-emulsie had de kleinste initiële druppelgrootte ( $D [4,3] = 8 \mu\text{m}$ ) en roomsnelheid (2,9  $\mu\text{m} / \text{s}$ ). FO-emulsie gestabiliseerd door complexe biodeeltjes had een goede fysische stabiliteit gedurende 28 dagen opslag en tegen verschillende stressomstandigheden waaronder een breed bereik van pH (2-9), zoutconcentratie (0-500 mM) en temperatuur (40, 60 en 80 °C gedurende 30 minuten) zonder tekenen van instabiliteit en afsmering. De metingen van peroxidewaarde (PV) en thiobarbituurzuur (TBA) gedurende 28 dagen opslag bij 4 °C en 50 °C vertoonden de verhoogde oxidatie door de temperatuur en opslagtijd te verhogen. De complexe deeltjes als Pickering-emulgatoren waren succesvol in het onderdrukken van de FO oxidatie en -vertering.

## LIST OF ABBREVIATIONS AND SYMBOLS

<sup>13</sup> CNMR	Carbon nuclear magnetic resonance
<sup>1</sup> HNMR	Proton nuclear magnetic resonance
AG	Arabic gum
ALA	Alpha linolenic acid
ANOVA	Analysis of variance
CI	Creaming index
CLA	Conjugated linoleic acid
CLSM	Confocal laser scanning microscopy
Cryo-SEM	Cryo-scanning electron microscopy
DOE	Dodecane oil-in-water Pickering emulsion
FDA	Food and drug administration
FFA	Free fatty acid
FI	Flocculation index
FO	Flaxseed oil
FOE	Flaxseed oil-in-water Pickering emulsions stabilized by complexes
FP	Flaxseed protein
FPFOE	Flaxseed oil-in-water emulsions stabilized by flaxseed protein
FTIR	Fourier transform infrared
GI	Gastrointestinal
HDL	High density lipoprotein
HDO	Hydrogen deuterium oxide
HIPPEs	High internal phase Pickering emulsions
LDL	Low density lipoprotein



LH	Lipid hydroperoxide
MAG	Monoacyl glycerol
MDA	Malondialdehyde
MW	Molecular weight
N	Nitrogen
O/W	Oil-in-water
O/W/O	Oil-in-water-in-oil
OD	Optical density
PDI	Polydispersity index
PHOs	Partially hydrogenated oils
pI	Isoelectric point
PS80	Polysorbate 80
PUFA	Polyunsaturated fatty acids
PV	Peroxide value
r	Protein to polysaccharide ratio
SDS	Sodium dodecyl sulfate
SDS-PAGE	Sodium dodecyl sulfate-polyacrylamide gel electrophoresis
SFM	Water soluble flaxseed mucilage
SGI	Simulated gastrointestinal
SIF	Simulated intestinal fluid
SSA	Specific surface area
STD	Standard deviation
T	Thymol
TAG	Triacylglycerol
TBA	Thiobarbituric acid

TBARS	Thiobarbituric acid reactive substances
TC	Total concentration
TCA	Trichloroacetic acid
USA	United States of America
UV	Ultra violet
W/O	Water-in-oil
W/O/W	Water-in-oil-in water
W/V	Weight/volume
WP	Whey protein
$\Delta G$	Gibbs free energy change
$\gamma$	Oil-water interfacial tension
$\theta$	Contact angle

## Table of contents

ACKNOWLEDGMENTS .....	v
Samenvetting .....	vii
LIST OF ABBREVIATIONS AND SYMBOLS .....	viii
Table of contents.....	xi
Chapter 1: Literature Review .....	1
1.1 Introduction .....	2
1.2 Basic principles of Pickering stabilization.....	3
1.3 Food applications of plant-based Pickering emulsions .....	8
1.4 PhD research strategy .....	11
Chapter 2: Plant-based Pickering stabilization of emulsions using soluble flaxseed protein and mucilage nano-assemblies .....	15
2.1. Introduction .....	17
2.2. Materials and methods .....	19
2.2.1. Materials .....	19
2.2.2. Extraction of flaxseed mucilage .....	19
2.2.3. Flaxseed protein extraction .....	20
2.3. Flaxseed protein and mucilage characterization.....	20
2.3.1. Proximate analysis .....	20
2.3.2. 1-D 1H and 13C nuclear magnetic resonance (NMR) spectroscopy.....	21
2.3.3. SDS-PAGE analysis .....	21
2.4. Fabrication of particles through acid titration .....	21
2.5. Turbidimetric analysis .....	22
2.6. Particle characterization .....	22
2.6.1. Charge density .....	22
2.6.2. Zeta-potential .....	22
2.6.3. Particle size .....	22
2.6.4. Fourier transform infrared spectroscopy (FTIR).....	23
2.6.5. Interfacial tension.....	23
2.6.6. Contact angle .....	23
2.7. Emulsion preparation.....	24
2.8. Emulsion characterization .....	24
2.8.1. Droplet size distribution .....	24

2.8.2. Cryo-scanning electron microscopy (Cryo-SEM) and confocal laser scanning microscopy (CLSM).....	25
2.9. Statistical analysis.....	25
2.3. Results and discussion.....	26
2.3.1. Flaxseed protein and mucilage characterization.....	26
2.3.2. NMR.....	26
2.3.4. Surface charge properties.....	31
2.3.5. Optical density measurement.....	34
2.3.6. Particle size.....	37
2.3.7. FTIR.....	40
2.3.8. Contact angle ( $\theta_w$ ).....	42
2.3.9. Interfacial tension.....	43
2.3.10. Emulsion characterization.....	44
2.3.10. 1. Effect of the FP to SFM ratio, total biopolymer concentration and oil volume fraction on droplet size distribution.....	44
2.3.10.2. Microstructure evaluation.....	48
2.4. Conclusions.....	51
Chapter 3: Bioparticles of flaxseed protein and mucilage enhance the physical and oxidative stability of flaxseed oil emulsions as a potential natural alternative for synthetic surfactants .....	53
3.1. Introduction.....	55
3.2. Materials and methods.....	57
3.2.1. Materials.....	57
3.2.2. Extraction and characterization of flaxseed mucilage and protein.....	57
3.2.3. Preparation of complex particles.....	57
3.2.4. Fabrication of Pickering emulsions.....	57
3.2.5. Pickering emulsion characterization.....	57
3.2.5.1. Droplet size distribution.....	57
3.2.5.2. Accelerated creaming stability.....	58
3.2.5.3. Microstructure characterization.....	58
CLSM (Leica TCS-SP5, Germany) was also applied for the microstructure characterization (section 2.8.2.).....	58
3.2.6. Influence of stress conditions.....	58
3.2.7. Lipid oxidation determination.....	59
3.2.7.1. Iodometric assay.....	59
3.2.7.2. Thiobarbituric acid reactive substances assay (TBARS).....	60

3.2.8. Statistical analysis .....	60
3.3. Results and discussion .....	61
3.3.1. FO Pickering emulsion .....	61
3.3.2. Microstructure evaluation .....	63
3.3.3. Influence of stress conditions.....	66
3.3.4. Effect of pH .....	66
3.3.5. Effect of ionic strength .....	68
3.3.6. Effect of thermal treatment .....	70
3.3.7. Oxidative stability of FO Pickering emulsions .....	71
2.10. Conclusions.....	77
Chapter 4: Effect of thymol and Pickering stabilization on in-vitro digestion fate and oxidation stability of plant-derived flaxseed oil emulsions .....	79
Abstract .....	80
4.1. Introduction .....	82
4.2. Materials and methods .....	84
4.2.1. Materials .....	84
4.2.2. Preparation of FP-SFM complexes .....	84
4.2.3. Fabrication of FO-loaded emulsions with and without thymol.....	84
4.2.4. Emulsions droplet size determination .....	84
4.2.5. Confocal laser scanning microscopy (CLSM).....	85
4.2.6. Lipid oxidation determination .....	85
4.2.6.1. Peroxide value.....	85
4.2.6.2. Thiobarbituric acid reactive substances assay.....	86
4.2.7. In-vitro digestion .....	86
4.2.8. Gastric conditions .....	87
4.2.9. Intestinal conditions.....	87
4.2.10. Thymol bioaccessibility.....	88
4.2.11. Statistical analysis .....	88
4.3. Results and discussion.....	88
4.3.1. FO-loaded Pickering emulsions.....	88
4.3.2. Oxidative stability of FO Pickering emulsions .....	91
4.3.3. Digestion fate and bioaccessibility assessment of thymol .....	96
4.4. Conclusions.....	102
Chapter 5: Conclusions and future research.....	104

References.....	108
CURRICULUM VITAE.....	132

# Chapter 1: Literature Review

## 1.1 Introduction

A vast variety of food products exists in which oil and water are present as two immiscible phases. A system to overcome this challenge is known as an emulsion; a phase is dispersed in another in the presence of surfactants: oil-in-water (O/W) (e.g. milk and mayonnaise), water-in-oil (W/O) (e.g. butter and margarine), water-in-oil-in-water (W/O/W), or oil-in-water-in-oil (O/W/O) are just some examples of emulsions. They could be an ideal delivery system for bioactive compounds, including carotenoids, essential oils and fatty acids and some phenolic compounds (e.g. curcumin) through incorporation of these added-value compounds into the lipid phase. Emulsions are increasingly applied not only in food products, but also in personal care, medicine, agrochemical, and topical delivery products.

Emulsifiers are traditionally used to stabilize liquid-liquid or liquid-gas phases by their amphoteric properties. On the other hand, much of the recent research has been focused on biopolymers with surface activity. Pickering emulsions, particle-stabilized emulsions, have attracted considerable interest because of their advantages over conventional emulsions which are stabilized by surfactants. These surfactant-free emulsions have superior stability against coalescence in comparison to low molecular weight emulsifiers (Pickering, 1907a, Schröder et al., 2018a). Additional benefits of Pickering emulsions include improving physicochemical stability, enhanced functionality, and having a surfactant-free label (Schröder et al., 2018a). Inorganic or synthetic particles such as clay, silica, and latex have been used for Pickering stabilization of emulsions while there is growing interest in using food-grade particles from organic and natural sources especially for food applications (Rayner et al., 2014). One of the options for food grade particles are plant-based particles, including proteins, polysaccharides, their



combination, and waxes, which have no reported adverse side effects. Both O/W and W/O emulsions can be formulated utilizing these particles with an appropriate wettability, and particle size (Duffus et al., 2016).

## **1.2 Basic principles of Pickering stabilization**

In 1907, Spencer Umfreville Pickering believed that emulsions stabilized using organic substances such as milk proteins, starch, and saponin would become spontaneously de-emulsified due to stress conditions, including pH variation and high ionic strength (Pickering, 1907a). He reported that paraffin emulsions prepared by solid particles which were not soluble in the oil phase and had little tendency towards the aqueous phase, were both resistant to coalescence and did not show spontaneous de-emulsification. Since then, emulsions stabilized using solid particles at the interface are known as 'Pickering emulsions'. One of the differences between Pickering emulsions and conventionally stabilized emulsions is related to their interface; Pickering stabilized oil droplets have usually a higher surface load and thickness due to the adsorption of particles than normal emulsions (Madadlou et al., 2016). Another considerable difference is the emulsifier dynamic exchange at the interface of conventional emulsions, which is not seen in Pickering emulsions (Schmitt and Ravaine, 2013).

Pickering stabilization relies on colloidal particles which can inhibit droplet coalescence and phase separation in different types of emulsions, including O/W, W/O, or multiple emulsions (Rousseau, 2013). Different qualifications have been considered for the particles to be capable of Pickering stabilization. First of all, the particles should not have a tendency (solubility) for neither the hydrophobic nor the hydrophilic phases, meaning that they can be wetted partially by both phases; theoretically, particles exerting a contact angle of 90° at the interface are

considered as the optimum. In addition, the particles should be able to efficiently adsorb at the interface. Moreover, the size of the particles is believed to be one order of magnitude smaller than that of the ultimate emulsions (Xiao et al., 2016a). In fact, the free energy for detachment of a spherical particle from an oil-water interface is expressed through the following equation:

Equation 1.1

$$\Delta G = \pi r^2 \gamma_{OW} (1 - |\cos \theta|)^2$$

where  $r$  is the radius of particle,  $\gamma$  is the oil-water interfacial tension, and  $\theta$  is the contact angle. It is obvious that the movement of a hydrophobic particle into the oil phase needs a lower detachment energy than into the water phase and vice versa for a hydrophilic particle (Rayner et al., 2014). Thus, the free energy of a particle with a contact angle of  $90^\circ$  to detach into both phases is equal and thereby this particle mainly deposits at the oil-water interface, which is a prerequisite for Pickering stabilization. For instance, in terms of nanometer range particles, if the detachment energy is higher than the Brownian thermal energy of the particles, they remain at the interface.

In addition to wettability, size and shape of the particles are other factors which could influence the formation and characteristics of Pickering emulsions. As a rule of thumb, it has been claimed that the size of particles should be initially about one-tenth of the desired emulsion droplet size (Sedaghat Doost et al., 2019b, Berton-Carabin and Schroën, 2015, Rayner et al., 2014). However, it should be taken into consideration that the continuous phase and the lipid phase are usually homogenized to form the emulsions droplets using semi-high energy methods such as high shear (rotor-stator) homogenizers. This mixing may decrease the size

distribution of particles before they can adsorb onto the interface. The mean droplet size of the emulsions is also linked to the shape of the particles by a factor defined as the aspect ratio (the length to the width ratio of a particle). Generally, there is no control over the shape of particles and they may take any shape depending on different parameters such as their composition or environmental conditions such as pH and solvent type. Particles with a higher aspect ratio have a higher capability to wet both phases and thereby suitable for stabilization. As an example, micron-sized spindle like hematite particles with an aspect ratio above 4.6 are an ideal case (Schröder et al., 2018a). For a more detailed description about the basic theory of Pickering stabilization, the readers are referred to a book chapter by Schröder et al. (2018a).

One of the main areas of interest in recent research activities in the field of food science is the exploration of proper building blocks and appropriate fabrication methods for production of food-grade Pickering emulsions which has been reviewed by Tavernier et al. (2016). Two commonly used functional ingredients, which are mostly applied for stabilizing edible Pickering emulsions, are proteins and polysaccharides (Dickinson, 2017). Plant-based proteins and polysaccharides offer some advantages over their animal counterparts, including a lower risk of infection and contamination, no limitations in terms of cultural food habits and vegetarian consumers, economic advantages and versatility compared to animal-based ingredients (González-Pérez and Arellano, 2009, Joye and McClements, 2014). This section overviews the newly documented literature focusing on plant based biopolymeric particles as appropriate Pickering candidates.

Protein-polysaccharide interactions can be used as a source of preparing bioparticles which have the combined favorable properties of both biopolymers and

their synergistic effects. Most of the plant proteins have limited applications due to their poor solubility and sensitivity to pH, salt and temperature. The association of a polysaccharide with these plant proteins can modulate their functional properties especially at and around their isoelectric point (pI). Proteins and polysaccharides can be linked together through covalent interaction (conjugation) as a result of Maillard reaction or non-covalent interactions (complexation) such as electrostatic interactions between oppositely charged polysaccharides and proteins. Maillard type reactions, also called glycosylation, are known to provide permanent conjugates through dry or wet heating and molecular crowding of the mixture of proteins and polysaccharides. It has been reported that emulsions stabilized with protein-polysaccharide conjugates have a thicker interfacial layer in comparison to emulsions stabilized by individual proteins; the molecular weight of the applied polysaccharide is responsible for this increased thickness (Akhtar and Ding, 2017). Yang et al. (2015) reported that the obtained conjugates from the glycosylation of soy proteins with soy polysaccharides, after reaction for 3 days at 60 °C and 75% relative humidity, prevented coalescence in the fabricated O/W emulsion.

Electrostatic interactions can occur when oppositely charged biopolymers are present in the mixture, resulting in soluble or insoluble complexes depending on the strength of the interaction. At pH values close to the pI of the protein, soluble complex particles are assembled which are stable due to their surface charge. However, at pH values where the formed complex particles have equal opposite charges and the net surface charge is zero, phase separation (precipitation) between the insoluble complexes (coacervates) and solvent occurs (Sedaghat Doost et al., 2019b). There are several studies on using different protein-polysaccharide electrostatic complexes as particulate emulsifiers. However, only a

few studies on the application of plant based complex particles for Pickering stabilization have been published and most studies have been focused on complexes/conjugates of animal proteins, particularly milk proteins.

Yildiz et al. (2018) prepared different plant protein-polysaccharide complexes obtained from complexation between pea or soy protein aggregates and Arabic gum, pectin, and modified starch. All the complexes had an improved solubility around the protein's pI while the pea protein complexes had a higher solubility and surface hydrophobicity leading to better interfacial and emulsifying properties in comparison to soy protein complexes. Overall, based on their results, the pea protein-starch complexes were the most suitable particles for emulsion stabilization. Dai et al. (2018) and Zhu et al. (2019a) evaluated zein nanoparticles complexed with Arabic and corn fiber gum, respectively, as Pickering emulsifiers which were obtained through electrostatic interaction and hydrogen bonds between the gum and the fabricated zein nanoparticles by anti-solvent precipitation. In both studies, the wettability of the zein particles was tuned for O/W Pickering stabilization by the addition of gum. Moreover, the addition of gum to zein nanoparticles increased the particle size and the positively charged particles became negatively charged which was an evidence for the adsorption of gum molecules at the surface of the zein particles. The assembly of plant proteins with polyphenols has also been reported to improve their ability as Pickering emulsifiers. Moreover, it can enhance the oxidative stability of the stabilized emulsion. It was reported that the assembly of tannic acid, as a natural polyphenol, modified the particle-particle interactions and the interfacial behavior of zein nanoparticles via hydrogen bonding of tannic acid and the consequent decrease of the particle hydrophobicity. Therefore, the adsorption rate of zein particles

decreased, leading to a full coverage of the stabilizing particles at the interface due to the provided sufficient time (Zou et al., 2017). It was also reported that the wettability of zein particles can be tuned to near neutral by this hydrogen bonding interaction with tannic acid which is sufficient for Pickering stabilization of O/W emulsions (Zou et al., 2015). In a further study, it was suggested that the rheology and the gel strength of the zein-tannic acid stabilized Pickering emulsions can be tuned through the variation of particle hydrophobicity which can be obtained by altering the tannic acid proportion (Zou et al., 2018). Recently, Pham et al. (2019) reported that the complexation of flaxseed protein with flaxseed polyphenols and hydroxytyrosol improved not only the interfacial and emulsifying ability of the protein, but also the oxidative stability of the emulsified flaxseed oil.

### **1.3 Food applications of plant-based Pickering emulsions**

The utilization of these emulsions in food applications has been widely explored on lab scale. For instance, the design and development of multi-functional food products to fulfill modern consumer demands like feeling outstanding sensorial features is of high importance. However, there are no well-known commercial products in which the use of Pickering emulsions has been claimed. There are, on the other hand, some interesting attempts where the use of Pickering emulsions in food products has been reported. Wang et al. (2018) introduced cellulose nanofibers and its palm oil Pickering emulsions as fat alternatives for replacing 30 and 50% of the original fat of pork-emulsified sausages. The formulated products showed almost comparable sensory characteristics to the control, which makes them appropriate for developing low fat meat products. In a different study, Yano et al. (2017) developed gluten-free rice bread without using additives. Bread with equal specific volume to wheat bread was obtained when rice flour with low starch

damage was used as the main ingredient. Microstructure monitoring of the bubble wall in the fermenting batter demonstrated a “stone-wall” like structure analogous to the microstructure of Pickering emulsions, rather than that of a typical wheat dough. Furthermore, the surface tension of the dispersed solution of flour with low starch damage was lower than that of flour with high starch damage suggesting a hypothetical mechanism in which Pickering stabilization facilitated swelling of the batter/bread (Yano et al., 2017).

Further to these examples, there are numerous reports, where Pickering emulsions stabilized with plant-based particles were used to encapsulate and protect bioactive ingredients, to enhance their nutritional value or for oil structuring purposes. These researches open a promising route based on Pickering emulsions in food formulations. Bioactive compounds have health benefits, including antioxidant, anticancer, and anti-inflammatory properties. However, their sensitivity to pH, light, and thermal treatments as well as their hydrophobic or crystalline nature with a low water solubility may limit their utilization in food products (Sedaghat Doost et al., 2018c, Sedaghat Doost et al., 2019a). Encapsulation has been extensively considered as a means of delivery for these compounds. For instance,  $\beta$ -carotene as the most common carotenoid with a high sensitivity to oxidation was incorporated into Pickering emulsions produced with wheat gluten nanoparticles or wheat gluten nanoparticle- xanthan gum complexes. In this study, it was shown that encapsulation within Pickering emulsions was effective at protecting  $\beta$ -carotene from chemical degradation during storage (Fu et al., 2019). In a different application, zein-chitosan complex particles as a carrier for curcumin were introduced to protect emulsion droplets from peroxidation. The formation of

an antioxidant interface in the presence of curcumin considerably enhanced the oxidative stability of the emulsions (Wang et al., 2015).

In terms of encapsulation, essential oils, naturally occurring compounds with appreciable antioxidant and antimicrobial features (Sedaghat Doost et al., 2018a, Sedaghat Doost et al., 2018b), need to be encapsulated due to their low water solubility, strong scent and flavor and environmental sensitivity. Thymol as a major compound of some essential oils was loaded into zein/gum Arabic nanoparticle-stabilized Pickering emulsions which enabled to inhibit the growth of *E. coli*. Additionally, Pickering emulsions showed a controlled-release effect on thymol due to the protective effect of the stable interfacial layer of complex particles (Li et al., 2018).

A stable interfacial layer of Pickering candidates around the oil droplets might make these structures suitable for designing anti-obesity formulations. High internal phase Pickering emulsions (HIPPEs) stabilized with gliadin/chitosan colloid particles showed that the fraction of free fatty acids released was below 30% for all HIPPEs, reflecting that HIPPEs restricted the digestion rate of the inner oil (Zhou et al., 2018b). In another study, Pickering emulsions stabilized by zein/tannic acid complex colloidal particles also slowed down the release rate of free fatty acids during *in vitro* simulated digestion (Zou et al., 2015), which is potentially beneficial for anti-obesity purposes. Pickering emulsions can also be used as templates to structure low-viscosity liquid vegetable oils into soft solids and oleogels. This strategy can be achieved through HIPPEs formulations of food-grade particles (Hu et al., 2016). HIPPEs systems can be introduced as a good substitute for margarine formulations which contain partially hydrogenated oils (PHOs) (Jiao et al., 2018b). Due to the food safety hazards announced by FDA, PHOs are not allowed to be



used in food production in USA since 2018 (Zhou et al., 2018b). HIPPEs templated oleogelation provides some health beneficial effects through reducing the dietary fat amount and controlling the fat digestibility and replacing PHOs with zero trans-fat and less saturated fats (Hu et al., 2016, Zeng et al., 2017).

#### **1.4 PhD research strategy**

In this study, the water soluble fraction of flaxseed (*Linum usitatissimum* L) mucilage (SFM) and flaxseed protein (FP) were used as biopolymers to prepare Pickering stabilizer nanoparticles since they both have a plant origin and nutritional benefits. FP can be isolated from defatted flaxseed meal, which is a by-product of the flaxseed oil industry and represents 20-30% of the seed weight depending on genetic and geographical origin (Kaushik et al., 2016b, Liu et al., 2018b, Tirgar et al., 2017). This plant protein contains a salt-soluble globulin with high molecular weight (MW) (linin, 252-320 kDa) and a water-soluble albumin with a lower MW (conlinin, 16-18 kDa) (Bekhit et al., 2018, Nwachukwu and Aluko, 2018). FP as a sustainable source of protein can prevent coronary heart disease, kidney diseases and cancer (Wang et al., 2010, Kaushik et al., 2016b, Bekhit et al., 2018), lowering the blood pressure as a source of bioactive peptides (Nwachukwu et al., 2014, Liu et al., 2018b), and can be used as an antidiabetic and antifungal (Nwachukwu and Aluko, 2018, Bekhit et al., 2018). This protein can be used as an alternative for animal-origin proteins for consumers with allergies since it is rich in aspartic acid, glutamic acid, leucine and arginine. There is no published report indicating that consuming FP as a part of a normal diet can cause allergy (Muir and Westcott, 2003). The water-soluble flaxseed mucilage (SFM) is another by-product of the flaxseed oil industry (approximately 7-10% of seed dry mass) which is naturally occurring in the outer layer of the flaxseed hull; it can be extracted easily by soaking

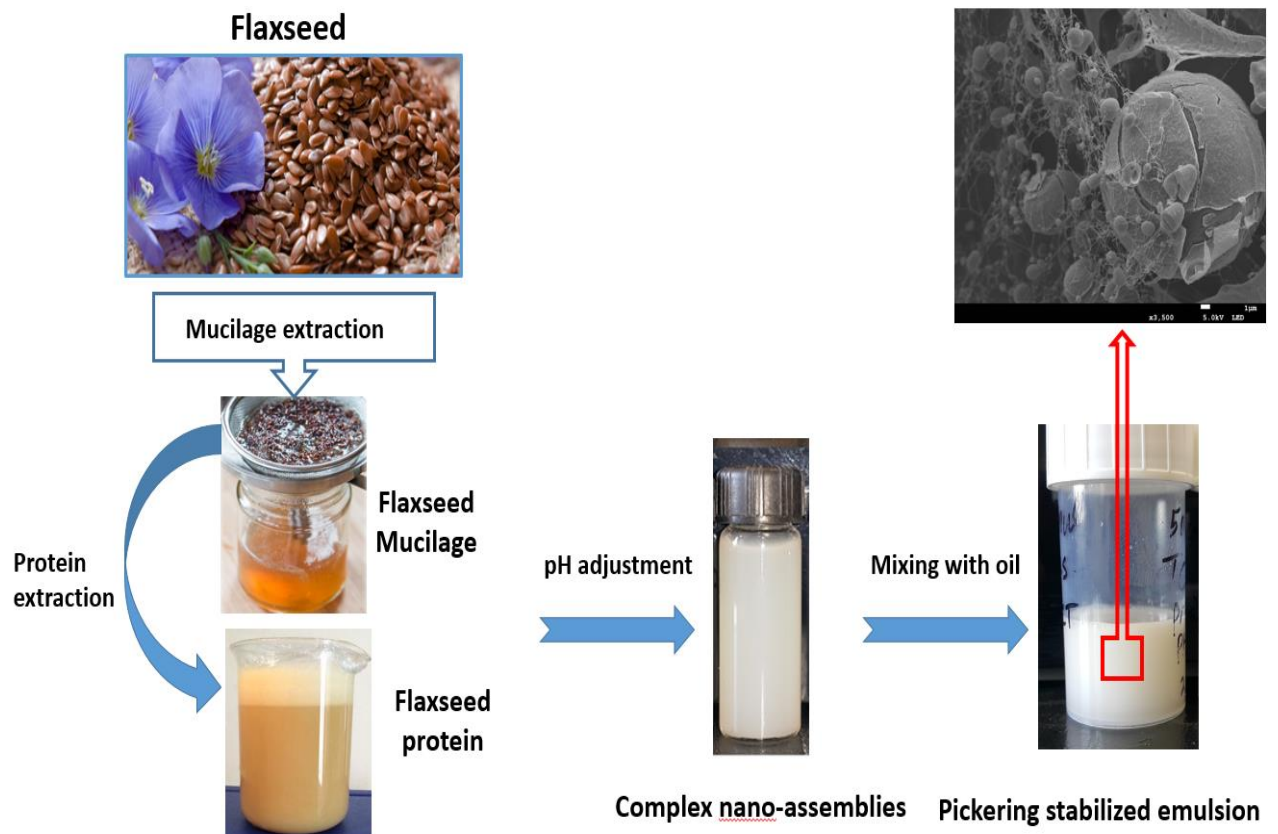
the seeds in water (Cui et al., 1994, Bekhit et al., 2018). The production of mucilage by pericarp (seed coat), which is released by the seed hydration, have multiple biological roles. These include helping the seed hydration, facilitation of seed germination under water logged conditions, decreasing the seed loss by adherence to soil, and increasing the seed dispersal by attachment to animals (Western, 2012). This gum consists of two main components, a neutral fraction consisting of  $\beta$ -D-(1 $\rightarrow$ 4) xylan with L-arabinose and D-galactose, and an acidic fraction containing L-rhamnose, D-galactose and D-galacturonic acid (Khalloufi et al., 2009, Liu et al., 2016c). In this study, the extracted flaxseed mucilage was further separated into a water soluble (SFM) and insoluble fraction. Consumption of SFM can reduce the blood glucose and cholesterol in diabetics (Thakur et al., 2009) as well as prolongation of the satiety and reducing the incidence of obesity by regulating the gut microbiota (Liu et al., 2018b, Luo et al., 2018). SFM also has the advantages of its relatively low cost in comparison to most of the conventional gums and its sustainable world-wide supply (Cui and Mazza, 1996).

FP and SFM were used in this work as plant-based biopolymers instead of animal-based ones due to several advantages, including a lower risk of infection and contamination, no limitations in terms of cultural and religious food habits and vegetarian consumers, and being more economic, sustainable and versatile. The aim of this study was to modulate the solubility and functional properties of FP at and around its isoelectric pH by complexation with SFM via electrostatic interaction and assemble food-grade and plant-based nanoparticles for the purpose of Pickering stabilization of oil-in-water emulsions. These surfactant free Pickering emulsions due to their superior stability against coalescence and oxidation were then applied as a delivery system for flaxseed oil (FO) which is known to be a rich

vegetable source of polyunsaturated fatty acids (PUFA), especially alpha linolenic acid ( $\omega$ -3 fatty acid) with lots of health benefits. However, the poor water solubility and susceptibility to oxidation of FO result in a loss of functionality and lead to off-flavours, which limits its application in food products. Therefore, the aim is to fabricate physically and chemically stable food-grade and plant-based Pickering emulsions based on complex particles of FP-SFM assembled through electrostatic interactions for the purpose of delivering FO as a functional oil for the fortification of water-based food products such as beverages and juices.



## Chapter 2: Plant-based Pickering stabilization of emulsions using soluble flaxseed protein and mucilage nano-assemblies



### Redrafted from:

**NIKBAKHT NASRABADI, M.**, GOLI, S. A. H., SEDAGHAT DOOST, A., ROMAN, B., DEWETTINCK, K., STEVENS, C. V. & VAN DER MEEREN, P. 2019. Plant based Pickering stabilization of emulsions using soluble flaxseed protein and mucilage nano-assemblies. *Colloids and Surfaces A: Physicochemical and Engineering Aspects*, 563, 170-182.

# Abstract

A straightforward and green method of stabilizing emulsions was developed using plant-based particles from complexation of flaxseed protein (FP) and the soluble fraction of flaxseed mucilage (SFM). The extracted SFM was characterized using  $^1\text{H}$  and  $^{13}\text{C}$  NMR. The effect of pH, total concentration (TC) and FP to SFM ratio on the formation of assemblies was investigated by light scattering, surface charge and optical density measurements. The selected negatively charged complex particles were submicron in size and had a near neutral wettability. These nano-assemblies were utilized to fabricate Pickering emulsions. The effect of the FP to SFM ratio, TC and oil content was evaluated on the droplet size of the Pickering emulsions. The droplet size variation of the emulsions stabilized by the selected complex particles and protein only was also monitored during 30 days of storage and the flocculation and coalescence indices were evaluated. On comparing the emulsifying ability of the complex particles with protein particles at pH 3, native FP resulted in poor formation and stability of emulsions due to the aggregation while complex stabilized emulsions were stable with no variation in the droplet size during storage. The microstructure of the emulsions was demonstrated utilizing Cryo-SEM and CLSM. The complexation was able to improve the functionality of FP for emulsion stabilization. The fabricated FP-SFM Pickering emulsions have potential application for the encapsulation of lipophilic bioactive compounds in natural and plant based food, beverage, and pharmaceutical formulations.

## 2.1. Introduction

Pickering emulsions are emulsions stabilized by solid particles, which are partly wetted by oil and water and act as emulsifiers. These emulsions are more stable against coalescence and Ostwald ripening than conventional emulsions (Dickinson, 2010). Recently, the focus on Pickering stabilized foams and emulsions is shifting from using inorganic particles to the utilization of organic and food grade particles from biological origin for food and pharmaceutical applications (Xiao et al., 2016a). The shift to edible and more sustainable bio-based materials especially those which are of plant origin, in food products is motivated by the incompatibility and/or consumer acceptance of inorganic particles whereby plants are generally more effective to transform raw ingredients into added-value products as compared to animals (Lam et al., 2014). Recent studies showed the ability of various particles derived from plant biopolymers such as polysaccharides (cellulose (Tenorio et al., 2017), lignin (Silmore et al., 2016), starch (Song et al., 2015, Timgren et al., 2011)) and proteins (gliadin (Hu et al., 2016), kafirin (Xiao et al., 2016b), pea (Liang and Tang, 2014), peanut (Jiao et al., 2018a) and soy proteins (Liu and Tang, 2016)) to stabilize foams and emulsions (Xiao et al., 2016a, Dickinson, 2017, Sedaghat Doost et al., 2018b). Polysaccharides and proteins may also be associated either through Maillard or electrostatic interactions to fabricate surface-active complexes with advantages of both biopolymers. Moreover, the complexation of proteins with polysaccharides can potentially improve the pH and salt sensitivity of proteins specifically at or around their isoelectric point (pI) where proteins would aggregate (Dickinson, 2008). Complexes can be formed by the electrostatic interaction between a polysaccharide and a protein at certain pH condition, where these two biopolymers carry opposite charge. These complexes are relatively stable due to their surface charges, which ensures their interaction with solvent molecules and

hence their solubility. Having said this, when the net charge of the complexes is zero due to the equal number of opposite charges carried by the two biopolymer, the complex particles become insoluble resulting in their precipitation (Turgeon et al., 2003). By designing the conditions of the biopolymer self-assembly such as pH, protein to polysaccharide ratio, total concentration and ionic strength, the size of the complex bioparticles can be controlled. These nano-assemblies can be simply obtained through pH adjustment and then be used as Pickering stabilizers (Dickinson, 2008). For instance, Humblet-Hua et al. (2013) prepared oil-in-water emulsions with egg white proteins (ovalbumin and lysozyme)-high methoxyl pectin complexes. Recently, some studies evaluated the emulsifying ability of complex particles of whey proteins with various polysaccharides such as chitosan (Chang et al., 2018), pectin (Trujillo-Ramírez et al., 2018), arabic gum (Estrada-Fernández et al., 2018), and almond gum (Sedaghat Doost et al., 2019b). As opposed to particles of animal origin, there are only a limited number of studies on Pickering emulsions which are stabilized by plant-based complex particles. Liu et al. (2010) reported that electrostatic complexation of arabic gum with pea protein can improve its functional properties such as solubility, emulsifying and foaming ability. Kong et al. (2017) also studied the influence of different preparation routes and pH on the stability of soy protein isolate/gum arabic stabilized emulsions.

In this work, FP-SFM colloidal complex particles were self-assembled by adjusting the pH, which is a straightforward and green way to fabricate complex nanoparticles followed by the evaluation of their properties. Then, 'surfactant free' Pickering emulsions were prepared using these plant based nano-assemblies through high-shear homogenization and finally the stability and microstructure of these emulsions were further studied.



## **2.2. Materials and methods**

### **2.2.1. Materials**

Brown flaxseeds (*Linum usitatissimum*) of Norman cultivar were purchased from a local market in Isfahan, Iran. The seeds were sieved and the intact seeds were utilized for further experiments. Sodium chloride, sodium acetate, and ethanol (> 99%) were provided by VWR PROLABO Chemicals (Belgium). Tricaprylin oil was provided by IOI Oleo GmbH (Witten, Germany). Deuterium oxide (heavy water, 99.9%) was purchased from Euriso-tope® (Saint-Aubin Cedex, France). All other chemicals used in this study were analytical grade and purchased from Merck (Darmstadt, Germany). Ultrapure water purified by a Milli-Q filtration system (0.22 µm) (Millipore Corp., Bedford, MA, USA) was used for the analyses and preparation of all aqueous solutions.

### **2.2.2. Extraction of flaxseed mucilage**

Flaxseed mucilage from raw flaxseed was extracted according to the previously reported method of Cui et al. (1994) with minor modifications. Flaxseeds were sieved and washed with deionized water for 1 min at room temperature to remove surface dust. Briefly, the cleaned flaxseeds were mixed with Milli-Q water at ratio of 1:13 (w/v) and left at 80°C while shaking at 200 rpm for 2 h. The extracted flaxseed mucilage was filtered through a 40-mesh screen and precipitation was performed by addition of three volumes of 96% ethanol. After filtration, the precipitated flaxseed mucilage was then dried inside a freeze-drier (Alpha 1-2 LD plus, Christ) and stored in a sealed bag at 4°C for further analysis. In order to obtain a pure and water soluble fraction, the dried mucilage was dissolved in water (1.5 % w/w) and was stored at 4°C overnight to achieve complete hydration. Then, it was ultra-centrifuged (44814 g, 35 min) at 25°C. The supernatant was collected and 0.02%w/v sodium azide as an antimicrobial agent was added before storage

in the refrigerator for further analysis. The concentration of soluble mucilage was determined by means of drying a certain amount of supernatant at 105°C overnight. This experiment was performed after each extraction.

### **2.2.3. Flaxseed protein extraction**

Mucilage-free seeds were dried inside an oven (50°C) and then milled by a coffee grinder followed by passing through a 0.5 mm mesh. The meal was defatted according to the method reported by Karaca et al. (2011). In order to extract the protein according to the methods of Tirgar et al. (2017) , the defatted meal was suspended in Milli-Q water with the ratio of 1:5 (w/v) and the pH was adjusted to 8.5-9 using 1 M and 0.1 M NaOH solution. The mixture was stirred for 1 h at ambient temperature (20°C) followed by centrifugation at 15300 g for 3 min at 4°C. The resulting residue was re-suspended in water at a ratio of 1:5 (w/v) at pH 8.5 - 9 for 1 h, followed by centrifugation (15300 g, 30 min, 4°C). The supernatants were pooled and adjusted to pH 3.8 with 0.1M HCl for protein precipitation. Centrifugation (18000g, 30min, 4°C) was applied to recover the precipitate. The protein solution was freeze-dried and stored in a sealed bag at 4°C until needed. The freeze-dried protein powder was dissolved in water (pH 8.6) followed by stirring for 1 h at 40 °C to dissolve the protein. The extract was centrifuged at 3076g for 20 min to separate insoluble impurities. The supernatant was freeze-dried and stored at 4°C until further use.

## **2.3. Flaxseed protein and mucilage characterization**

### **2.3.1. Proximate analysis**

The moisture, fat, and ash content of the flaxseed, SFM, and FP were determined according to the standard AOAC methods (2003). The nitrogen (N) content was obtained by DUMAS combustion of the dry sample in an Elemental Analyzer - Isotope Ratio Mass Spectrometer (EA-IRMS) (20–22, SerCon, Cheshire, UK)

using helium as carrier gas at 1000°C. A calibration curve was made with a known concentration of ammonium sulphate as standard. As a control, a casein standard with known concentration was used. The protein content was calculated with a conversion factor of 6.38. The carbohydrate content was obtained by the difference between all previous fractions from 100%. All the measurements were carried out in triplicate and the average  $\pm$  standard deviation were reported.

### **2.3.2. 1-D $^1\text{H}$ and $^{13}\text{C}$ nuclear magnetic resonance (NMR) spectroscopy**

The freeze-dried SFM powder (0.5% w/v) was dissolved in deuterium oxide containing 5 mM sodium acetate as an internal standard and  $^1\text{H}$ -NMR spectra were recorded utilizing a Bruker Avance III Nanobay 400 MHz spectrometer equipped with a 5 mm PABBO BB probe. The measurements were carried out at 25 °C. 2% w/v of SFM was used to acquire the  $^{13}\text{C}$  spectrum for 16 h at 30°C.

### **2.3.3. SDS-PAGE analysis**

Sodium dodecyl sulfate-polyacrylamide gel electrophoresis (SDS-PAGE) analysis was carried out on the extracted FP. The acrylamide content of the separating and stacking gel was 12% and 5%, respectively. The sample solutions were prepared in 0.125 M Tris–HCl buffer containing 1% (w/v) SDS, 2% (v/v) mercaptoethanol (ME), 20% (v/v) glycerol and 0.025% (w/v) bromophenol blue and heated in boiling water for 5 min prior to electrophoresis. Then, staining of the gels was performed for protein with Coomassie Brilliant Blue.

## **2.4. Fabrication of particles through acid titration**

FP and SFM stock solutions were separately prepared. The protein mixture was left for stirring on a magnetic stirrer for two hours at 50°C followed by pH adjustment to 8.6 using 1 M NaOH. The stock solutions were stored at 4°C for complete hydration. Individual FP and SFM as well as their mixtures at different protein to

polysaccharide ratios (90:10, 70:30, 50:50, 30:70, 10:90) and different total concentration (TC=0.15, 0.30 and 0.45 wt%) were prepared. Acidification was achieved through the addition of 0.1 M HCl (pH range of 3–7) or 0.3 M HCl (pH range of 1.5-3.0). Alkalization was applied by adding 0.1 M NaOH (pH range of 7–9) dropwise and pH values were monitored by a pH meter.

## **2.5. Turbidimetric analysis**

Optical density measurements were employed to characterize the formation of soluble and insoluble complexes by structural rearrangements as a function of pH, protein to polysaccharide ratio and TC using a UV-visible spectrophotometer (VWR, Belgium) at 600nm. Milli-Q water was used as a blank reference. All these measurements were carried out in triplicate using separate stock solutions.

## **2.6. Particle characterization**

### **2.6.1. Charge density**

140 ml of FP (0.225 wt%), SFM (0.225 wt%) and FP-SFM mixture (50:50, TC=0.45 wt%) were prepared and were titrated from pH 6.0 down to pH 2.0. The streaming potential signal was measured by a Charge Analyser II (Rank Brothers Ltd., Cambridge, England) equipped with streaming potential cell.

### **2.6.2. Zeta-potential**

The zeta-potential of the protein (in a 0.25% solution) and complexes (50:50, TC=0.45 wt%) were determined using a Zetasizer 2c (Malvern Ltd, UK). The samples were diluted prior to analysis with a solution with the same pH. The reported values are the mean of three repetitions  $\pm$  STD.

### **2.6.3. Particle size**

The size of the particles was measured using Photon Correlation Spectroscopy (Model 4700, Malvern Instruments, U.K.) at a scattering angle of 150° at 25 °C. The samples were diluted before analysis with a solution with the same pH to avoid

multiple scattering. The light intensity correlation function was analyzed based on the multimodal method while the z-average diameter was obtained by cumulant analysis. Each measurement was an average of 10 runs.

#### **2.6.4. Fourier transform infrared spectroscopy (FTIR)**

Fourier transform infrared (FTIR) spectroscopy (Shimadzu IR Affinity-1, Kyoto, Japan) was used to determine the functional groups present within the molecular structure of the complex particles with the ratio of 50:50 and TC=0.45 wt% at pH 3 and of individual FP and SFM. The freeze-dried powder of the samples was used to record the FTIR spectra in the wavelength range 400-4500  $\text{cm}^{-1}$  and a 4  $\text{cm}^{-1}$  resolution with 20 scans and then analyzed using LabSolutions IR software (V2.15, 2016).

#### **2.6.5. Interfacial tension**

The interfacial activity of FP (0.225%), SFM (0.225%) and the complex FP-SFM particles with a protein to mucilage ratio of 50:50 and TC=0.45% at the tricaprylin oil-water interface was measured by monitoring the evolution of the interfacial tension ( $\gamma$ ) with time using an automated drop shape tensiometer (Tracker, Teclis, I.T.C., France). One drop of each sample was automatically formed with the aid of a pendant needle into a glass cuvette containing tricaprylin oil phase. The shape of the drop was analyzed to record changes in interfacial tension over a period of time. The density of the samples was measured using an Anton-Paar DM5000 (Belgium) density meter. The temperature was kept constant at 25°C during the interfacial tension measurement utilizing a water bath.

#### **2.6.6. Contact angle**

The freeze-dried powders of FP-SFM nanoparticles with a ratio of 70:30 and 50:50 and SFM prepared at pH 3 were compressed to produce tablets by compacting the

powder under pressure of 89.2 MPa for 5 min. The contact angle ( $\theta_w$ ) of a sessile drop of water (10  $\mu$ L, pH 3) on the tablets was measured using a drop shape analysis system DSA 10 Mk2 (Krüss GmbH, Germany) and approximating the contour of the droplets in the image with a circle fitting using the Young-Laplace equation.

## **2.7. Emulsion preparation**

Emulsions were prepared by homogenizing the particle dispersion (ratio of FP:SFM 70:30 and 50:50, TC=0.45 wt%) at pH 3 with tricaprylin oil as lipid phase (2.5% w/w) using a high shear blender (type S 50N-G 45 F, IKA®-Werke, Germany) for 5 min at 24000 rpm. For comparison, an emulsion with only FP (0.225%, pH 3) was also processed in a similar manner.

## **2.8. Emulsion characterization**

### **2.8.1. Droplet size distribution**

The volume-weighted average droplet size ( $D[4,3]$ ) of emulsions after the preparation and during the storage for 30 days was monitored using a MasterSizer 3000 (Malvern Instruments Ltd, Malvern, Worcestershire, UK) equipped with a wet sample dispersion unit (Malvern Hydro MV, UK). The samples were diluted with a dilution liquid with the same pH as the solution prior to the measurement. The refractive index of the dispersed phase and of water as continuous phase were taken as 1.45 and 1.33, respectively. All determinations were conducted on individual samples at least in triplicate.

The flocculation index (FI) of stored (after 24 h) emulsions, as well as the coalescence index between 0 h and 24 h was investigated. The emulsions were diluted in deionized water with and without 1% (w/v) SDS, and the  $d[4,3]$  and SSA (specific surface area) of the droplets was determined. The percentage of FI and CI was calculated as follows (Liang and Tang, 2013);

$$\text{Flocculation index (FI)} = \left[ \left( \frac{d_{24h} [4,3] \text{ in water}}{d_{24h} [4,3] (\text{in } 1\% \text{ SDS})} \right) - 1 \right] \times 100$$

$$\text{Coalescence index (CI)} = \left[ \left( 1 - \frac{SSA_{24h} (\text{in } 1\% \text{ SDS})}{SSA_{0h} (\text{in } 1\% \text{ SDS})} \right) \right] \times 100$$

where  $SSA_{0h}$  is the specific surface area at zero time (fresh emulsion), and  $SSA_{24h}$  is the specific surface area 24 h after emulsion preparation.

### **2.8.2. Cryo-scanning electron microscopy (Cryo-SEM) and confocal laser scanning microscopy (CLSM)**

The microstructure of the emulsions stabilized by nanocomplexes with a FP to SFM ratio of 50:50 and TC= 0.45% wt was evaluated using Cryo-SEM. Droplets of the sample were placed on the specimen holder and frozen in liquid nitrogen transferred to the preparation chamber (PP3010T Cryo-SEM preparation system, Quorum Technologies, UK). After fracturing and sublimation, they were sputter coated with platinum prior to taking photograph utilizing a JSM-7100 (Jeol Europe, Belgium).

Confocal laser scanning microscopy (CLSM) (Leica TCS-SP5, Germany) was utilized to visualize Pickering emulsions. Native FP and FP-SFM nano-assemblies prepared at pH 3 (50:50, TC=0.45% wt) and oil phase were stained by Rhodamine B and Nile red, respectively. The excitation and emission wavelength of Rhodamine B were set as 532 and 560-600 nm, respectively. Nile red was excited at 488 nm and detected at 680-700 nm.

### **2.9. Statistical analysis**

All measurements were carried out at least in triplicate and results were reported as means  $\pm$  standard deviations (SD). One-way analysis of variance (ANOVA) was carried out on the data using SPSS software using a level of significance of  $p < 0.05$ .

## 2.3. Results and discussion

### 2.3.1. Flaxseed protein and mucilage characterization

The chemical composition of flaxseed as well as flaxseed protein and mucilage is given in Table 2.1.

Table 2.1. Chemical composition of the flaxseed used, as well as of the derived FP and SFM fractions. The values are in weight percentage  $\pm$  SD.

	Carbohydrate	Protein	Moisture	Ash	Fat
Flaxseed	35 $\pm$ 0.6	15.5 $\pm$ 1.6	7.5 $\pm$ 0.4	3 $\pm$ 0.7	39 $\pm$ 0.8
Flaxseed protein	10.5 $\pm$ 0.4	64.5 $\pm$ 1.1	15.5 $\pm$ 0.5	7.6 $\pm$ 0.4	1.9 $\pm$ 0.3
Flaxseed mucilage	79.8 $\pm$ 0.1	12.9 $\pm$ 0.1	3.5 $\pm$ 0.3	2.7 $\pm$ 0.1	1.1 $\pm$ 0.3

These results were partly different from what Kaushik et al. [26] reported on the chemical components of the extracted flaxseed mucilage, which were lower in protein (9.4 $\pm$ 0.9% protein) and slightly higher in carbohydrate (81.3 $\pm$ 1.4% total carbohydrate). This difference could be due to different varieties of flaxseed since they used the golden type instead of the brown variety. Moreover, the conditions of mucilage extraction such as seed to water ratio (1:18), temperature (50°C) and the speed of shaking (300 rpm) were quite different from this study. Furthermore, in our work the water soluble fraction of flaxseed mucilage was purified by ultracentrifugation. The SFM extraction efficiency was 9 wt% which was consistent with the results of Kaushik et al. [26].

### 2.3.2. NMR

The proton NMR spectrum of SFM is given in Figure 2.1-a. The signals at 1 - 1.5 ppm are caused by the proton resonances of  $-CH_3$  groups of the fucose and rhamnose residues and signals at 2.6 - 3.4 ppm could be attributed to the  $-CH_2-$  group in the propyl and/or  $-CH_2-O$  group of ethyl at position 3 of some of the glucosyl residues (Kaushik et al., 2017, Cui et al., 1995, Kaewmanee et al., 2014,



Qian et al., 2012a). The sharp peak around 1.9 ppm belongs to the sodium acetate, which was used as an internal standard. There is no signal in the region between 2.0 and 2.2 ppm showing the lack of acetylated sugars. Mikshina et al. (2012) reported that the signal at 3.53 ppm correlated with galactose of galactan. Moreover, they mentioned that the amount of rhamnose branched with terminal galactose from the total branched rhamnose residues could be estimated from the ratio of the signal intensities at 3.53 ppm and 1.31 ppm in the  $^1\text{H}$  spectrum of the polysaccharide. The signals between 4.43 and 5.41 ppm are attributed to anomeric protons except the sharp peak at 4.7, which was due to the water (HDO). Among these peaks, the signal at 5.25 ppm arises from the rhamnose residues of a rhamnogalacturonan backbone (Kaewmanee et al., 2014). The signals at 4.65, 4.96, and 5.01 ppm were assigned to (1,4)-linked- $\beta$ -D-Galactopyranose (G4), (1,4)-linked- $\beta$ -D-Galacturonic acid (GA4), and (1,3,4)-linked- $\beta$ -D-Galacturonic acid (GA34). Two signals at high field (1.25 and 1.29 ppm) were assigned to the H-6 of (1,2)-linked- $\alpha$ -L-rhamnopyranose (R2), and (1,2,4)-linked- $\alpha$ -L-rhamnopyranose (R24), respectively (Ding et al., 2015). The small peaks between 5.0-5.2 ppm were assigned to the H-1 of arabinose residues (1,5)-linked- $\alpha$ -L-Arabinofuranose (A5), (1,3,5)-linked- $\alpha$ -L-Arabinofuranose (A35), (1,2,3,5)-linked- $\alpha$ -L-Arabinofuranose (A235), and terminal  $\alpha$ -L-Arabinofuranose (AT) (Ding et al., 2015). Four linkage patterns at 4.1, 3.92, 3.84, 3.77 ppm revealed that the carbon atoms are mainly of  $\beta$ -configuration (Liang et al., 2017b). Overall, the proton NMR of SFM was in good agreement with the previously reported spectrum of flaxseed gum (Kaushik et al., 2017).

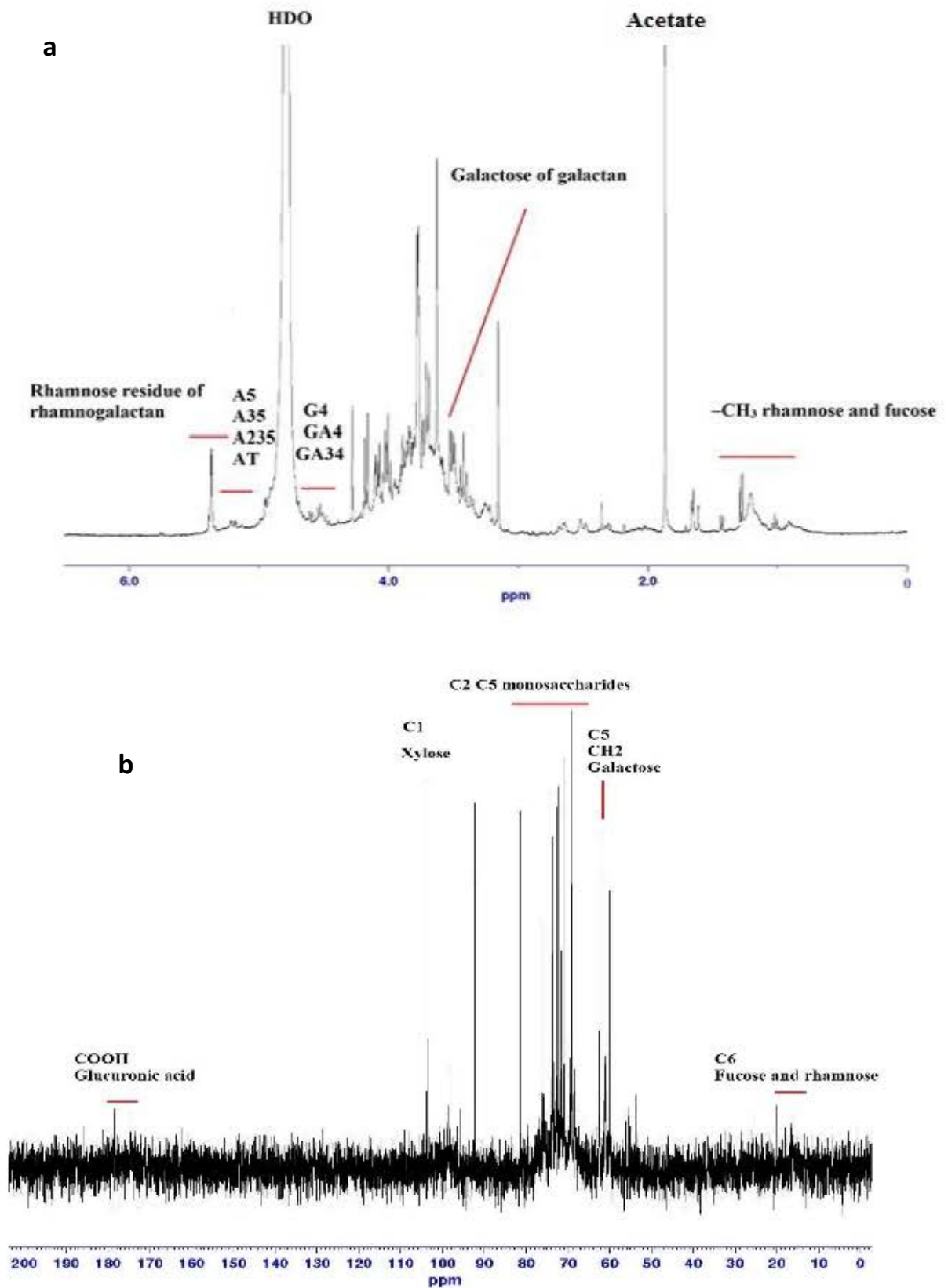


Figure 2.1. a)  $^1\text{H}$  and b)  $^{13}\text{C}$  NMR spectra of SFM.

The  $^{13}\text{C}$  NMR spectrum of SFM shown in Figure 2.1-b is in a good agreement with previously reported spectra (Warrand et al., 2005b, Cui and Mazza, 1996, Kaushik et al., 2017). The resonances at 16.2 and 17.6 ppm originated from the C-6 of fucose and rhamnose, respectively (Cui and Mazza, 1996, Qian et al., 2012a). Resonances between 65 – 85 ppm are attributed to carbons 2 and 5 of monosaccharides. Signals at 90 - 110 ppm are attributed to anomeric carbons (Liu et al., 2016a). The signals at 81, 78 and 62 ppm are for C2, C3 and C5 of 1,3-linked arabinose residues, respectively (Warrand et al., 2005b). The signals at 97 (C1) and 77 (C4) ppm revealed a  $\beta$ -anomeric conformation of the 1,4-linked D-xylopyranose backbone (Kaushik et al., 2017). The peak at 99 ppm originated from the CH group in the cyclic group of rhamnose. The small peak at 102 arose from galactose and the chemical shift signal at 104 ppm is attributed to the C-I carbon of xylose (Cui and Mazza, 1996, Qian et al., 2012a). The peaks between 173-180 ppm evidence the existence of glucuronic acid (Qian et al., 2012a, Liu et al., 2016a).

Warr et al. (2003) and Qian et al. (2012b) showed that the extracted mucilage from the flaxseeds contains two fractions; a neutral and an acidic fraction. The neutral fraction is an arabinoxylan comprised of  $\beta$ -D-(1,4)-xylan backbones which gives the polymer an extended structure. According to the literature, the neutral fraction has a weight-based average MW of approximately 1200-1500 kDa (Qian et al., 2012b, Warrand et al., 2005a). The acidic fraction with a rhamnogalacturonan backbone containing L-rhamnose, D-galactose, and D-galacturonic acid (Liu et al., 2018b) is composed of two sub-fractions with MWs of 650 and 17 kDa (Warr et al., 2003, Qian et al., 2012b). The anionic nature of the acidic fraction due to the presence of D-galacturonic acid, which is an uronic acid with carboxylic groups,

provides the opportunity to have an electrostatic interaction with proteins below their isoelectric point (pI) (Warr et al., 2003, Qian et al., 2012b).

### **2.3.3. SDS-PAGE**

The signal bands of SDS-PAGE for extracted FP are shown in Figure 2.2. According to Nwachukwu and Aluko (2018), both albumin and globulin fractions are present in the extracted FP. Among the bands that were observed for FP, those corresponding to 14.4 and 25 kDa were more intense. Oomah and Mazza (1998) reported four predominant polypeptides in flaxseed meal products with molecular weight (MW) of 14, 24, 25, and 34 kDa, and also a number of other minor bands, while Tirgar et al. (2017) reported 25–30 kDa and 35–40 kDa as the predominant bands. The 24.6 kDa (20-27 kDa) component was reported to correspond to basic subunits while the 30 and 35 kDa components correspond as the acidic subunits in the flaxseed globulin. The subunit composition of the protein is certainly dependent on the flaxseed variety (Nwachukwu and Aluko, 2018, Tirgar et al., 2017).

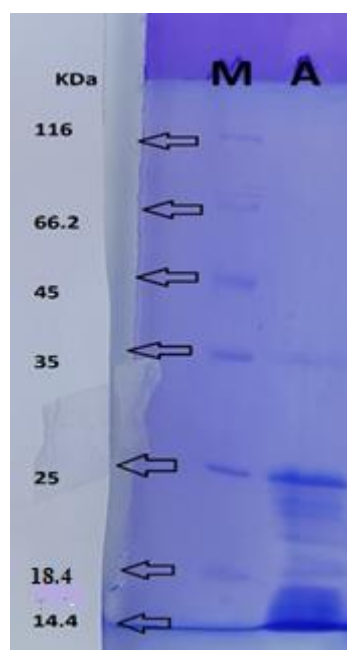


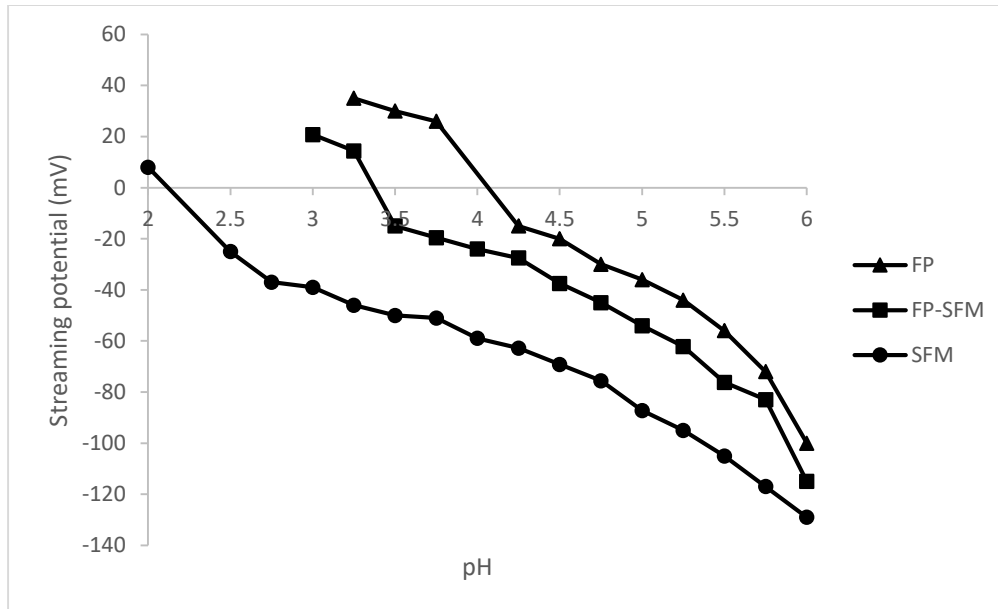
Figure 2.2. SDS-PAGE profile of the extracted FP (lane A) and the molecular weight marker (lane M).

#### 2.3.4. Surface charge properties

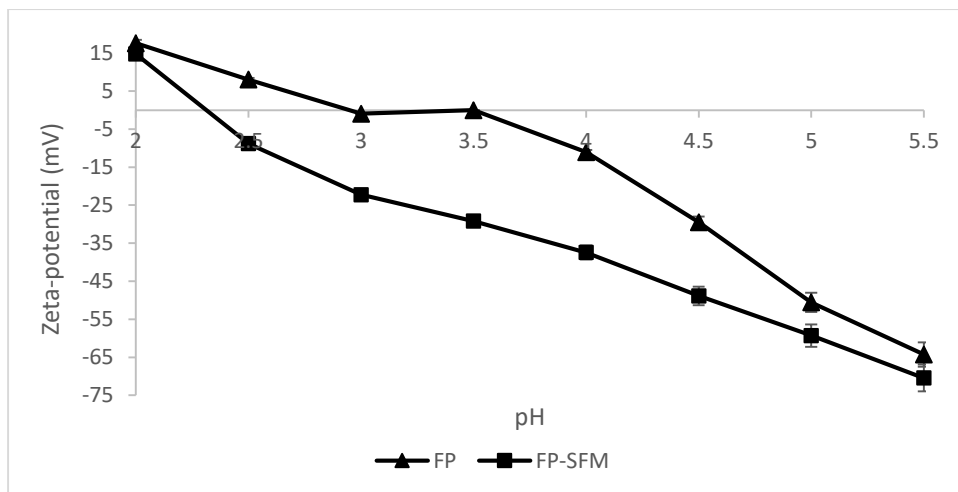
The flaxseed protein pI has been reported to be at 3.8 - 4.2 in previous studies (Kaushik et al., 2016b, Karaca et al., 2011). The pI is dependent on the composition of the protein and on the measurement technique. Nwachukwu and Aluko (2018) have recently reported that flaxseed protein consists of two globulins (salt soluble) and albumin (water soluble) fractions with different molecular weights of 10 – 50 kDa and 10 kDa with a minor content of 40 kDa, respectively. Moreover, the globulin fraction has a higher amount of hydrophobic amino acids (sulphur amino acids) and a higher surface hydrophobicity in comparison to the albumin fraction (Liu et al., 2018a, Nwachukwu and Aluko, 2018). Subsequently, the globulin fraction has a lower solubility at all pH conditions with the lowest solubility at pH 5. However, the albumin fraction due to the higher amount of negatively-charged amino acids and carbohydrates is more soluble with a minimum at pH 3

(Nwachukwu and Aluko, 2018). The aggregation and precipitation occurred in FP at pH 3, 3.5 and 4 (Figure 2.3-c). Thus, these values are close to the points where each fraction has the lowest solubility.

a)



b)



c)

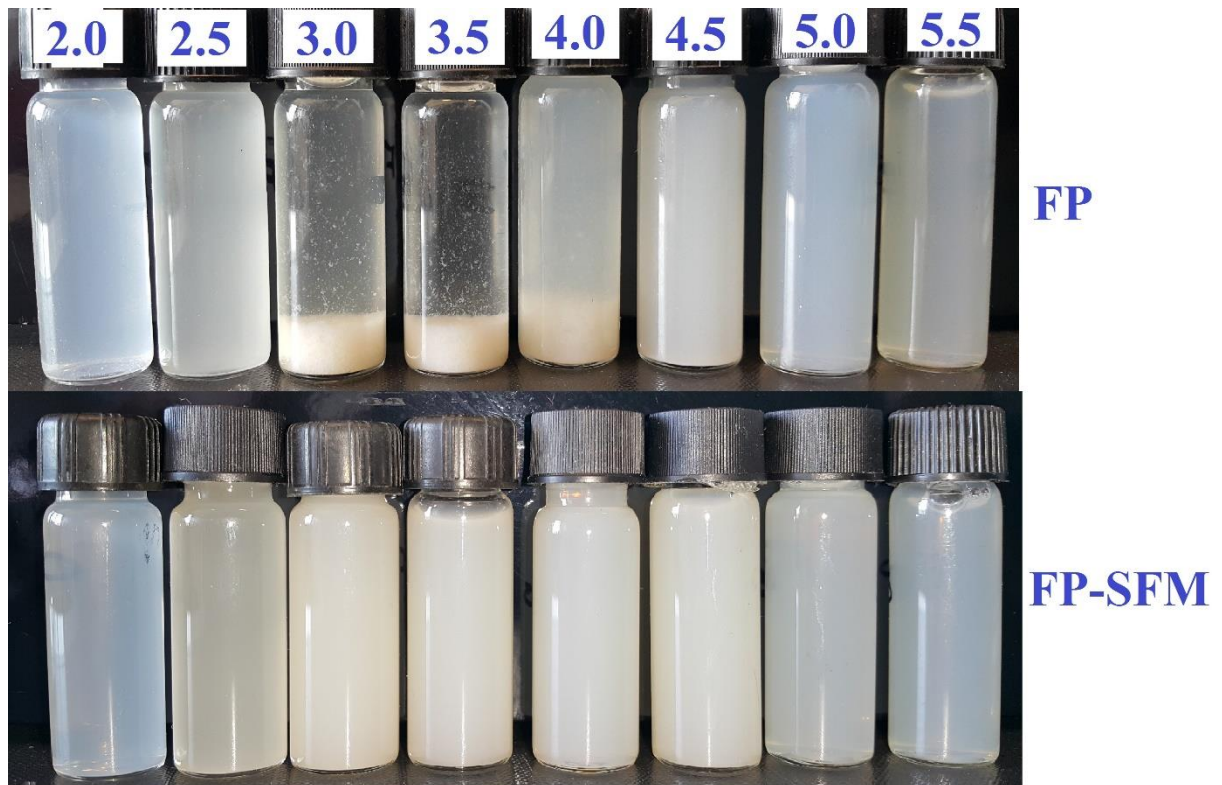


Figure 2.3. a) Charge titration curve of FP, SFM and the mixture with the FP to SFM ratio of 50:50 and TC = 0.45 wt % and b) Zeta potential values as a function of pH for the individual FP and FP-SFM 50:50 complex particles with TC = 0.45 wt % . All data represent mean  $\pm$  standard deviation ( $n = 3$ ). C) Visual appearance of individual FP and FP-SFM mixtures (TC = 0.45 wt %) at different pH values.

Figure 2.3-a shows the charge titration curve of the FP, SFM and the complex particles with a ratio of 50:50 and TC = 0.45 wt %. SFM is an anionic gum in the studied pH range due to the existence of D-glucuronic acid (Figure 2.1-b) (Liu et al., 2015) with a  $pK_a$  of 2.25, which is consistent with the results of Kaushik et al. (2015). In terms of FP, the point of zero charge (at pH around 4.0 to 4.2) coincides with the  $pI$  of the FP (pH 3.8 - 4.2) reported previously by (Kaushik et al., 2016b, Karaca et al., 2011)). The presence of SFM decreased the  $pI$  of the FP, which can be due to the binding of the anionic mucilage to the cationic patches of the protein. Figure 2.3-b presented that the zeta potential of FP had the net neutrality and low surface charge at pH 3 to 4, which is in agreement with the visual investigation that

at all these three pH values, there was aggregation and precipitation (Figure 2.3-c). The Zeta potential of FP-SFM mixture at a 50:50 mixing ratio and TC = 0.45 wt% as a function of pH indicated that the assembled particles are negatively charged and the net neutrality occurred at below pH 2.5. It can be seen in Figure 2.3-c that the complexation between FP and SFM prevented the aggregation and precipitation of protein at and around its pI and this might be due to the increase in surface charge.

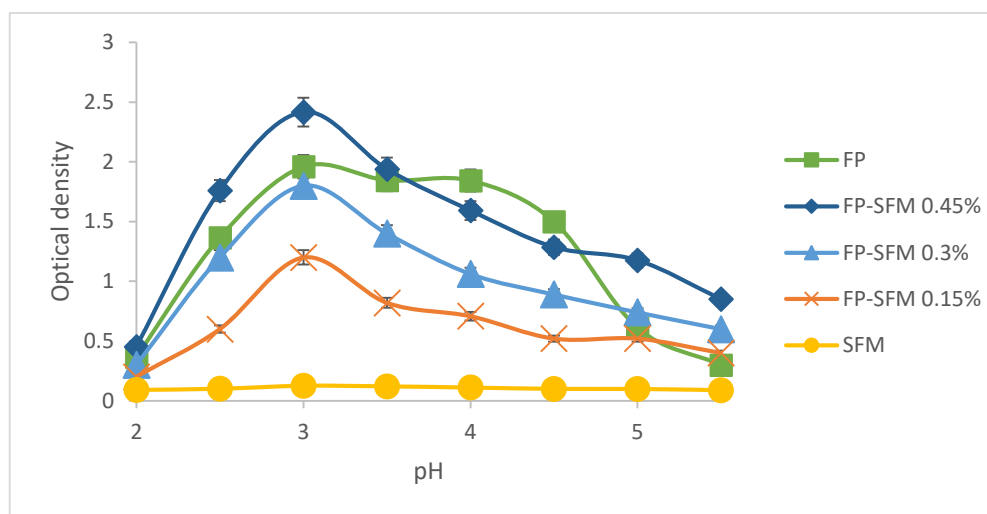
### **2.3.5. Optical density measurement**

The variation in optical density (OD) during the acid titration was measured for individual FP and SFM as well as the mixtures of FP and SFM with different TC (Figure 2.4-a). For FP alone, the OD started increasing from pH 5 downwards followed by a plateau between pH 4.00 and 3.00 (corresponding to a maximum OD of 1.96 at pH 3) and then decreased with lowering the pH down to 2. This high OD value at these pH values could be related to the solubility reduction of FP at and around its pI, which is consistent with the outcomes of surface charge measurements and visual investigation (Figure 2.3) (Bengoechea et al., 2011). In terms of SFM, the OD displayed a very slight variation between pH 2 and 5.5.

The OD profile of the mixed FP-SFM systems with different TC had a fairly similar trend. However, increasing the TC led to a higher values of the OD, which is mainly through increasing the number of complexed biopolymer particles (Figure 2.4-a). Our results are in agreement with the findings of Liu et al. (2015) for bovine serum albumin and gum from whole flaxseed, where the trend of the optical density profile was independent from the TC while higher TC values had a higher OD.



**a**



**b**

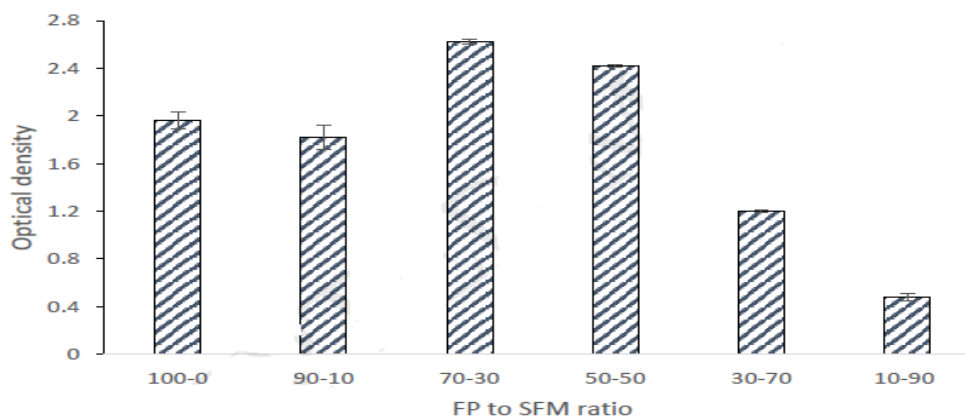


Figure 2.4. Optical density (turbidity values) as a function of pH for a) individual FP and SFM and the FP-SFM mixed system at ratio ( $r$ ) of 50:50 with a total solid concentration of 0.15, 0.3 and 0.45 wt %. b) Effect of different FP to SFM ratios on the optical density of the complexes prepared at pH 3 and a total concentration of 0.45 wt %.

Whereas the streaming potential results (Figure 2.3-a) indicated that in FP-SFM mixtures both biopolymers carry a negative charge at a pH above the pI of the protein, still even at pH 5.0 and 5.5 the optical density of the mixture with TC= 0.45 wt% is higher than of the protein alone indicating some electrostatic interactions

between the SFM and positive parts on the protein. The interaction between proteins and polysaccharides at the protein pI and higher pH values where both are net negatively charged, is also possible. This could be due to the fact that protein molecules have some positively charged patches via their protonated amines ( $-\text{NH}_3^+$ ) groups interacting with negative carboxyl groups of polysaccharides (Ru, Wang, Lee, Ding, & Huang, 2012). Nevertheless, at relatively extreme low and high pH values associated with the severe electrostatic repulsion between similar charges the interaction will be limited. As the pH was lowered, the formation of complexes between oppositely charged polymers increased and the OD reached its highest value at  $\text{pH}_{\text{opt}}$  (3.0). Moreover, at this pH the mixture of FP-SFM with TC= 0.45 wt% had higher OD than individual FP, which is a good indication of the formation of either large particles and/or higher number of complex particles. As the pH was lowered further, it resulted in a decline in OD, indicating the fact that complexes began to dissociate as the negatively charged sites of SFM became protonated. The dissolution of electrostatic complexes occurred near pH 2.0 where a similar optical density was observed for the mixture and for the protein only (Liu et al., 2010, Kaushik et al., 2015). The addition of SFM leads to the stabilization of proteins against aggregation and precipitation via increasing the surface charge density at pH values close to the pI of the FP. At pH 3.0 (the optical density peak) the maximum production of complexes occurred. Nanoparticles are usually soluble complexes, which may be considered as a precursor of insoluble complexes or coacervates (Lv et al., 2014). Le and Turgeon (2013) reported that interpolymer complexes between polysaccharide chains and proteins can be formed at  $\text{pH} \geq \text{pI}$  of the protein for  $\beta$ -lactoglobulin-xanthan gum due to intramolecular interactions. In their study, the mobility of XG was reduced in the

system, which acted as nuclei. By decreasing the pH, the proteins diffused to the XG chain and aggregated. At this point, soluble complexes formed due to attractive interactions and then the interpolymeric complexes appeared.

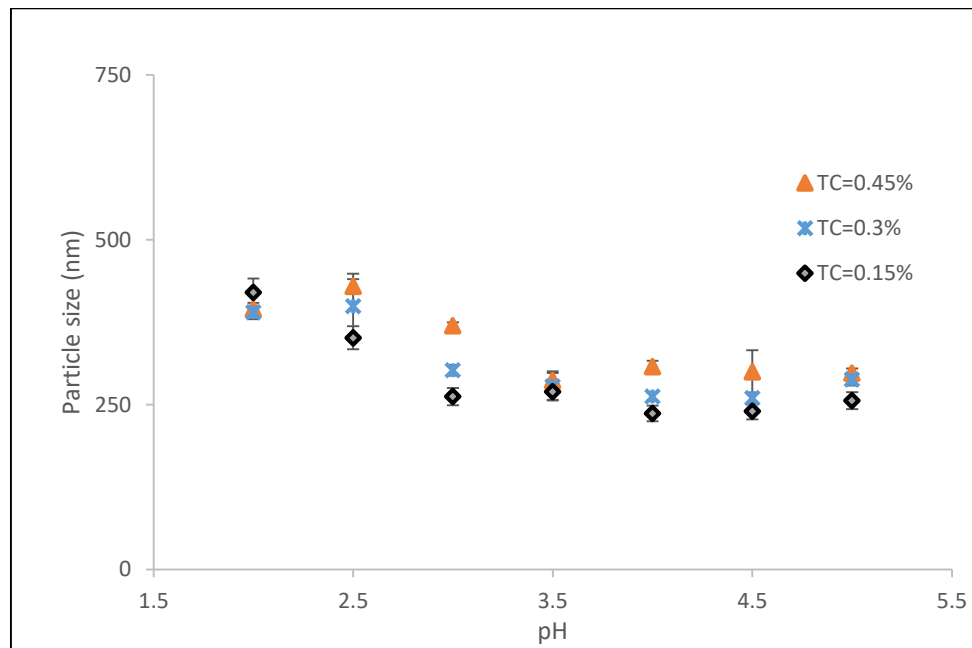
The OD variation of FP-SFM was studied at pH 3 and a fixed TC (0.45 wt%) in order to understand the effect of FP to SFM ratio on the interaction between the biopolymers (Figure 2.4-b). Aggregation and precipitation occurred for the FP and the 90:10 ratio and their OD was not significantly ( $p > 0.05$ ) different. At this ratio, the concentration of the SFM was not enough to prevent the aggregation at the studied pH conditions. At all other ratios, there was no precipitation. It is obvious that the optical density of mixtures except the ones with 30:70 and 10:90 ratio is higher than of the individual FP solution, which can be a sign of the formation of complex particles.

#### **2.3.6. Particle size**

As presented in Figure 2.5-a, the diameter for the 50:50 ratio complex particles with different total concentrations was evaluated as a function of pH. At high pH values dissociation of the assembled particles occurred because of repulsion between the biopolymers, as both the FP and SFM carry like charges (Figure 2.3), which led to a smaller particle size. This was consistent with the OD results at high pH values where the OD became lower. However, the optical density was higher than the FP alone, showing that there exist particles. On the other hand, the dissociation of the complexes at low pH conditions, led to the formation of a small number of large aggregates based on both OD and size measurements. At pH = 3, which is below the FP pI, there is an electrostatic interaction between the oppositely charged FP and SFM whereby a high number of complex particles are assembled. These outcomes are in agreement with results of optical density

measurements, where the biopolymer mixture has the highest turbidity at pH 3 (TC = 0.45 wt%, 50:50 ratio). A similar trend was observed for the size of the particles at different TC under different pH values. Despite of the higher optical density at pH 3 (Figure 2.4-a), the size of the particles was marginally larger at pH 2.5 for all TC values. This is due to the fact that at pH 3 a larger number of soluble complexes with smaller size were assembled: according to the light scattering theory, the optical density is related to the particle size in a non-monotonous way (Bohren & Huffman, 2008). The size of native protein particles with a concentration of 0.225 wt% at different pH values was also evaluated. Due to the aggregation (Figure 2.3-c), no successful measurements could be performed for individual FP at pH values of 3.0, 3.5 and 4.0, which indicates the presence of supermicron aggregates in the protein solution. However, for pH 2.0, 4.5 and 5.0 the z-average particle diameter was  $381 \pm 5$  nm,  $592 \pm 25$  nm and  $210 \pm 3$  nm, respectively. Smaller particle size and prevention of aggregation and precipitation in the presence of SFM was a clear sign of having electrostatic interaction between the SFM and FP, which was confirmed with the outcomes of surface charge and optical density measurements.

a



b

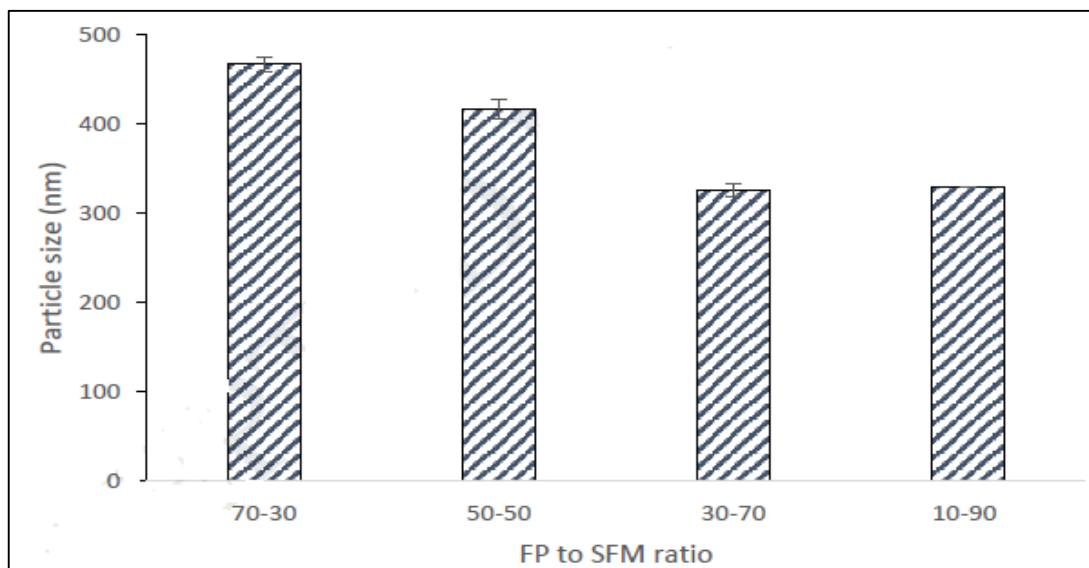


Figure 2.5. a) pH dependence of the z-average particle diameter (nm) as a function of pH for FP-SFM complex systems with 50:50 FP to SFM ratio with a total solid concentration of 0.15, 0.3 and 0.45% (w/w). b) The effect of FP to SFM ratio on the size of the particles prepared at pH 3 and a total concentration of 0.45wt%. Each measurement was made in triplicate.

The effect of the protein to mucilage ratio on the average size of the particles at a fixed TC=0.45 wt% and pH = 3 is shown in Figure 2.5-b. For the ratio of 100:0 and 90:10 the particle size measurement was not successful due to aggregation of the

protein near its pI and the size of the obtained particles was in micrometer range (data not shown). Moreover, for the 0:100 ratio, there was still a problem in measuring but this time due to the low scattering intensity. The particle size was reduced by increasing the amount of the SFM. As a result of electrostatic interaction, the anionic SFM wrapped around the protein molecules and prevented the aggregation by providing a sufficient repulsion. Due to the compaction and the electrostatic repulsion, the size of the complex particles decreased.

Overall, the complex particles assembled at pH 3 were selected for further analysis and fabrication of Pickering emulsions. This point had the highest optical density with relatively small particle size (around 300 nm) indicating the formation of higher number of soluble and small particles. Moreover, at this pH the assembled particles were negatively charged and stable due to the surface charge while the native protein had aggregation and precipitation as a result of near zero surface charge.

### **2.3.7. FTIR**

The changes in the functional groups of the complex particles were characterized by FTIR spectroscopy. Figure 2.6 represents the FTIR spectra of SFM, FP, and the FP-SFM complex particles (FP:SFM = 50:50, TC=0.45 wt%, prepared at pH 3). It is seen that the functional groups present in the complex particles are in close resemblance with the functional groups of SFM and FP. The strong and broad absorption band at  $3323\text{ cm}^{-1}$  is due to the existence of hydroxyl groups which confirms the presence of the glucosidal linkage. The peak at  $1608\text{ cm}^{-1}$  in SFM is caused by the stretching of vibration of C=O stretching of carbonyl groups which is a typical saccharide absorption and is attributed to the vibration of amide I, as the SFM is a gum that contains protein (Liu et al., 2016b, Liang et al., 2017b). The peak at  $1420\text{ cm}^{-1}$  represents the C=O stretching of the -COOH group of uronic

acid (D-glucuronic acid as corroborated by the results of  $^1\text{H}$  and  $^{13}\text{C}$  NMR in Figure 2.1 and the negative charge of SFM) in SFM which disappeared in the complex particles. This indicates the interaction between carboxyl groups of SFM and amine groups of FP. The peak at  $1039\text{cm}^{-1}$  in SFM is due to the stretching of the C-O bond of pyranose (Espinosa-Andrews et al., 2010, Liang et al., 2017b). The FTIR spectrum of the complex particles exhibited corresponding peaks at  $3304\text{ cm}^{-1}$  and  $2960\text{ cm}^{-1}$  showing the presence of O-H stretching bonding and  $-\text{CH}_2$  stretch in aromatic rings, similar to the individual SFM with a shift to  $3271\text{ cm}^{-1}$  and  $2922\text{ cm}^{-1}$ , respectively (Jain et al., 2016, Bouaziz et al., 2016). The peaks at  $2997$  and  $3197\text{ cm}^{-1}$  are attributed to the C-H stretching of aliphatic groups attached at different positions in globular proteins (Jain et al., 2015). The amide I peak position in FP occurred in the region of  $1600\text{-}1700\text{ cm}^{-1}$  (mainly C=O stretch), the amide II band in the region of  $1500\text{-}1600\text{ cm}^{-1}$  (C-N stretch coupled with N-H bending mode) and the amide III band in the region of  $1300\text{ cm}^{-1}$  (N-H bending mode coupled with C-N stretch) (Sun et al., 2017, Kaushik et al., 2016a, Chung et al., 2005). There was a slight shift in vibrations and different intensities in the amide I and amide II groups of FP in the complex particles in comparison to FP. Moreover, it was observed that the amide III peak at  $1300\text{ cm}^{-1}$  in FP disappeared in the FP-SFM complex particles. There was also a slight shift for the peaks at  $1035\text{ cm}^{-1}$  to  $1039\text{ cm}^{-1}$ . Bands at  $1160\text{ cm}^{-1}$  were associated to the stretching of C-O in FP, which disappeared in FP-SFM complex particles, indicating the effect on the protein structure due to interaction between SFM and FP. Xu et al. (2015) reported similar results for the fabrication of xanthan-lysozyme complex nanoparticles via electrostatic interactions. These results due to the changes particularly in the carbonyl-amide region suggested the existence of electrostatic interaction between

protonated amine groups  $\text{NH}_3^+$  of FP and dissociated carboxyl groups  $\text{COO}^-$  of SFM in the complex particles.

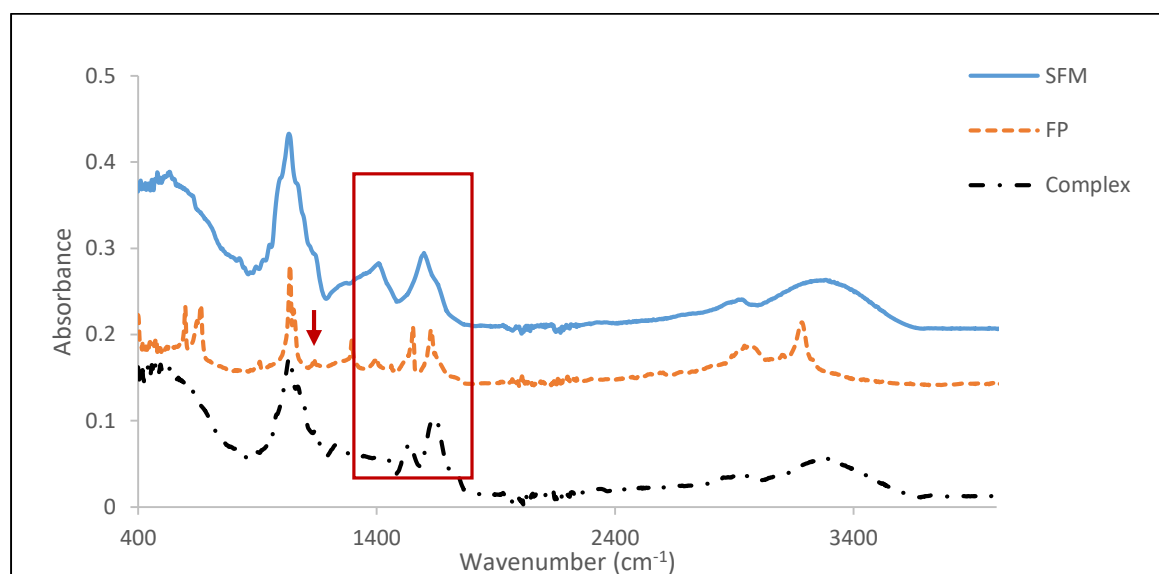


Figure 2.6. FTIR profile of SFM, FP, and the FP-SFM complexes formed at  $\text{pH}=3$  with a ratio of 50:50.

### 2.3.8. Contact angle ( $\theta_w$ )

A contact angle of  $90^\circ$  induces the best wettability condition for preparing Pickering emulsions to obtain the suitable steric repulsion. In this case, particles at the interface can be wetted by the both phases. However, there are several studies reported that particles with contact angle  $60\text{-}90^\circ$  are able to stabilize Pickering oil-in-water emulsions since they can penetrate the oil phase and be wetted by the continuous phase simultaneously (Aveyard, Binks, & Clint, 2003; (Dai et al., 2018, Sedaghat Doost et al., 2019b).

Surfaces of compressed tablets prepared with nanoparticles at  $\text{pH } 3$  with a ratio of 70:30 and 50:50 had a contact angle of  $82^\circ \pm 2.0$  and  $67^\circ \pm 3.0$ , respectively. This indicates that the nanocomplexes are neither extremely hydrophobic nor hydrophilic, which is suitable for being used as a Pickering stabilizer (Zou et al., 2015). Moreover, the results revealed that by increasing the proportion of mucilage in the nanoparticles, the value of  $\theta_w$  decreased. The contact angle of SFM was



around  $28^\circ \pm 2.0$  which shows its hydrophilic nature. Dai et al. (2018) had similar results for zein-arabic gum complexes, where the presence of gum in the zein particles also decreased the contact angle: the  $\theta_w$  value of zein-AG particles at a mass ratio of 1:1 was  $89^\circ$  while this value was above  $90^\circ$  for the plain protein, which is not suitable for the stabilization of oil-in-water emulsions. In another study, Sedaghat Doost et al. (2019b) reported that whey protein-almond gum complexes had a contact angle of  $58^\circ$  indicated that the surface of the complexes was partially wetted by water droplets. Thus these complex particles were not primarily hydrophobic or hydrophilic and suitable for Pickering stabilization of emulsions.

### **2.3.9. Interfacial tension**

The most important step in the formation of emulsions is the adsorption of molecules at the oil-water interface. The time dependence of the interfacial tension ( $\gamma$ ) of the FP, SFM and complex particles at the tricaprylin oil-water interface is shown in Figure 2.7. The complex particles and SFP had a lower interfacial tension in comparison to SFM, which might promote a better interfacial adsorption (Sharma et al., 2015). The adsorption of complex particles at the oil-water interface caused a decrease down to  $8.6 \text{ mN.m}^{-1}$  in the interfacial tension. Interestingly, the formation of the nanoparticles by combination of FP and SFM had no significant influence on the interfacial tension changes of the protein. Humblet-Hua et al. (2013) reported that the interfacial tension at the n-hexadecane–water interface stabilized by ovalbumin-pectin complexes was the same as that of interfaces stabilized by plain ovalbumin while the complexes formed viscoelastic interfacial films with higher dilatational modulus. The same results were reported by Speiciene et al. (2007) for whey protein-chitosan complexes and Schmitt et al. (2005) for  $\beta$ -lactoglobulin-arabic gum complexes.

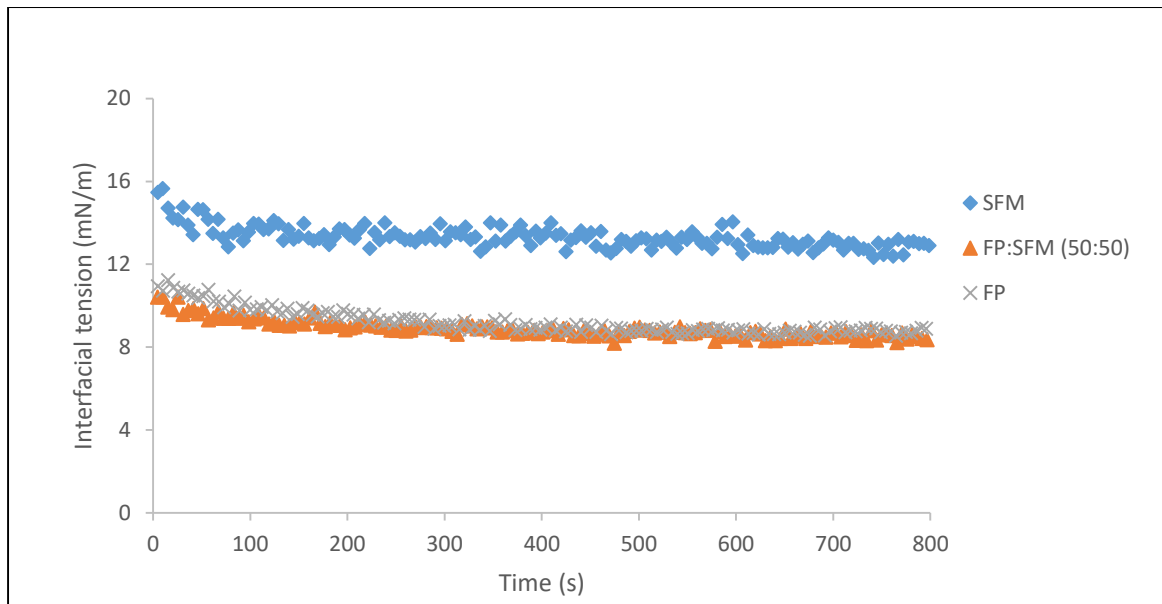


Figure 2.7. Interfacial tension variation at the oil-water interface of SFM, FP and FP-SFM particles at pH=3 ( $r= 50:50$ ,  $TC=0.45$  wt%).

### 2.3.10. Emulsion characterization

#### 2.3.10. 1. Effect of the FP to SFM ratio, total biopolymer concentration and oil volume fraction on droplet size distribution

The influence of FP to SFM ratio on the droplet size of emulsion was investigated to clear up the predominance and effectiveness of the size or contact angle of particles on the emulsion stability. As it is clear from Table 2.1, emulsions containing the 50:50 FP to SFM ratio had a smaller droplet size than the ones with 70:30 ratio and their droplet size was constant during 30 days of storage (Figure 2.8-a). However, a slight shift to bigger droplet size was observed in the droplet size distribution of the emulsions stabilized with the 70:30 ratio (data not shown). As it was mentioned before, the complex particles with FP to SFM ratio of 50:50 had a lower contact angle than those with 70:30 ratio, while the size of particles was smaller. Thus, it seemed that smaller particles are more effective to protect Pickering emulsions against flocculation, coalescence and instability. This effect was previously reported by Madivala et al. (2009) and Alargova et al. (2004) that

particles with different size can react in a different manner at the oil-water interface, resulting in a different oil droplet size.

Table 2.2. Mean z-average diameter ( $d_{43}$  and  $d_{32}$ ) values of tricaprylin Oil-in-water Pickering emulsions stabilized by complex particles with different FP to SFM ratio ( $r$ ), total biopolymer concentration (TC) and oil volume fractions.

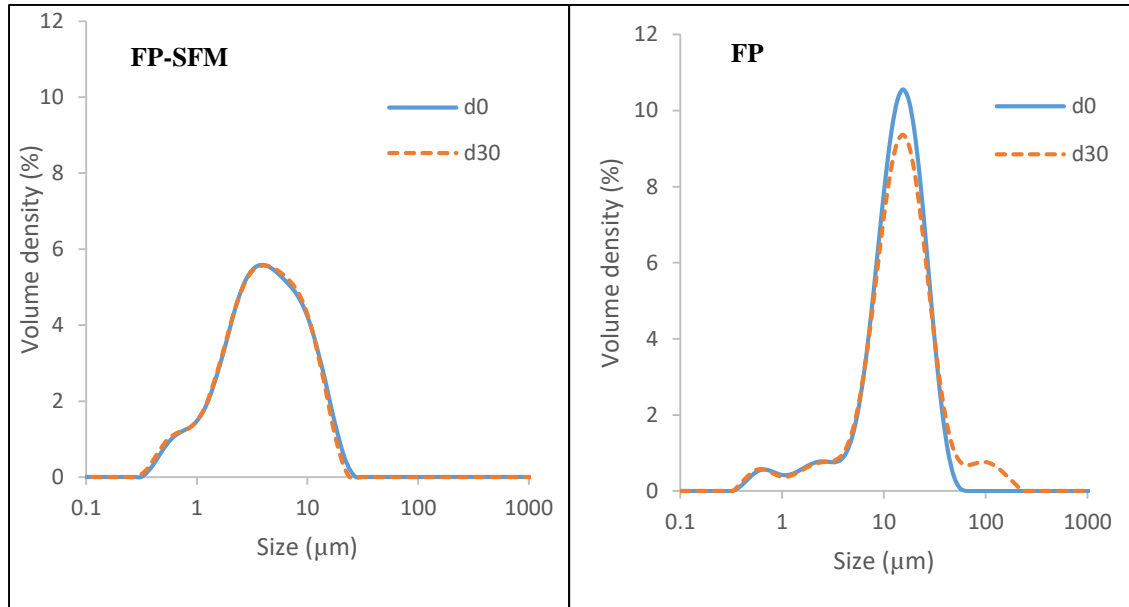
FP/SFM	TC	Oil (%)	Time (d)	$d_{43}$	$d_{32}$
<b>70:30</b>	0.4	2.5	0	$7.73 \pm 0.71$	$2.51 \pm 0.55$
<b>50:50</b>	5			$5.82 \pm 0.68$	$2.84 \pm 0.71$
<b>50:50</b>	0.1	2.5	0	$11.7 \pm 1.00$	$4.39 \pm 0.51$
	5			$8.78 \pm 0.99$	$3.31 \pm 0.72$
	0.3				
<b>50:50</b>	0.4	1.0	0	$4.75 \pm 0.43$	$1.84 \pm 0.34$
	5	5.0		$9.76 \pm 0.73$	$3.93 \pm 0.53$
<b>50:50</b>	0.4	2.5	30	$5.61 \pm 0.64$	$2.86 \pm 0.37$
	5				

Values are means  $\pm$  SD from triplicate repetitions.

In another series of experiments, the FP to SFM ratio and oil content was fixed at 50:50 and 2.5 wt% and the total concentration of particles was varied. The droplet size of emulsions stabilized with different particle concentrations is presented in Table 2.2. In all the three cases, an initial stable emulsion was obtained and the results showed that emulsions containing 0.15 and 0.3 wt% particles had a bigger oil droplet size in comparison to 0.45 wt%. Therefore, these two particle concentrations were probably insufficient to efficiently cover the emulsion droplets preventing the recoalescence of the droplets during the Pickering stabilization.

Moreover, at higher biopolymer concentration, the higher viscosity of the continuous phase could help the stabilization of oil droplets.

**a**



**b**

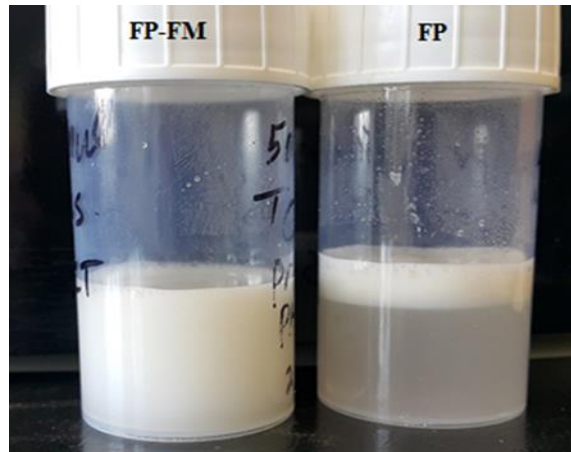


Figure 2.8.a) The size distribution of 2.5% o/w emulsion after preparation and 30 days of storage at pH 3 with the complex particles at FP to SFM ratio of 50:50, TC=0.45 wt% and the FP at a same condition and b) The visual appearance of the 2.5% o/w emulsion at pH 3 stabilized with the complex particles at FP to SFM ratio of 50:50, TC=0.45 wt% and the native FP stabilized emulsions prepared at a same condition 1 hour after the preparation.

The effect of the oil to water volume ratio at a fixed particle concentration (TC = 0.45 wt%) and FP to SFM ratio (50:50) was studied. As presented in Table 2.1, the emulsion containing 5% w/w tricaprylin oil had the biggest mean droplet size revealing that an insufficient number of particles was available to cover the

interfaces and to prevent the re-coalescence of the oil droplets during homogenization. The oil-in-water emulsion with 2.5% oil content was selected because there was no significant difference ( $p > 0.05$ ) between the droplet diameter of 1 and 2.5% O/W emulsions. Besides, from an application point of view, stable emulsions with high oil content are desired.

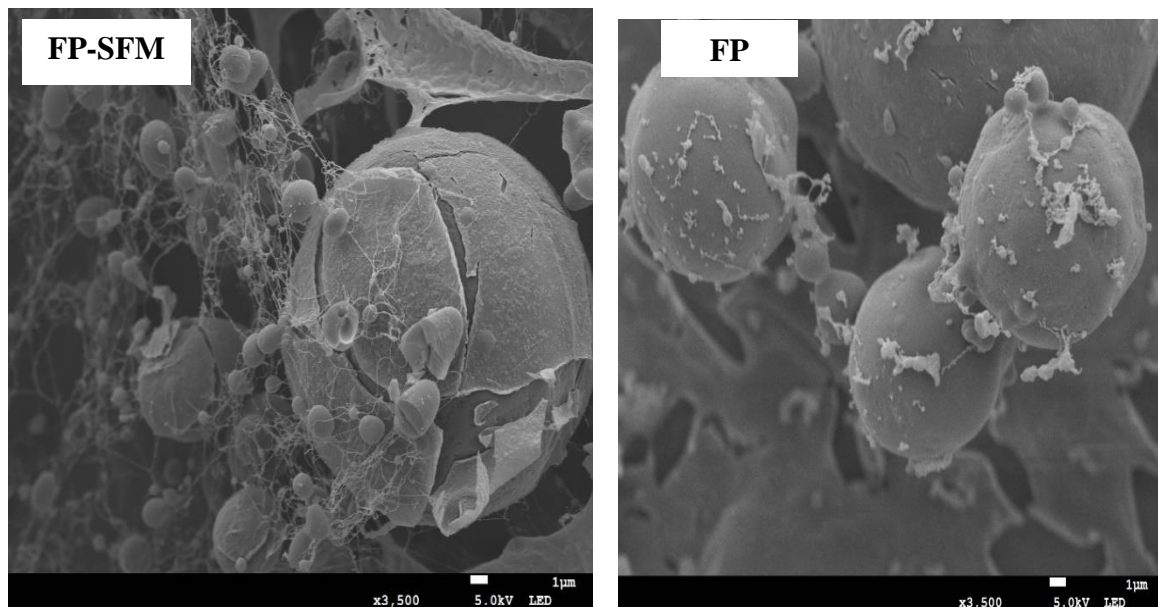
The dispersion containing 0.45 wt% complex particles with FP to SFM 50:50 ratio and an oil volume fraction of 2.5 wt% at pH 3 was selected according to the above discussion. The average size of the emulsion droplets was 5-6  $\mu\text{m}$  after preparation with no creaming or sedimentation (Figure 2.8-b). The droplet size distribution of this Pickering emulsion showed that there was no increase in oil droplet size. However, the protein particles at the same concentration (0.225 wt%) and pH formed an emulsion with larger droplet size (Figure 2.8-a,b). This was due to the fact that at pH 3, which is close to the pI of the FP, aggregation occurs between the protein particles.

The flocculation and coalescence indices (FI and CI) of FP-SFM stabilized emulsions with FP to SFM ratio of 50:50 and TC= 0.45 wt% were not significantly different from zero (i.e.  $-0.7 \pm 12.0$  and  $-3.1 \pm 9.6$ , respectively). However, these values were  $14.7 \pm 1$  and  $4.7 \pm 0.1$  for the emulsion, which was stabilized by FP only. These observations indicated that for the both FP and complex stabilized emulsions the flocculation of oil droplets played the chief role in the instability and for the complex stabilized emulsion no coalescence occurred. These results are in line with the size measurement of droplets during the 30 days of storage (Figure 2.7-a).

### 2.3.10.2. Microstructure evaluation

The microstructure of Pickering emulsions containing 2.5 wt% oil stabilized by FP-SFM nanoparticles (TC = 0.45 wt%) and protein only at pH 3 was evaluated by Cryo-SEM and CLSM. As can be seen in Figure 2.9-a, the globular FP which interacted with fibrous SFM anchored onto the oil-water interface and triggered the stabilization of the emulsion. The oil droplets are surrounded by the nanoparticles, which also provide steric hindrance to the coalescence of droplets. It is clear that there was an intramolecular interaction between mucilage and protein at pH 3 which is consistent with the results of Le and Turgeon (2013) that it is possible to have intramolecular interactions between protein aggregates and polysaccharide at  $\text{pH} \geq \text{pI}$  of protein. Figure 2.9-a also represents the SEM photographs of FP stabilized emulsions.

a



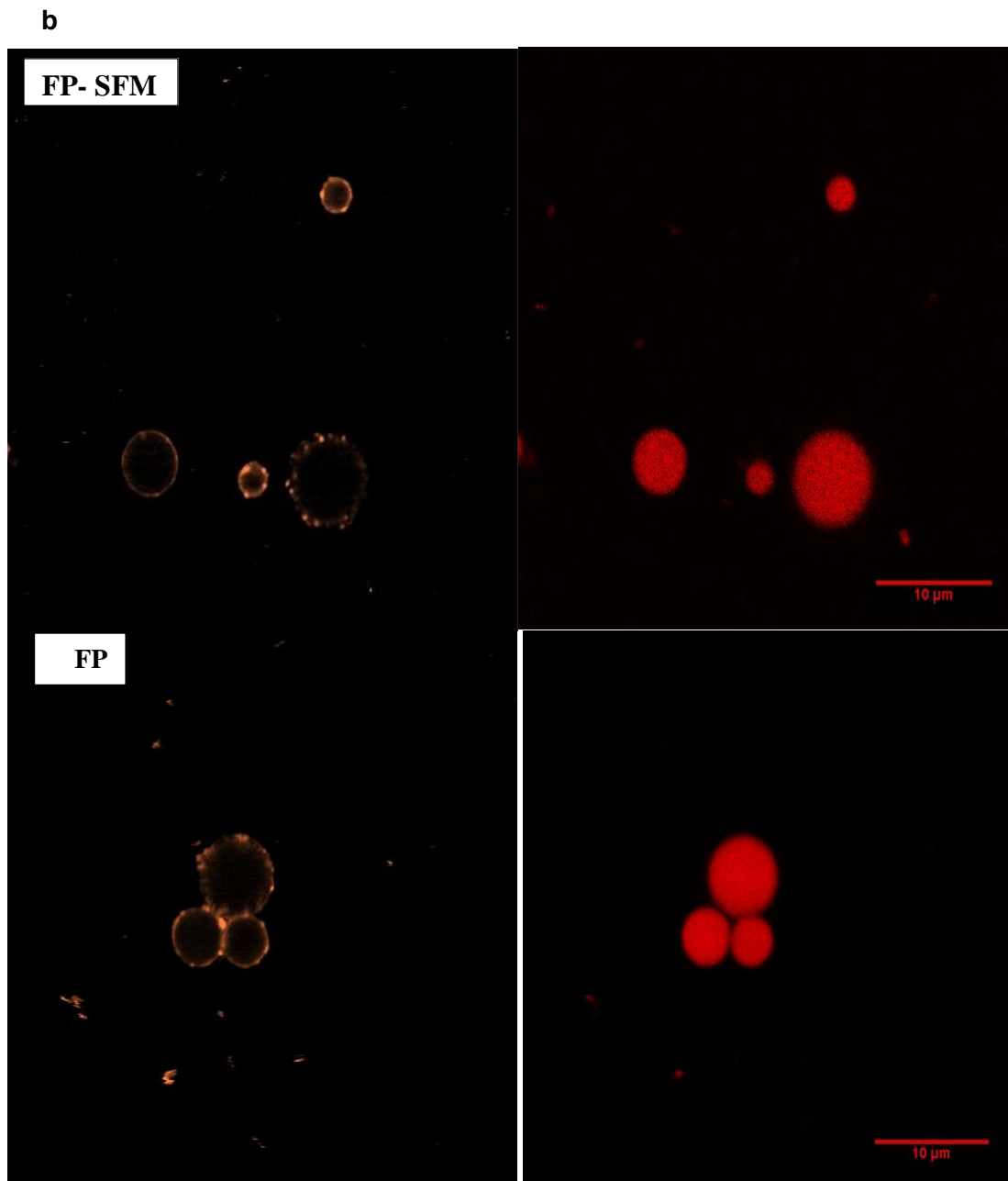


*Figure 2.9. a) Cryo-SEM and b) confocal images of the FP-SFM and FP particles responsible for the stabilization of oil droplets in an emulsion containing 2.5 wt% tricaprylin oil and 0.45 wt% complex nanoparticles at pH 3.*

The CLSM micrographs presented in Figure 2.9-b show that the aggregation of FP particles is associated with the flocculation of oil droplets in FP stabilized emulsion while no aggregation and flocculation of particles or oil droplets was observed for FP-SFM particle stabilized emulsion. The presence of SFM at pH 3 prevents the aggregation of FP particles. Moreover, the formation of an interfacial and surrounding architecture around oil droplets can be a confirmation of O/W Pickering emulsion. In both FP and complex particle stabilized emulsions the oil

droplets were covered with a Rhodamin-B fluorescent layer which is an indicator for the adsorption of protein-containing particles on the interface which is in line with the results of interfacial tension measurements. The uniform and compact formed interface layer by complex particles around oil droplets provide a strict barrier against flocculation and coalescence for the Pickering emulsions.

The pictures showed that when the FP only was used as an emulsifier, strong red fluorescence signals were floating around in the continuous phase of the emulsion. This could be an evidence that electrostatic interaction between FP and SFM due to the prevention of aggregation facilitated the accumulation of the particles around the oil droplet. On the other hand, it could be possible that larger structures in FP due to the aggregation are larger to see as independent particles in comparison to the complex particles.

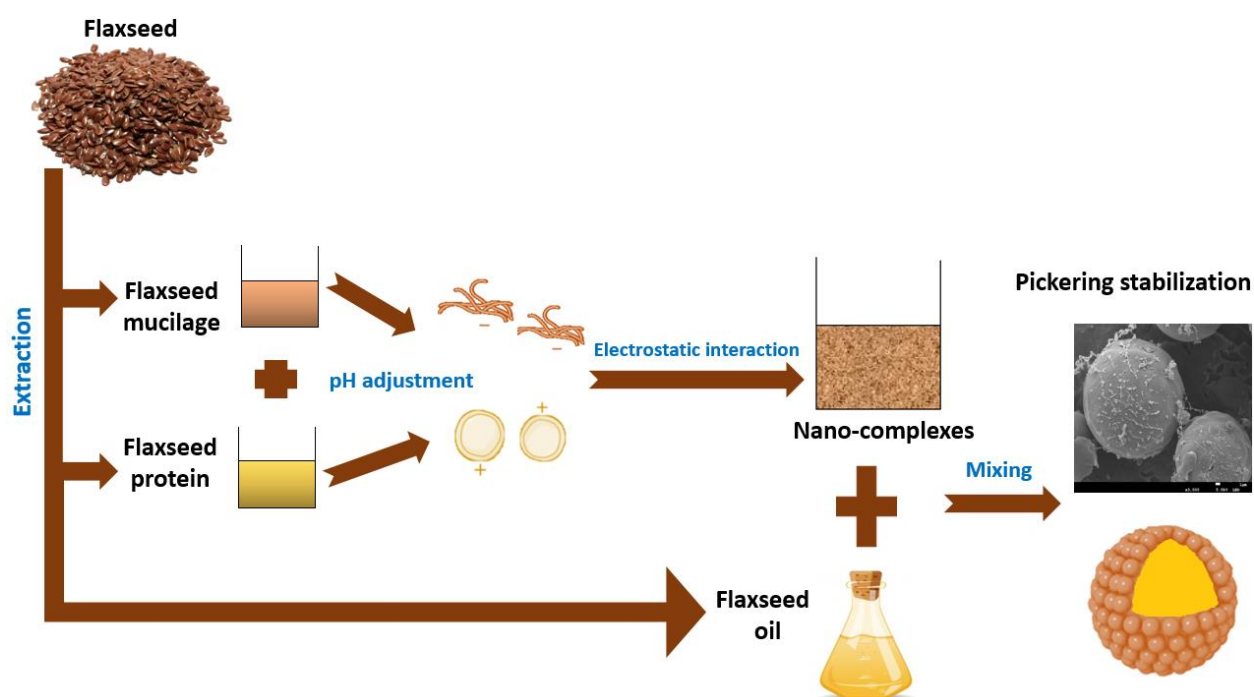


## **2.4. Conclusions**

Based on our results, the formation of complex nanoparticle consisting of FP and the soluble portion of flaxseed mucilage is possible at a wide pH range with no precipitation. It can be concluded that the electrostatic interaction between FP and the SFM can prevent the aggregation and further precipitation of the protein at and around its isoelectric pH, which can solve the solubility problem at this pH. The SFM binding decreased the electrostatic repulsion between the FP molecules and the anionic mucilage formed electrostatic bridges between cationic patches on the protein. The soluble complexes can provide an electrostatic repulsion in addition to the creation of a steric protective layer around the oil droplets. Furthermore, these soluble complexes are able to decrease the interfacial tension and have a higher rate of adsorption on the oil droplet surface due to their smaller size in comparison to insoluble complexes. Considering the fact that the emulsion cannot be stabilized properly with FP around its pI, it can be concluded that adsorbing FP-SFM complex nanoassemblies onto the interface introduces a protecting coating resisting flocculation and coalescence. The results suggest that FP-SFM complex nano-assemblies exhibit a good potential as a food-grade and plant based Pickering stabilizers for surfactant free oil-in-water emulsions even at acidic pHs.



## Chapter 3: Bioparticles of flaxseed protein and mucilage enhance the physical and oxidative stability of flaxseed oil emulsions as a potential natural alternative for synthetic surfactants



### Redrafted from:

**NIKBAKHT NASRABADI, M.,** GOLI, S. A. H., SEDAGHAT DOOST, A., DEWETTINCK, K., & VAN DER MEEREN, P. 2019. Bioparticles of flaxseed protein and mucilage enhance the physical and oxidative stability of flaxseed oil emulsions as a potential natural alternative for synthetic surfactants. *Colloids and Surfaces B: Biointerfaces*, 184, 110489.

# Abstract

Flaxseed protein (FP) and mucilage (FM) complex bioparticles as sustainable ingredients were assembled by electrostatic interaction for plant-based Pickering stabilization of flaxseed oil (FO)-in-water emulsions. The effect of FO content (1 - 5 wt%) on droplet size and accelerated creaming stability of the emulsions was evaluated. 2.5 wt% FO emulsion had the smallest initial droplet size ( $D[4,3] = 8 \mu\text{m}$ ) and creaming velocity ( $2.9 \mu\text{m/s}$ ). The microstructure of the emulsions was observed using Cryo-SEM, confocal and optical microscopy, showing a thick layer of the particles on the oil surface responsible for the stabilization. The physical stability of FO emulsion stabilized by complex bioparticles was higher against various environmental stress conditions (pH, salt and temperature) compared to plain FP- and polysorbate 80-stabilized emulsions. For instance, the droplet size of FP-stabilized (pH 3) emulsion increased from 21 to 38  $\mu\text{m}$  after thermal treatment (80 °C) whereas particles stabilized emulsion had a negligible increase in its size distribution. The latter emulsion also remained stable during 28 days of storage and it displayed good stability against a wide range of pH (2-9) and salt concentration (0-500 mM) with no sign of instability and oiling-off. The complex particles as Pickering emulsifiers were successful to depress the FO oxidation at 4 °C and 50 °C. This study could open a promising pathway for producing natural and surfactant-free emulsions through Pickering stabilization using plant-based biopolymer particles for protecting lipophilic bioactive components.

### 3.1. Introduction

Flaxseed (*Linum usitatissimum* L.) oil (FO), also known as linseed oil, is a vegetable source of polyunsaturated fatty acids (PUFA), especially alpha linolenic acid ( $\omega$ -3 fatty acid) (Liang et al., 2017a). The consumption of FO is associated with prevention of various diseases such as cardiovascular diseases, incidence of obesity, and cancer (Liang et al., 2017a, Shim et al., 2014). Despite its health benefits, FO is susceptible to oxidation and has a low water solubility with a low intake (the recommended intake worldwide is 250 mg/d) (Lemahieu et al., 2015). Thus, it is necessary to find an appropriate delivery system for FO to enrich food products. Most of the previous encapsulations of FO were based on spray-drying (Gallardo et al., 2013, Tonon et al., 2011, Carneiro et al., 2013). However, the high temperatures needed for drying may cause oxidation (Kolanowski et al., 2006). A straightforward approach is to incorporate FO within an emulsion-based system. Synthetic surfactants are widely used for forming and stabilizing conventional emulsions which may cause taste alteration and even health hazards (Benetti et al., 2019). Therefore, researchers are keen to find appropriate natural alternatives especially plant-based ones which are biodegradable, environmental friendly, biocompatible, sustainable and cheap (Zhu et al., 2019b, Ladjal Ettoumi et al., 2016).

More recently, particle-stabilized emulsions known as Pickering emulsions provide a new strategy for encapsulation and transport of lipophilic bioactive components and drugs in food and pharmaceutical applications (Harman et al., 2019, Sufi-Maragheh et al., 2019, Liu et al., 2019). These surfactant-free emulsions have superior stability, especially against coalescence, Ostwald ripening and changes to processing conditions (pH, salt, and temperature) in comparison to conventional

emulsions (Schröder et al., 2018b, Lam et al., 2014, Wu et al., 2015). Moreover, the adsorbed particles at the interface can provide a strong physical and chemical barrier against interacting pro-oxidants in the continuous phase and the surface-active lipid hydroperoxides at the interface (Kargar et al., 2012, Wang et al., 2015). The formed thick interfacial layer could improve the oxidative stability of O/W emulsions (Kargar et al., 2012). For instance, it is also reported that zein-chitosan complex particles were successful to improve the oxidation stability of the stabilized Pickering emulsion due to the formation of a protective barrier at the interface (Wang et al., 2015).

The aim of this work was to fabricate physically and chemically stable flaxseed oil-in-water Pickering emulsions using FP-FM complex bioparticles. First, FP and FM were extracted and characterized and then complex FP-FM particles with appropriate size and contact angle were assembled based on the results obtained in chapter 2. Pickering emulsions were characterized by particle size distribution, accelerated creaming stability, Cryo-SEM and confocal laser scanning microscopy. The stability of the emulsions under environmental stress conditions such as variations in pH, salt concentration, or temperature was determined. The physical and oxidative stability of FO-in-water Pickering emulsions was also monitored during 28 days of storage. The effectiveness of natural and plant-based FP-FM particles was compared with polysorbate 80 (PS 80). Polysorbate 80 is a synthetic food-grade surfactant that finding an appropriate alternative for this emulsifier is highly encouraged due to its health concerns (Sedaghat Doost et al., 2018a).

## **3.2. Materials and methods**

### **3.2.1. Materials**

Flaxseed oil were purchased from a local market in Isfahan, Iran. the rest of the materials details are given in section 2.2.1.

### **3.2.2. Extraction and characterization of flaxseed mucilage and protein**

Flaxseed mucilage and protein were extracted and characterized based on the methods given in sections 2.2.2, 2.2.3 and 2.3.

### **3.2.3. Preparation of complex particles**

FP and FM stock solutions (0.5 weight (wt) %) were separately prepared in Milli-Q water and were stored at 4 °C overnight for complete hydration. The FP-FM complex particles were assembled at pH 3 with a protein to polysaccharide ratio (r) of 50:50 and total concentration (TC) of 0.45 wt% section 2.4.

### **3.2.4. Fabrication of Pickering emulsions**

Flaxseed oil-in-water emulsions (1, 2.5, 5 wt%) were prepared by homogenizing the particle dispersion (0.45% w/v) at pH 3 using a high shear blender (Ultra-Turrax 50N-G, IKA®-Werke, Germany) for 5 min at 24000 rpm. For the sake of comparison, FP-stabilized (0.225% w/v) emulsions (FPFOE) and polysorbate 80-stabilized emulsions (PS80) were prepared in a same manner with the selected FO content and 0.45% w/v PS 80 concentration.

### **3.2.5. Pickering emulsion characterization**

#### **3.2.5.1. Droplet size distribution**

The droplet size distribution of the emulsions was measured immediately after emulsification and during 28 days of storage using the method given in section 2.8.1. The refractive index of the dispersed phase and of water as continuous phase was taken as 1.48 and 1.33, respectively whereas the imaginary refractive index was assumed to be 0.01.

### **3.2.5.2. Accelerated creaming stability**

The accelerated creaming stability of the emulsions containing different oil phase content (1, 2.5 and 5 wt% FO) was investigated using a LUMIfuge<sup>®</sup> 116 particle separation analyzer (LUM GmbH, Germany). 0.4 ml of the emulsions was poured into a polycarbonate cell. The sample within the cell was exposed to a centrifugation force of 1147 g for 1 h at room temperature (25 °C) during which the device recorded the light transmission through the sample and the movement of the emulsion droplets as a function of sample height in the test tube. The creaming velocity was calculated using front tracking data analysis according to Sedaghat Doost et al. (2017).

### **3.2.5.3. Microstructure characterization**

The morphology and microstructure of FO emulsions stabilized by complex nanoparticles at pH 3 was visualized using a Cryo-SEM JSM-7100 (Jeol Europe, Belgium) as explained in section 2.8.2.

CLSM (Leica TCS-SP5, Germany) was also applied for the microstructure characterization (section 2.8.2.).

Photographs of the Pickering emulsions stabilized by complex particles and plain FP at pH 3 were acquired using a light microscope (Olympus-CX40, Hamburg, Germany) connected to an Axiocam ERc5s camera (ZEISS, Germany).

### **3.2.6. Influence of stress conditions**

The stability of FO Pickering emulsions (FOEs) was evaluated by measuring the droplet size and visual appearance of emulsions before and after exposure to different pH, ionic strength, and temperature conditions. The evaluation was performed by comparison with plain FP stabilized emulsions (FPFOE) and a



reference conventional FO emulsion stabilized with polysorbate 80 as a commonly used surfactant (PS80).

To evaluate the effect of pH, the fresh emulsions were adjusted to pH 2, 3, 5, 7 and 9 using 0.1 M NaOH or HCl. Moreover, emulsions were diluted (1:1; v/v) with sodium chloride solution to provide a final salt content of 0, 125, 250 and 500 mM. In addition, emulsions were incubated at different temperatures (20, 40, 60 and 80 °C) in a water bath for 30 min covered by aluminium foil and cooled down to room temperature (25 °C) under running tap water. The stability of these stressed emulsions was evaluated during 7 days of storage at room temperature (25 °C) in a dark place.

### **3.2.7. Lipid oxidation determination**

Two series of fresh samples were placed in sealed screw cap glass tubes and stored up to 30 days in a refrigerator at 4 °C and in an oven at 50 °C. For this purpose, Pickering emulsion (FOE), polysorbate 80-stabilized emulsion (PS80) and bulk flaxseed oil (FO) were selected as treatments. Emulsions were sampled every 7 days and the amount of primary lipid oxidation products (lipid hydroperoxides, LH) was measured using the iodometric method and the secondary products (malondialdehyde, MDA) were also measured using TBARS assay.

#### **3.2.7.1. Iodometric assay**

LH content was determined as peroxide value (PV) through a modification of the method in the norm UNE 55-023 (Atarés et al., 2012). 2 g emulsion (2.5% FO) or 50 mg bulk oil was dissolved in 20 ml of a 3:2 (v/v) mixture of glacial acetic acid and isooctane in a 250 ml Erlenmeyer flask and was stirred well for 30 s to break the emulsion. 500 µl of saturated potassium iodide (KI) solution was added. After

1 min vigorous shaking, 30 ml water and 500 µl of 1% (w/v) starch as indicator was added and titration with 0.002 M sodium thiosulfate ( $\text{Na}_2\text{S}_2\text{O}_3$ ) solution was performed until the blue/purple color disappeared. The PV was calculated according the following equation;

$$\text{PV (mEq of oxygen/kilogram of sample)} = (\text{S} - \text{B}) \times \text{N} \times 1000/\text{W}$$

where, S is the volume of  $\text{Na}_2\text{S}_2\text{O}_3$  used by sample, B is the volume of  $\text{Na}_2\text{S}_2\text{O}_3$  used by blank, N is the normality of  $\text{Na}_2\text{S}_2\text{O}_3$  solution, and W is the sample mass (g).

#### **3.2.7.2. Thiobarbituric acid reactive substances assay (TBARS)**

The TBARS method was used to measure the MDA content to monitor the secondary oxidation products in emulsions according to the method described by Atarés et al. (2012) with some modifications. 0.1 ml emulsion was mixed with water up to 1 ml and mixed with 2 ml TBA solution which was prepared by dissolving 0.375 g of TBA (0.375% w/v) and 15 g of TCA (15% w/v) into 100 mL of 0.25 M HCl. Then the mixtures were kept in boiling water for 15 minutes and subsequently were cooled to room temperature with tap water. Afterwards, the obtained mixtures were centrifuged at 4000 rpm for 30 minutes and the supernatant was collected. Finally, the resultant MDA-TBA chemical compounds were detected by recording the absorbance using a UV-visible spectrophotometer (VWR, Belgium) at 532 nm against TBA solution. The MDA content was calculated from a standard curve made from 1, 1, 3, 3-tetraethoxypropane.

#### **3.2.8. Statistical analysis**

Statistical tests as described in section 2.9.

### 3.3. Results and discussion

#### 3.3.1. FO Pickering emulsion

Based on our previous work, the assembled FP-FM complex particles at pH 3 with a protein to polysaccharide ratio ( $r$ ) of 50:50 and total concentration (TC) of 0.45 wt% were negatively charged with a zeta-potential value of  $-22.3 \pm 0.1$  mV. The z-average diameter and polydispersity index (PDI) of the complex FP-FM particles were  $369 \pm 5$  nm and  $0.31 \pm 0.02$ , respectively. Thus, the complex particles were relatively small and have enough surface charge to make them stable against aggregation and precipitation.

The partial wettability is another key factor for particle stabilizing emulsions, which benefits sufficient adsorption on the interface to provide efficient steric repulsion against coalescence. The results suggested that the FP-FM complex nanoparticles at the selected pH and ratio had partial wettability ( $\theta_w = 67^\circ \pm 3.0$ ) and since they can be wetted by both water and oil phases, have the ability to stabilize Pickering emulsions.

The fabricated emulsions were apparently homogenous and stable against oiling-off and phase separation. The volume-weighted mean diameter ( $D[4,3]$ ) of emulsions with different FO content and 0.45 wt% particle content as a function of time is shown in Figure 3.2. For fresh emulsions, the emulsion containing 2.5 wt% FO had the minimum droplet size while during storage, its droplet size increased so that it was marginally higher than the emulsion with 1 wt% FO. The size increased by increasing the FO volume fraction up to 5 wt% both directly after preparation, and also during storage. At higher FO content, there might have not been enough particles present to cover the oil droplets during homogenization and to prevent their recoalescence. It can be seen from Figure 3.1 that the PS80

emulsion contained smaller droplets than particle stabilized emulsions (FOEs). This is a logical consequence of the faster adsorption kinetics of small molecular weight emulsifiers. Moreover, polysorbate 80 was capable to decrease the oil-water interfacial tension properly which facilitated droplet break up. Although the size of the emulsions with 2.5 and 1 wt% FO did not have a significant difference during storage, the emulsion with 2.5 wt% oil was selected for further experiments due to the capability to encapsulate more FO. This oil volume fraction makes it easier to satisfy the recommended daily intake of  $\omega$ -3 fatty acids (57 wt% of FO fatty acids) which is 250 mg/d (Lemahieu et al., 2015), for which about 40 ml of 2.5 wt% emulsion is needed.

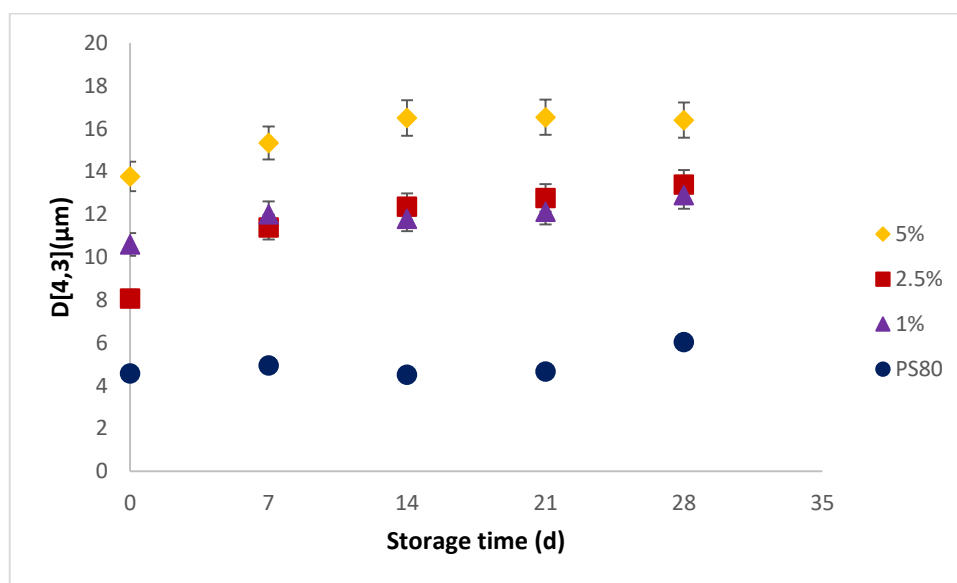


Figure 3.1. Volume-weighted mean diameter  $D[4,3]$  of flaxseed oil emulsions with different FO content (1, 2.5 and 5 wt%) and of a 2.5 wt % FO emulsion stabilized with 0.45 wt% polysorbate 80 (PS80) as a function of storage time.

The stability of the emulsions against creaming was investigated by an accelerated test using centrifugal photosedimentometry. In this method, creaming is accelerated as a result of centrifugation and the physical stability of the emulsions can be evaluated by monitoring the light transmission intensity. The slope of the

curve which shows the position of the interface between serum and cream phase during the centrifugation, displays the velocity of creaming. Comparing the creaming velocity of the Pickering emulsions, the emulsion with 2.5 wt% FO had a lower creaming velocity ( $2.91 \pm 0.03 \mu\text{m/s}$ ) than those with 1 wt% ( $3.11 \pm 0.02 \mu\text{m/s}$ ) and 5 wt% ( $5.6 \pm 0.08 \mu\text{m/s}$ ), respectively. The PS80 emulsion had the lowest creaming velocity among all of the studied emulsions ( $0.99 \pm 0.04 \mu\text{m/s}$ ). These accelerated creaming stability results were consistent with the droplet size measurements.

The emulsions remained stable with an almost constant droplet size during 28 days of storage and a relatively small creaming velocity. Therefore, the emulsion containing 2.5 wt% FO as the oil phase and 0.45 wt% FP-FM complex particles (r=50:50, pH= 3) as an emulsifier, was selected based on the droplet size and creaming velocity measurements for the further experiments in order to have the highest possible oil content without negative impact on the physicochemical stability.

### **3.3.2. Microstructure evaluation**

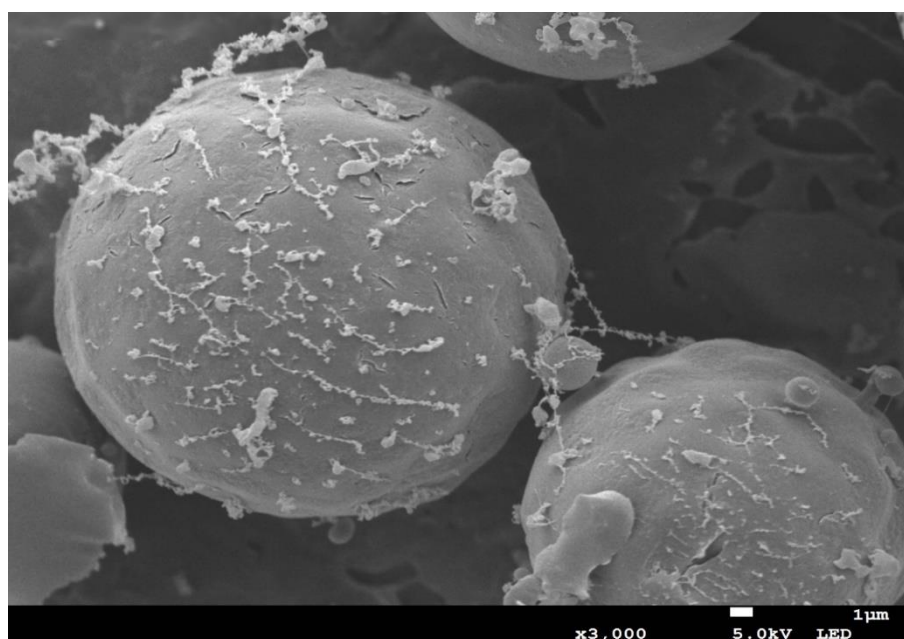
The microstructure and morphology of the 2.5 wt% FO Pickering emulsions stabilized with FP-FM complex particles was evaluated using Cryo-SEM and CLSM. The Cryo-SEM picture is displayed in Figure 3.2a which shows that the oil droplets were stabilized with adsorbed complex particles on their surface and confirms the droplet size measurements. It can be seen that the complex particles are anchored on the oil droplet surface which provides the Pickering stabilization against coalescence through steric and electrostatic repulsion.

Figure 3.2b shows a CLSM image of the 2.5 wt% FO Pickering emulsions where the biopolymer particles were stained with Rhodamin-B and FO was stained with

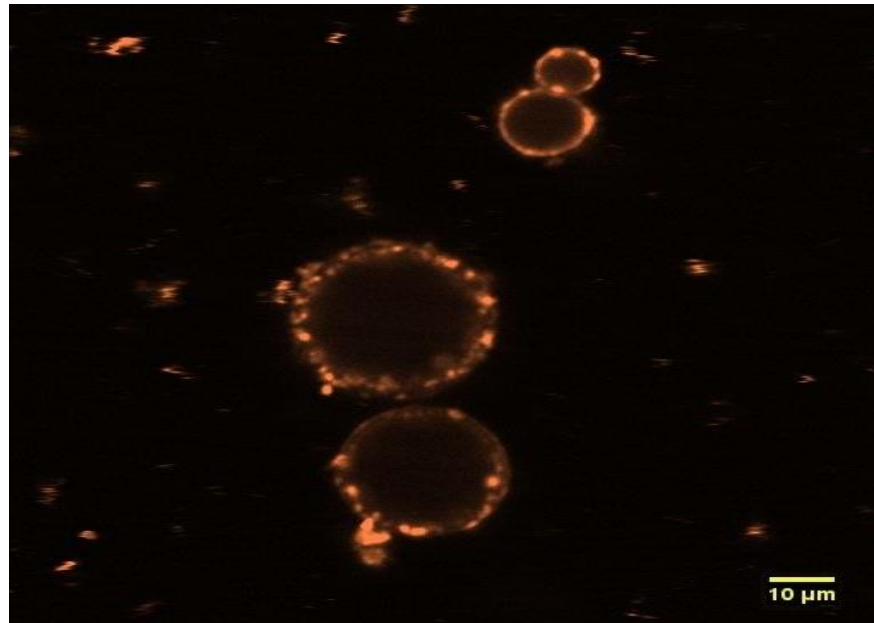
Nile red. The adsorption of the complex particles onto the oil-water interface and their coverage on the oil droplets for stabilizing the FO emulsion is clearly illustrated. The oil droplets are surrounded by the nanoparticles, which provide not only steric hindrance but also electrostatic repulsion to prevent aggregation and/or coalescence of the droplets.

The pictures obtained by optical microscopy from diluted 2.5 wt% FOE and FPFOE in Milli-Q water (1:10), are presented in Figure 3.2c. It can be seen from the picture taken of the FP-stabilized emulsion that the oil droplets were flocculated as a result of aggregation of the FP at pH 3 due to the lack of sufficient surface charge, which was not the case for FP-FM particle stabilized emulsions. These results are consistent with the results of droplet size measurements. Therefore, the complexation of FP with FM was successful in modulation of FP for preparing Pickering emulsifiers which should be able to stabilize emulsions against aggregation around the protein's pI.

**a**



**b**



**c**

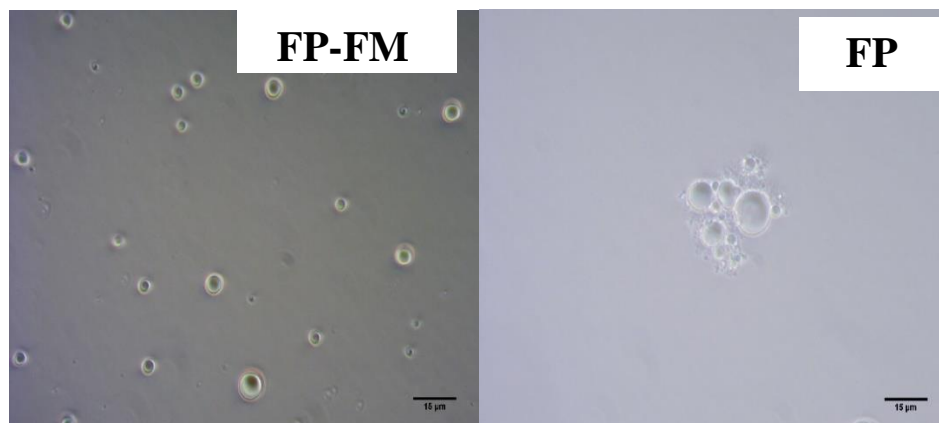


*Figure 3.2. a) Cryo-SEM and b) CLSM images of 2.5 wt% FO Pickering emulsion stabilized by complex FP-FM particles at pH 3. FO and FP-FM particles were stained by Nile red and Rhodamine B, respectively. c) Optical microscopic pictures of 2.5 wt% FO emulsions stabilized with FP-FSM complex particles and plain FP at pH 3 (scale bar: 15 μm).*

### **3.3.3. Influence of stress conditions**

As many foods may be subjected to undesirable conditions, such as processing, storage, transportation, and utilization, the selected FO Pickering emulsion (FOE) and PS80 type were subjected to different environmental stress conditions.

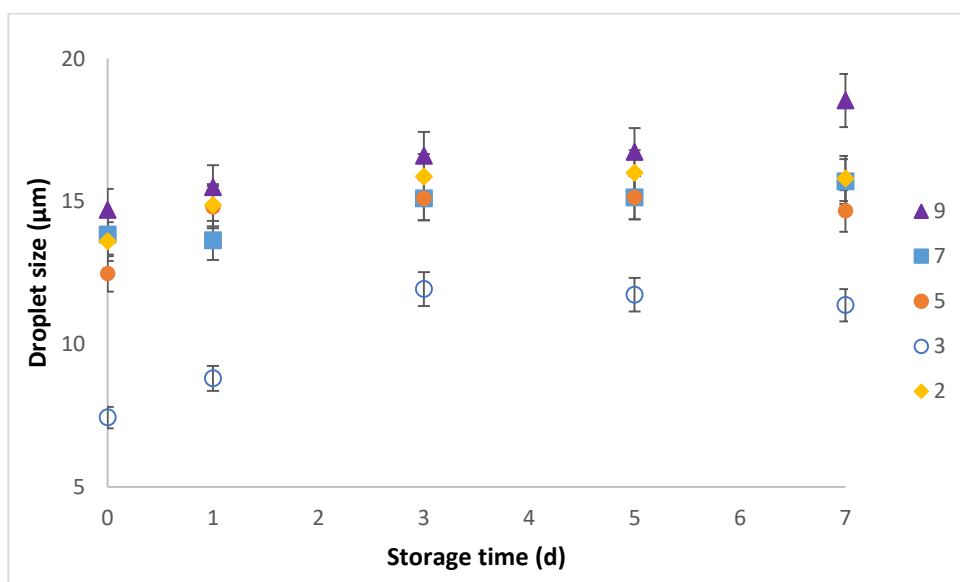
### **3.3.4. Effect of pH**

The droplet size of emulsions at different pH conditions was shown in Figure 3.3a. There was an increase in droplet size of the FO particle-stabilized emulsions at all the studied pH values in comparison to pH 3, which is the initial pH of the emulsion. As the results of our previous work suggested, based on the surface charge at higher pH values than 3.5, the FP is negatively charged. Therefore, due to the electrostatic repulsion between FP and FM, dissociation of complexes could occur. There is also dissociation of electrostatic complexes around pH 2 where both FP and FM carry positive charges due to the protonation of FM (Nikbakht Nasrabadi et al., 2019). The mean droplet diameter at pH 9.0 was slightly larger than at other pH values. The increased size at different pH conditions than pH 3 could be due to the aggregation. This aggregation at pH values including 5, 7 and 9 could be due to the depletion flocculation of the unadsorbed water-soluble polymer as well as bridging by weakly binding polymer binding to oppositely-charged groups on the protein since above the protein pI some positive patches are still present. Although the droplet size of the emulsions increased by changing the pH, the emulsions had a good stability because no breaking was observed in any of them. According to our previous study, at pH 3 the highest number of soluble complex particles were formed due to FP and FM self-assembly through electrostatic interaction (Nikbakht Nasrabadi et al., 2019). Therefore, the main purpose is to evaluate the stability at this pH. In our previous work, it was reported that the FP at pH 3, which is around its pI, due to the lack of sufficient surface charge, was prone to aggregation and



precipitation. It can be seen in Figure 3.3 that at ambient temperature the droplet size of the FP-stabilized emulsions at pH 8 was much smaller in comparison to pH 3; at these conditions, the negatively-charged adsorbed particles had sufficient surface charge to provide efficient electrostatic repulsion between the oil droplets. It is obvious that at other pH values far from its pI, protein would have a better performance as a result of sufficient surface charge and higher solubility (Ladjal-Ettoumi et al., 2016). Thus, it is not necessary to compare the stability of FP stabilized emulsions and complex-particle stabilized emulsions at different pH values. As polysorbate 80 is a non-ionic surfactant, pH did not have a significant effect on its emulsion droplet size (data not shown). This is in good agreement with previous work reported by Sedaghat Doost et al. (2017) who presented that the pH did not have a major influence on the physicochemical stability of emulsions emulsified using polysorbate 80 in the range of 3 to 7.

**a**



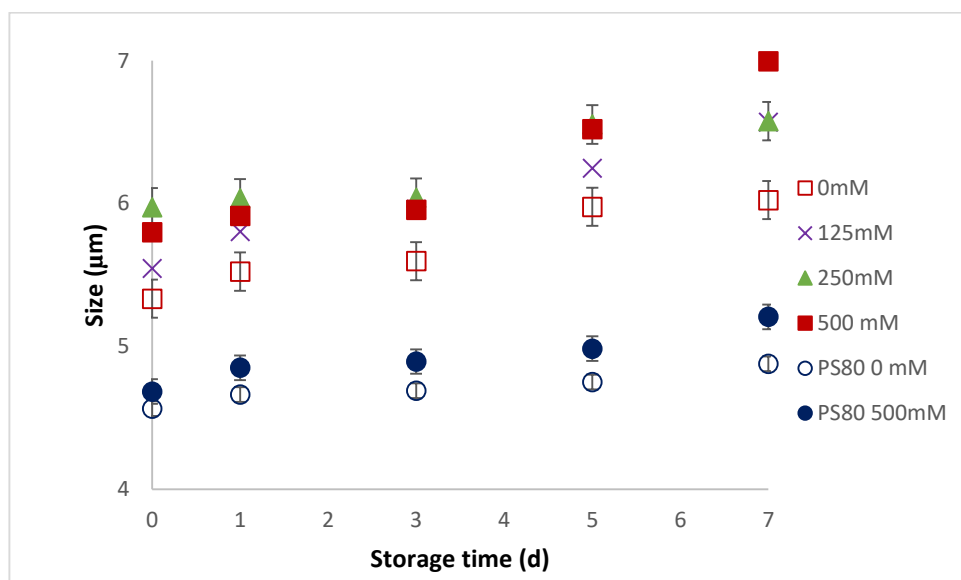
**b**

Figure 3.3. a) Effect of pH on the volume-weighted mean diameter ( $D[4,3]$ ) of the 2.5 wt% FO Pickering emulsion (FOE) during storage at ambient temperature (25 °C). b)  $D[4,3]$  of FOE and PS80 diluted (1:1; v/v) with deionized water (0 mM) or NaCl solution to provide a 500 mM salt content as a function of time at ambient temperature (25 °C).

### 3.3.5. Effect of ionic strength

Figure 3.3b depicts the droplet size of emulsions during 7 days of storage after dilution in a 1:1 (v/v) ratio with deionized water or NaCl solution to provide 0, 125, 250 and 500 mM salt concentrations, respectively. The observed differences in the droplet size of the FOE with 2.5 wt% FO presented in Figure 3.1 and the one displayed in Figure 3.3b as the FOE containing 0 mM salt, is due to the effect of dilution. It can be seen that both emulsions had a similar  $D[4,3]$  at the first day while during storage it became different. This could be due to the change in the interfacial tension after dilution. Although Pickering emulsions are mostly dependent on the size and contact angle of the stabilizing particles, the interfacial tension can be also affected by the size, contact angle and morphology of the particles (Tamayo Tenorio et al., 2017). It can be observed from Figure 3.3b that the  $D[4,3]$  of the emulsions increased in the presence of salt. For the Pickering emulsions, by

increasing the ionic strength the electrostatic repulsion between the oil droplets decreased which became more susceptible to flocculation and coalescence. This could be due to the fact that the added NaCl ions screen the charges of the adsorbed complexes, which according to our previous study (Nikbakht Nasrabadi et al., 2019) were negatively charged. Therefore, the electrostatic repulsion became less effective leading to flocculation (Ladjal Ettoumi et al., 2016). Another reason could be that increasing the ionic strength may lead to the breakage of complexes due to the decrease in the electrostatic interactions between the protein and polysaccharide. Thus, dissociation of some complex particles due to the weakened electrostatic interaction between FP and FM may occur. These findings were in agreement with the suggested results of Xiong et al. (2018) and Jones et al. (2010). However, the emulsions remained visually stable against oiling-off and phase separation with only a thin creaming layer at the top after the addition of salt during 7 days of storage. FP-FM particles prevent the droplet aggregation not only through electrostatic but also steric repulsion while polysorbate 80 stabilizes emulsions mainly through steric repulsion since it is a non-ionic surfactant (Sedaghat Doost et al., 2018b). Therefore, the latter emulsion is expected to have a stable droplet size upon increasing the ionic strength. As presented in Figure 3.3b, the  $D[4,3]$  of the PS80 stabilized emulsions after 7 days of storage did not have a significant difference ( $p > 0.05$ ) in the presence of salt in comparison to the absence of salt. In our previous work, it was displayed that FP was susceptible to pH since at and around its pI there was aggregation and precipitation due to the zero net surface charge and low solubility. It was shown that at pH 3 which was selected as the optimum pH for the assembly of complex particles, the FP had an unfavorable performance as a Pickering stabilizer in comparison to FP-FM

complex particles (Nikbakht Nasrabadi et al., 2019). Therefore, it would be expected that FP behave even worse in the presence of salt.

### **3.3.6. Effect of thermal treatment**

The effect of heat treatment on the stability of emulsions was investigated since food products are exposed to heat during their manufacturing, processing and storage. There was no change in the visual appearance of FOE and PS80 after exposure to any of the heat treatments (data not shown). There was no significant change in the droplet size of the PS80 and FOE at all the studied temperatures (Figure 3.4). Since at pH 3, there was aggregation and precipitation for the FP, it was not possible to investigate the effect of heat separately from pH on the stability of FP-stabilized emulsions. Therefore, the heat stability of FP emulsions was also evaluated at pH 8, which is the best pH for the electrosteric stabilization performance of FP due to the high negative surface charge and solubility. This provides the opportunity to evaluate the effect of thermal and pH stress conditions on the stability of the FP- and particle-stabilized emulsions independently. It can be seen in Figure 3.4 that at pH 3 at all the studied thermal treatments the droplet size of the emulsions stabilized with the FP were much higher than all other studied emulsions. At pH 8, the FP-stabilized emulsion had approximately the same droplet size as the particle stabilized emulsion up to 60 °C. This is due to the fact that globular proteins remain largely unaffected within this temperature region. By increasing the temperature of the thermal treatment to above the denaturation temperature of globular proteins (i.e. up to 80 °C), the volume-weighted average particle size of the FP-stabilized emulsion largely increased, even at pH 8 which is far from the FP pI, whereas the complex particles performed much better against this heat treatment. Therefore, the results revealed that the complexation with FM

was successful in modulation of the heat and pH susceptibility of the FP: electrostatic complexation of globular proteins with oppositely charged polysaccharides largely reduced their well-known heat sensitivity.

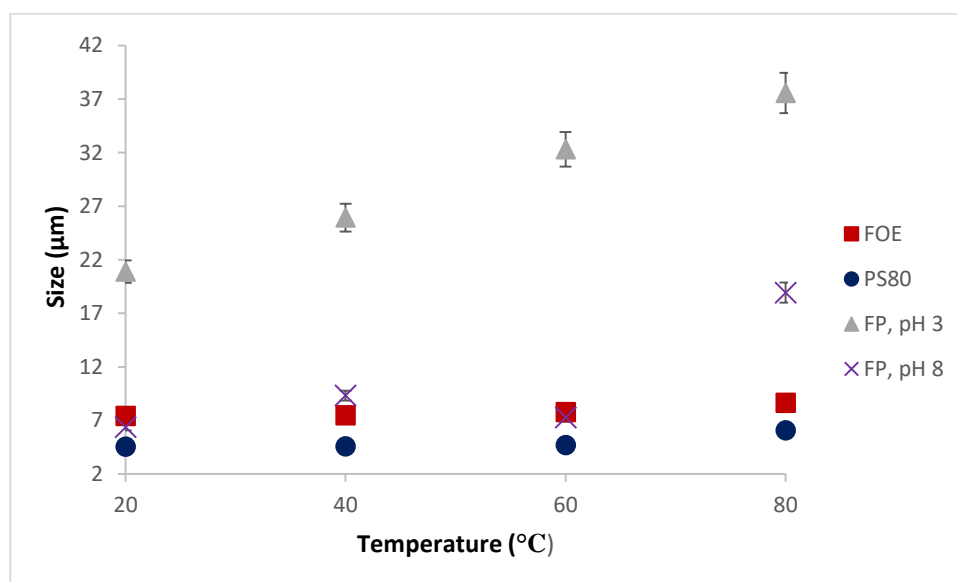


Figure 3.4. Effect of heat treatment on  $D[4,3]$  of 2.5 wt% FO O/W emulsions stabilized with either flaxseed protein (FP), complex particles (FOE) or polysorbate 80 (PS80) at different temperatures for 30 min.

### 3.3.7. Oxidative stability of FO Pickering emulsions

The oxidative status of the samples was assessed by monitoring the formation of primary and secondary products during 28 days of storage at two different storage temperatures as presented in Figure 3.5a,b. The content of lipid hydroperoxides (LH) as primary oxidation products gradually increased in bulk FO during 28 days of storage at 4 °C from 8 to 100 meq/kg oil, while it was more rapid especially during the first 7 days of storage at 50 °C. The LH content in Pickering FOE was significantly lower than in bulk FO at 4 °C and 50 °C at all the studied days except for the fresh samples. The initially higher content of LH in Pickering FOE could be due to the effect of the preparation and emulsification process on the oxidation of the FO (Figure 3.5a). The adsorption of complex FP-FM particles on to the O/W

interface provided a thick and compact protective layer around the FO droplets (Figure 3.2) against physical and chemical instability. The surrounding layer can behave as a physical and chemical barrier to pro-oxidants such as metals. It is consistent with the results of Yao et al. (2016) that the whey protein (WP)-arabic gum (AG) complex interfacial layer around conjugated linoleic acid (CLA) oil droplets could act as a barrier for isolating metals from LH which prevented the formation of free radicals. They also reported that the oxidative stability of CLA emulsions stabilized with complex particles improved in comparison to individual WP or AG stabilized emulsions due to its superior physical stability. Some other previous studies reported that complex particles including gliadin-chitosan (Zeng et al., 2017), zein-chitosan (Wang et al., 2015), and  $\beta$ -lactoglobulin-chitosan (Chang et al., 2018) in Pickering emulsions were successful to depress the oil oxidation in comparison to biopolymers such as proteins only. However, none of these particles was totally plant-based. Moreover, they used a cationic polymer, which might be thought to be more effective to prevent metal cation binding.

Particle stabilized emulsions at thermally accelerated conditions (at 50 °C) had a better oxidation stability in comparison to PS80. This could be due to the fact that complex particles can provide a thicker interfacial layer in comparison to polysorbate 80. Kargar et al. (2011) also reported that silica particle stabilized emulsions had a better oxidative stability than emulsions stabilized by small molecular surfactants (polysorbate 20). In another work they also suggested that food-grade particles (microcrystalline cellulose and modified starch) were able to reduce the rate of the oxidation (Kargar et al., 2012). They reported that the adsorbed particles at the interface reduced the contact between the oil droplets and the continuous phase which resulted in a reduction of the oxidation surface

area. It was also reported by Xiao et al. (2015) that the kafirin nanoparticle-laden interfacial due to a thicker interfacial barrier in comparison to polysorbate 80 was more successful to retard oil oxidation in the emulsion.

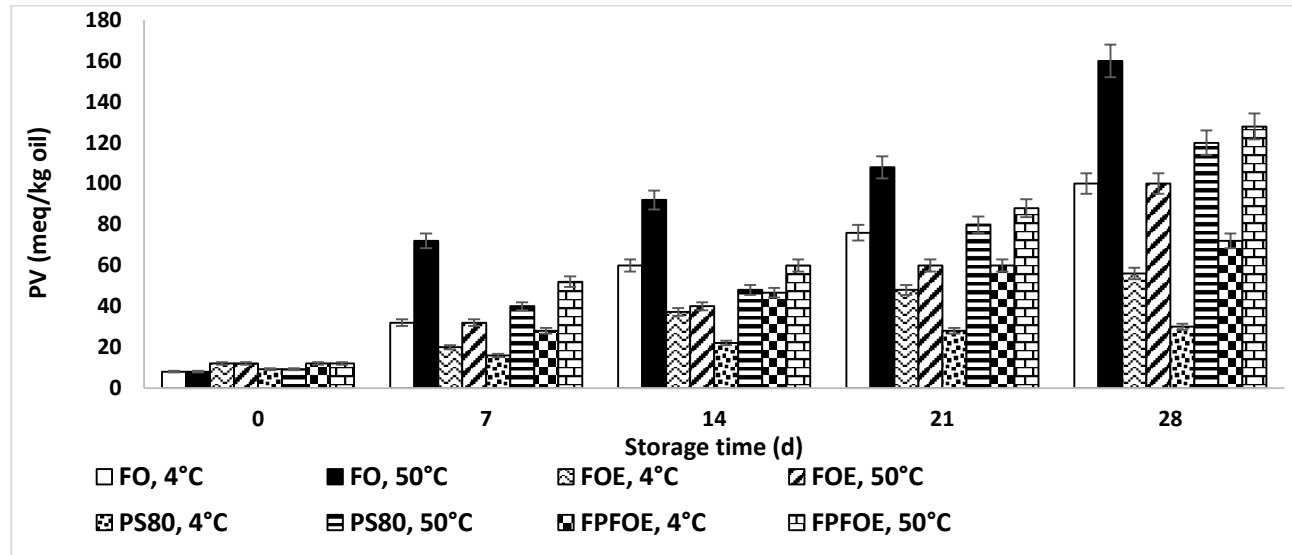
Moreover, the better oxidation stability of the Pickering FOE in comparison to PS80 could be due to its larger droplet size, hence having a smaller interfacial area. A smaller droplet size means a higher number of droplets and a larger contact surface between unsaturated lipids and prooxidant compounds such as metal ions which are dissolved in the aqueous phase. Furthermore, the larger interfacial area can increase the access of the oil phase to the dissolved oxygen in the aqueous phase (Berton-Carabin et al., 2014, Sedaghat Doost et al., 2019c). These results are in agreement with the suggested results of Xiao et al. (2015) who reported that PS80 emulsion due to its smaller droplet size and larger interfacial area had a severe oxidation compared to the Pickering emulsions stabilized by kafirin nanoparticles.

FP-stabilized emulsions had a higher LH content in comparison to FOE and PS80 during storage at both studied temperatures, which could be due to the inefficient anchoring of the FP particles as a result of their aggregation and precipitation at pH 3. At this pH, the protein particles were unsuccessful to stabilize the emulsion properly since they cannot adsorb to the interface efficiently and the adsorbed proteins also do not have the ability to provoke electrostatic repulsion between the oil droplets. Yi et al. (2019) reported that the adsorbed proteins to the interface were more effective in increasing the oxidation stability in comparison to non-adsorbed ones. However, the FPFOE had a better oxidation stability compared to bulk FO (Figure 3.5a). In fact, even unadsorbed proteins can interact with water soluble pro-oxidants and reagents including metal ions and free radicals. Proteins

as metal chelators have the ability to prevent that pro-oxidants reach the hydroperoxides located at the interface (Cheng et al., 2010, Berton-Carabin et al., 2014). It is reported by Silva et al. (2013) that FP had antioxidant and scavenging activity.



a



b

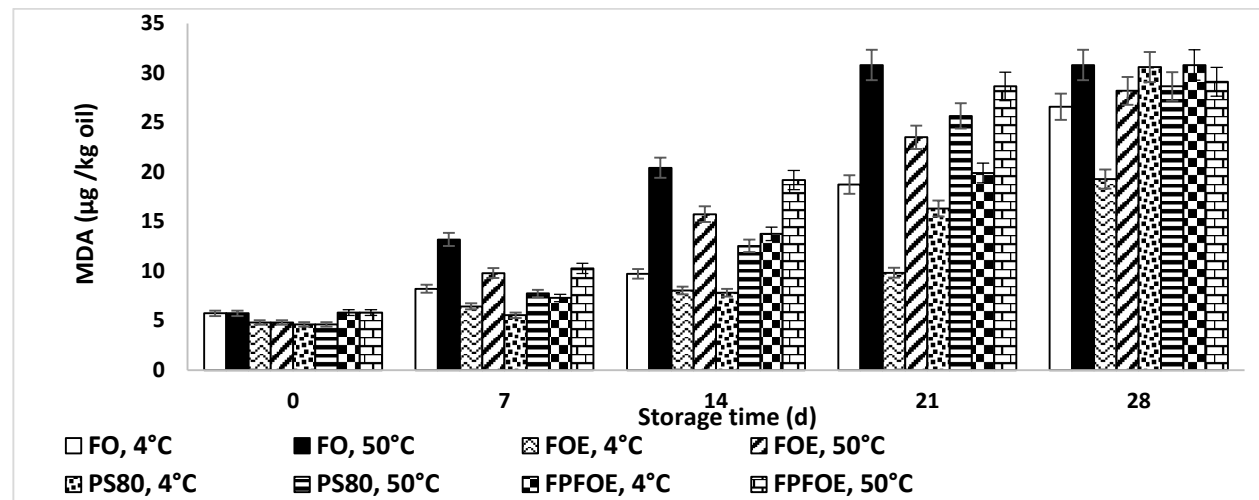


Figure 3.5. Influence of Pickering stabilization and storage temperature (4°C and 50°C) on a) peroxide values (PV, mEq of O<sub>2</sub> per kg of sample) and b) TBA values (µg malonaldehyde (MDA) per kg oil) of FO over 28 days of storage.

The MDA content as a secondary product of oxidation was monitored using the TBARS method which is displayed on Figure 3.6b. The MDA production rate at 50 °C is higher than at 4 °C for all the tested samples. The MDA content of FOE was lower than of bulk FO regardless of the temperature. Up to 21 days of storage at 4 °C, the MDA content of FOE and PS80 was similar while after this time the Pickering stabilization was more successful to retard the MDA formation.

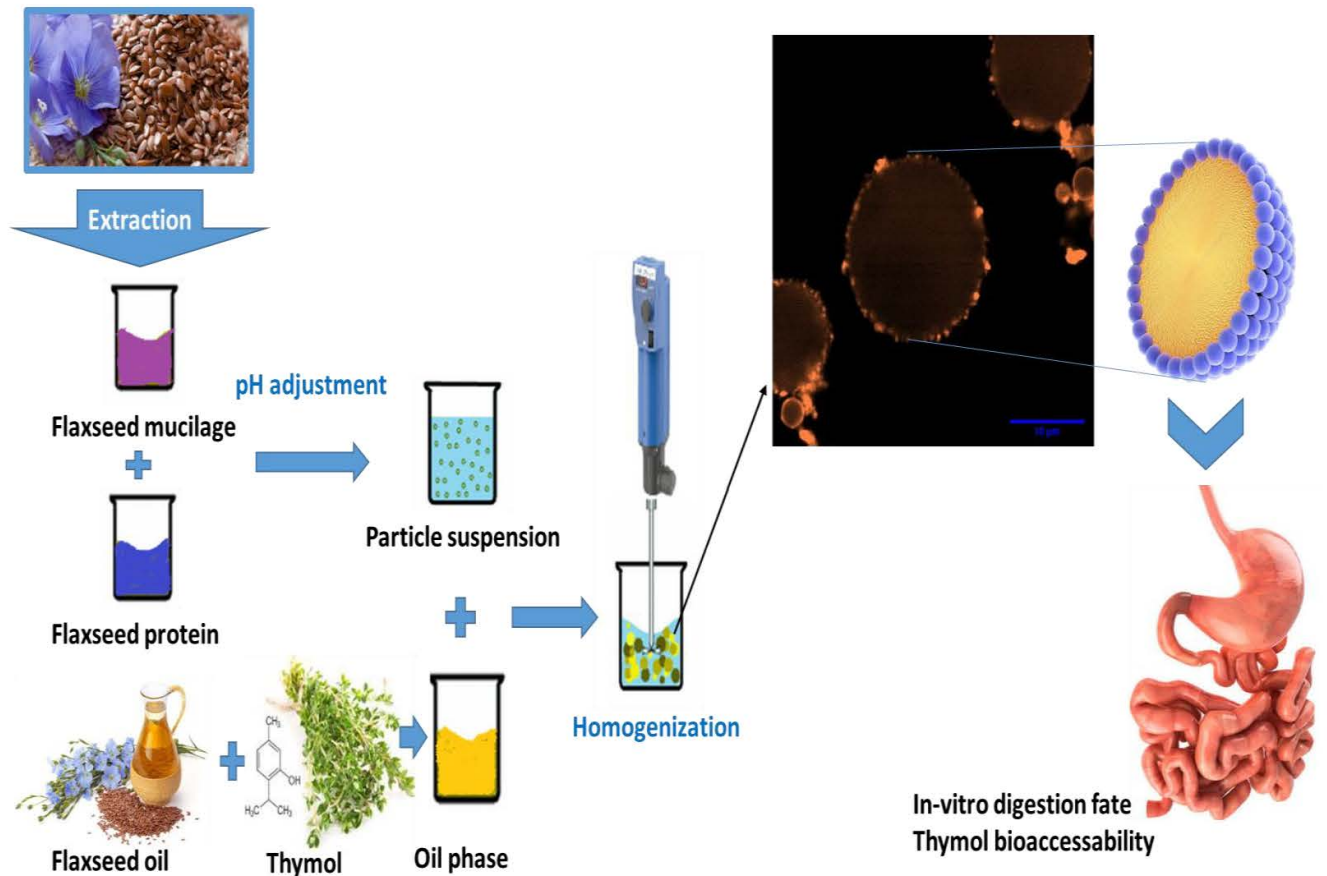
It is claimed that the droplet surface charge plays an important role on the oxidation process of emulsified oils since negatively charged droplets attract pro-oxidants such as metal ions, which are positively charged, to the interface. These metal ions at the interface accelerate the oil oxidation by LH decomposition (Liang et al., 2017a). Therefore, there are some reports that positively charged droplets due to the electrostatic repulsion between the pro-oxidants and the droplet surface have better oxidation stability (Zeng et al., 2017, Wang et al., 2015). In addition to the surface charge of the droplets, the interfacial thickness and composition are other important key factors that have an effect on the oxidation (Wang et al., 2015, Liang et al., 2017a). Thus, there are some reports which suggest that even negatively charged droplets with a thick and compact interfacial barrier can retard the oxidation (Chang et al., 2018). In our study, negatively charged FP-FSM complex particles depressed the production of both primary and secondary oxidation products compared to that in bulk FO due to the formation of a thick interfacial barrier against aqueous phase pro-oxidants.

## **2.10. Conclusions**

Complexation with polysaccharides can be used to improve the functionality of proteins, which are susceptible to pH, salt and temperature. The FP-FM complexes can be used as bioparticles for Pickering stabilization of FO emulsions. The complexation improved the heat stability of the FP-stabilized emulsions at 80 °C, which had a significant mean droplet size increase from 21 to 38 µm at pH 3, as there was a slight increase in mean droplet size of bioparticles stabilized emulsion with no sign of instability. The latter had also a reasonable physical stability against wide range of pH conditions (2-9) and salt concentrations (0-500 mM). Moreover, the oxidation stability of FO was increased in the Pickering emulsion form in comparison to the bulk oil. This was monitored by determination of PV and MDA content. The results suggested a lower PV and MDA content at the studied temperatures (4 and 50 °C) for bioparticles stabilized FO emulsion than bulk FO and FP-stabilized emulsion. Therefore, the results of this study suggested that the assembly of an interfacial architecture of the complex FP-FM particles around the FO droplets provides a good physicochemical stability in comparison to uncomplexed FP and to polysorbate 80 as a conventional synthetic surfactant. The information obtained in this study revealed that the complexation of FP with FM was successful to fabricate complex particulate stabilizers for FO emulsification. Moreover, the fabricated emulsions have the potential to be used as a delivery system for labile lipophilic bioactive components in food formulations.



# Chapter 4: Effect of thymol and Pickering stabilization on in-vitro digestion fate and oxidation stability of plant-derived flaxseed oil emulsions



## Abstract

The aim of this study was to evaluate the effect of bioparticle (consisting of flaxseed protein and polysaccharide) stabilization and addition of thymol on the oxidation stability and digestion fate of flaxseed oil (FO) emulsions compared to bulk FO and conventional emulsions stabilized by polysorbate 80 (PS80). Applying Pickering stabilization and thymol antioxidant simultaneously was a successful approach to retard FO oxidation. Lipid digestion was slower in complex particle stabilized emulsions compared to PS80 stabilized emulsions. The thymol bioaccessibility increased after incorporation into FO Pickering emulsions in comparison to the bulk oil. The results suggested that the combination of the Pickering stabilization and using dispersed thymol antioxidant in the oil phase can be used as a promising way of protecting highly unsaturated oils such as FO against oxidation. These emulsions are also applicable for designing functional foods with controlled lipid digestion to increase satiety and to reduce the incidence of obesity.



#### 4.1. Introduction

Flaxseed oil (FO) is a vegetable and sustainable source of  $\omega$ -3 fatty acids mainly  $\alpha$ -linolenic acid (ALA, 57% of total fatty acids), which is extracted from the flaxseed plant (also known as linseed, *Linum usitatissimum* L.). ALA has beneficial influences on the human health, including prevention of cardiovascular diseases (Bowen et al., 2016), immune and inflammatory disorders (Moura-Assis et al., 2018), and mental diseases such as depression (Pan et al., 2011), obesity and diabetes (Dátilo et al., 2018), and cancer (Bekhit et al., 2018). However, some of its properties may limit its utilization, including its hydrophobicity and susceptibility to oxidation (due to the high content of polyunsaturated fatty acids) leading to unfavorable off-flavors and odors as well as negating its nutritional and health benefits (Liang et al., 2017a). Therefore, this lipophilic bioactive oil needs to be incorporated into a colloidal delivery system to avoid the above-mentioned limitations (Bekhit et al., 2018, Shim et al., 2014).

Solid colloidal particles have been proven to be able to adsorb at oil-water interfaces to stabilize “Pickering emulsions” (Pickering, 1907b, Ramsden, 1903). These surfactant-free emulsions are believed to be less toxic and possess a higher stability against coalescence and Ostwald ripening in comparison to conventional emulsions (Sedaghat Doost et al., 2019b). For this purpose, there is a great demand for food-grade particles from natural resources, especially from plant-based origin due to their sustainability and being healthier, instead of using inorganic or synthetic particles (Rayner et al., 2014, Xiao et al., 2016a). The novelty of this study lies in the formulation of plant-derived emulsions which are increasingly of interest to different consumer groups especially for vegan communities. Several studies investigated various plant-derived and food-grade materials as particulate emulsifiers. Most of the focus of these studies was concentrated on the physical stability of the fabricated emulsions (Li and de Vries, 2018, Rayner et al., 2014). However, much less is known about the oxidative



stability of these emulsions (Kargar et al., 2012, Xiao et al., 2015). Therefore, more emphasis should be placed on the functionality of this delivery system on the oxidation of the lipophilic phase and its ability to improve the chemical stability. Pickering emulsions are found to have a good sustained release behavior of encapsulated lipophilic bioactive components such as retinol and curcumin as well as controlled lipid digestibility, making these systems suitable for the development of products presenting a low lipid absorption rate, which promotes satiety and reduces obesity (Tzoumaki et al., 2013, Zhou et al., 2018b, Shah et al., 2016). They can also be used as a delivery system for fat-soluble nutraceuticals.

For further improvement of the oxidative stability of FO emulsions and masking the undesirable flavors and odors of FO, thymol as a plant-based antioxidant was added to the oil phase. Thymol is a dietary phenolic monoterpene and a main constituent in the chemical composition of some essential oils extracted from thyme and oregano. It has antimicrobial (Zhang et al., 2014, Li et al., 2018, Bilenler et al., 2015), antifungal (Marchese et al., 2016), antioxidant (Sedaghat Doost et al., 2019c, Bilenler et al., 2015), anticancer (Islam et al., 2019), antidiabetic (Alu'datt et al., 2016), antiallergic and anti-inflammatory properties (Pivetta et al., 2018). However, its low water solubility and crystal form are obstacles for different applications as an alternative to synthetic additives (Sedaghat Doost et al., 2019b).

In this research, we used self-assembled particles obtained by complexation of flaxseed protein (FP) and the soluble fraction of flaxseed mucilage (SFM) to stabilize the emulsions. The effect of Pickering stabilization using these plant-derived particles on the oxidation stability and *in-vitro* simulated gastrointestinal (SGI) digestion of FO emulsions, was evaluated. To compare the functionality of the particles in the formulation of these emulsions, FO emulsions containing the commonly used

polysorbate 80 synthetic emulsifier (commercially available as Tween 80), were also prepared. The knowledge obtained from this study could be useful for designing plant-based colloidal delivery systems to better control the digestion and bioaccessability of hydrophobic nutraceuticals and drugs for food, beauty, and pharmaceutical applications.

## **4.2. Materials and methods**

### **4.2.1. Materials**

Thymol (2-isopropyl-5-methylphenol) was purchased from Sigma-Aldrich Co (St. Louis, MO, USA). Pepsin powder (from porcine gastric mucosa,  $\geq 400$  U/mg protein), pancreatin (from porcine pancreas,  $\geq 3 \times$  USP specifications) and lipase (Type II from porcine pancreas, 100-500 U/mg protein using olive oil with 30 min incubation) were also purchased from Sigma-Aldrich Co (St. Louis, MO, USA).

### **4.2.2. Preparation of FP-SFM complexes**

The complex particles were prepared as explained in section 2.4.

### **4.2.3. Fabrication of FO-loaded emulsions with and without thymol**

In order to fabricate 2.5 wt% FO oil-in-water emulsions, the particle dispersion as an aqueous phase was homogenized using a high-shear blender (Ultra-Turrax 50N-G 45 F, IKA®-Werke, Germany) with FO (thymol content 0 to 2%) for 5 min at 24000 rpm. The polysorbate 80 stabilized emulsion (PS80) and FP stabilized emulsion (FPFOE) were prepared in the same manner as the conventional emulsions.

### **4.2.4. Emulsions droplet size determination**

The droplet size of fresh emulsions and also during 20 days of storage was evaluated as expressed in section 2.8.1. The specific surface area (SSA,  $\text{m}^2/\text{kg}$ ) was calculated based on the Sauter mean diameter  $D_{3,2}$  using the following equation:

Equation 4.1.

$$\text{SSA} = \frac{6}{D_{3,2} \times \rho}$$

where  $\rho$  is the oil density which was determined to be 0.93 g/ml using an Anton-Paar density meter (DMA-5000, Belgium) at 20°C at atmospheric pressure.

#### **4.2.5. Confocal laser scanning microscopy (CLSM)**

CLSM (Leica TCS-SP5, Germany) was used for the microstructure characterization of FO-loaded emulsions with 2% thymol in the lipid phase which were stored for 20 days at 20 °C (section 2.8.2).

#### **4.2.6. Lipid oxidation determination**

Lipid oxidation experiments were performed by setting two series of fresh samples in sealed screw cap glass tubes covered by aluminum foil for 28 days in an incubator at 4 °C, and in an oven at 50 °C to accelerate the oxidation. For this purpose, a FO emulsion (FOE), thymol (0.5, 1, and 2 wt%)-FO emulsions (TFOEs), bulk flaxseed oil (FO) and bulk thymol (0.5, 1 and 2 wt%)-FO mixtures (TFOs) were analyzed. Sampling was conducted every 7 days to monitor the production of primary lipid oxidation products (lipid hydroperoxides, LH) using the peroxide value (PV), and the secondary products (malondialdehyde, MDA) using the thiobarbituric acid reactive substances assay (TBARS).

##### **4.2.6.1. Peroxide value**

PV was evaluated through the method in the norm UNE 55-023 (Atarés et al., 2012) with some modifications. 2 g emulsion or 50 mg bulk oil was weighted in a 250 ml Erlenmeyer flask and was dissolved in 20 ml of a 3:2 (v/v) mixture of glacial acetic acid and isooctane. After an efficient stirring for 30 s, 500  $\mu$ l of saturated potassium iodide (KI) solution was added and shaking was carried on for 1 min. 30 ml water was added and the solution was titrated using 0.002 M sodium thiosulfate ( $\text{Na}_2\text{S}_2\text{O}_3$ ) solution in the presence of 500  $\mu$ l of 1% (w/v) starch as indicator until the blue/purple color disappeared. The PV was calculated according to the following equation:

#### Equation 4.2

$$PV \text{ (mEq of oxygen/ kg of sample)} = (S - B) \times N \times 1000/W$$

where S is the volume of Na<sub>2</sub>S<sub>2</sub>O<sub>3</sub> used by the sample, B is the volume of Na<sub>2</sub>S<sub>2</sub>O<sub>3</sub> used by the blank, N is the normality of the Na<sub>2</sub>S<sub>2</sub>O<sub>3</sub> solution, and W is the sample mass (g).

#### 4.2.6.2. Thiobarbituric acid reactive substances assay

The MDA content was measured using the TBARS method according to the method described before by Atarés et al. (2012) with slight modification. 0.1 ml emulsion was diluted with water up to 1 ml and mixed with 2 ml thiobarbituric acid (TBA) solution which was prepared by dissolving 0.375 g of TBA (0.375% w/v) and 15 g of trichloroacetic acid (TCA, 15% w/v) into 100 mL of 0.25 M HCl. These were kept in boiling water for 15 min and were cooled down under tap water for 5 min. After centrifugation at 4000 rpm for 30 min, the supernatant was collected and the absorbance was read using a UV-Vis spectrophotometer (VWR, Belgium) at 532 nm against TBA solution. The concentration of MDA was determined from the standard curve prepared with 1, 1, 3, 3-tetraethoxypropane at a concentration range of  $1.42 \times 10^{-8}$  to  $4.54 \times 10^{-8}$  M ( $R^2 = 0.9994$ ).

#### 4.2.7. *In-vitro* digestion

FO, TFO, FOE, TFOE, FPFOE, TFPFOE (FO containing thymol stabilized with FP), PS80, and TPS80 (FO containing 2 wt% thymol stabilized with polysorbate 80) were exposed to the upper GI conditions to investigate the fate of their *in-vitro* digestion. Control experiments were also carried out by replacing FO with dodecane in FOE in order to exclude any decrease in pH-value due to other factors. These control emulsions were indicated as DOE. These were prepared as mentioned in section 4.2.3. For this purpose, samples were subjected to simulated gastrointestinal fluid

(SGF) and then simulated intestinal fluid (SIF) according to the standardized method reported by Minekus et al. (2014).

#### 4.2.8. Gastric conditions

10 ml emulsion was adjusted to pH 2 and then was added to 10 ml SGF which was composed of 0.275% NaCl and 0.32% pepsin (25000 u/ml) with pH 2. The mixture pH was adjusted to 2 and incubated at 37 °C for 2 h and agitated on an orbital shaker at 20 rpm. After two hours, the pH was adjusted to 7 before applying SIF conditions.

#### 4.2.9. Intestinal conditions

The lipid digestibility of the emulsions was determined using the free fatty acid (FFA) release during the simulated intestinal phase. 10 ml digesta from the gastric media for each sample was adjusted to pH 7 and then was added to 10 ml SIF which is composed of 0.3 mM CaCl<sub>2</sub>, 47 mM NaCl, 10 mM bile extract, 100 u/ml pancreatin (trypsin-based) to reach the concentration of 1.3 mg/ml in the final mixture, 0.4 mg/ml lipase 2000 u/ml in 50 mM phosphate buffer. Then, the pH of the digesta was adjusted to 7 again and the pH was maintained at 7.0 by dropping 0.1 M NaOH during 2 h at 37 °C. The amount of FFA released from the FO digestion was calculated from the volume of NaOH ( $V_{NaOH}$ ) used to neutralize these FFA from the following equation at 10 min interval, assuming that all triacylglycerols (TAG) are hydrolyzed in two molecules of FFA and one molecule of monoacylglycerol (MAG):

Equation 4.3

$$\%FFA = \left( \frac{V_{NaOH} \times M_{NaOH} \times MW_{lipid}}{2 \times W_{lipid}} \right) \times 100$$

$M_{NaOH}$  is the molarity of the NaOH (0.1 M),  $MW_{lipid}$  is the average molecular weight of FO (875.38 g/mol), and  $W_{lipid}$  is the weight of the lipids.

In addition, the droplet size of the samples was monitored during the digestion process.

#### **4.2.10. Thymol bioaccessibility**

The bioaccessibility of thymol in the FO Pickering emulsions was determined after the *in vitro* digestion process mentioned-above. The digesta were centrifuged at 16,000 rpm for 30 min at 4 °C. The middle transparent layer was diluted 100 times with hexane and was vortexed for 5 min. After standing until two separate transparent phases appeared, the upper phase was transformed to measure the absorbance at 275 nm to determine the thymol concentration. The calibration curve was prepared previously using standard solutions with 0.01–0.1 mg/mL thymol dissolved in hexane. The bioaccessibility of thymol was then calculated as the ratio of the amount of thymol found in the digest volume to the initially present amount (Aravena et al., 2016, Pan et al., 2014)

#### **4.2.11. Statistical analysis**

Statistical tests were performed as section 2.9.

### **4.3. Results and discussion**

#### **4.3.1. FO-loaded Pickering emulsions**

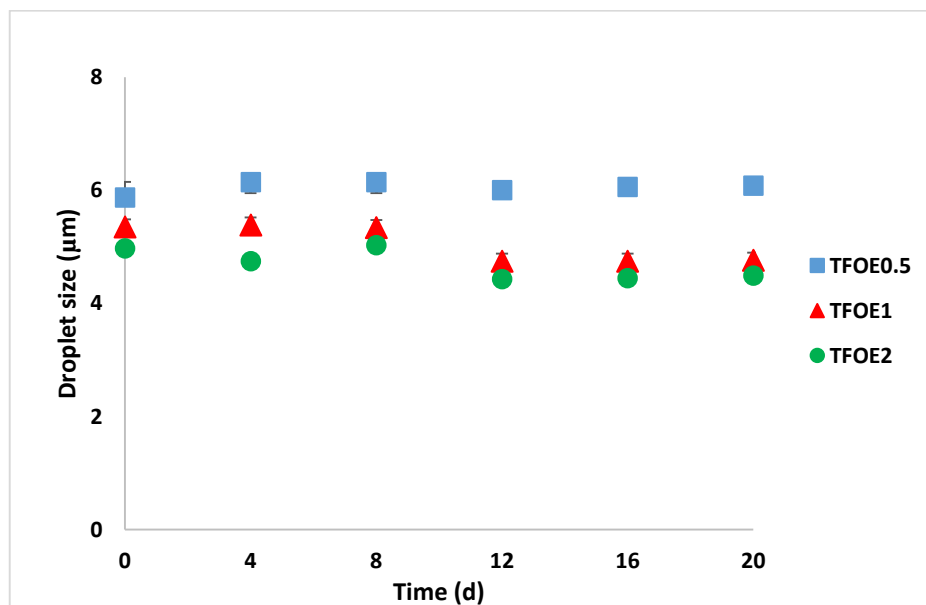
Initially, FO-loaded oil-in-water emulsions with variable thymol content were characterized in terms of visual appearance and droplet diameter. Thymol was added to FO-emulsions since its antioxidant activity has been shown in several studies (Sedaghat Doost et al., 2019c).

It was observed that the prepared emulsions were opaque and homogenous with no sign of instability (data not shown). The droplet size measurements revealed that the volume-weighted mean diameter of fresh 2.5 wt% FO emulsion (FOE) in the absence of thymol was  $7.19 \pm 0.03 \mu\text{m}$ . Interestingly, there was a slight decrease in the mean droplet diameter of emulsions by addition of 0.5, 1 and 2% thymol to the lipid phase: the diameter of the corresponding emulsions was  $5.9 \pm 0.1$ ,  $5.4 \pm 0.1$ , and  $5.0 \pm 0.0 \mu\text{m}$ , respectively. This indicated that the addition of thymol affects the droplet size

which could be due to the fact that thymol changed the interfacial tension between the lipid and continuous phase.

From a functionality and application point of view, it is desired that the formulated delivery system has a sufficient long-term stability. The droplet size variation of emulsions can provide practical information about their physicochemical stability. Thus, the mean diameter of FO-loaded emulsions containing thymol was monitored during long-term storage at ambient temperature. The results in Figure 4.1.a indicated that 2.5 wt% FO-loaded emulsions carrying variable amounts of thymol did not show a noticeable size variation during long-term storage. The visual appearance assessment of these samples also exhibited no considerable changes, which was in line with the droplet size analysis results (data not shown).

a)



b)

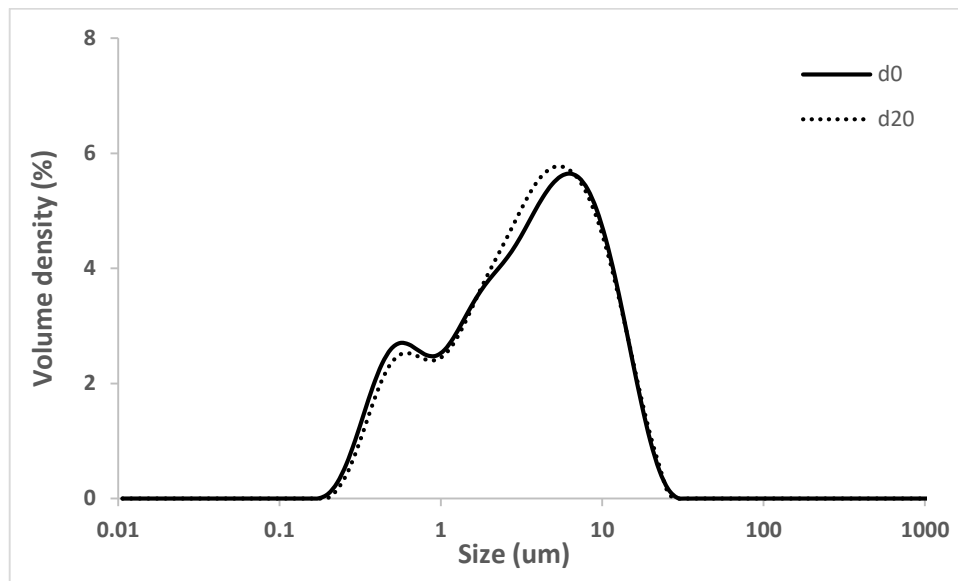


Figure 4.1. (a) Volume-weighted mean diameter  $D[4,3]$  variation of 2.5 wt% FO Pickering emulsions with different thymol content (0.5, 1 and 2 wt%) during 20 days of storage at 20 °C and (b) size distribution of fresh FO emulsions containing 2% thymol and after 20 days of storage .

The droplet size distribution of fresh FO emulsion containing 2 wt% thymol and after 20 days of storage is also displayed in Figure 4.1-b. The morphology and microstructure of this system after 20 days of storage was also visualized using CLSM (Figure 4.2). At a first glance, it was obvious that the oil droplets were still present with a spherical morphology while the particles were accumulated at the oil-water interface responsible for the stabilization.



a)

b)

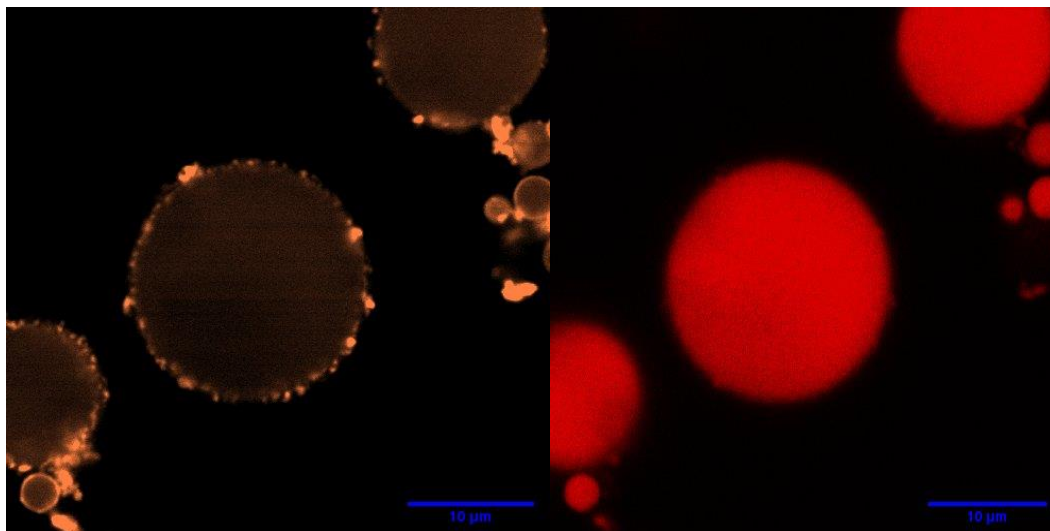


Figure 4.2. CLSM images of 2.5 wt% FO Pickering emulsion containing 2 wt% thymol stabilized by complex FP-SFM particles at pH 3. The particles and flaxseed oil were stained by Rhodamine B (a) and Nile red (b), respectively.

#### 4.3.2. Oxidative stability of FO Pickering emulsions

The oxidation process in bulk FO with and without thymol was initially monitored at refrigerator and oxidation accelerated conditions in terms of LH and MDA creation. From the results presented in Figure 4.3.a&c, it was visible that mixing thymol with the bulk FO led to a significant ( $p < 0.05$ ) decrease in the PV and TBA values after 28 days of storage at 4 °C depending on the thymol content. By contrast, the storage of FO bulk oil at 50 °C resulted in the formation of a higher amount of LH and MDA which is a consequence of the faster oxidation of polyunsaturated fatty acids at elevated temperatures (Figure 4.3.b&d). The statistical analysis exhibited that 0.5% thymol was not sufficient to retard oxidation at 50 °C, as was the case when the FO was stored at 4 °C. On the other hand, by addition of 1 or 2% thymol, a significantly lower amount of LH and MDA were present. This indicates clearly that addition of thymol slowed down the oxidation of FO. The fact that thymol has antioxidant activity is due to the -OH group on its aromatic ring that can eliminate free radicals by donating H• and hence decreases the propagation of the LH (Gursul et al., 2019). However, its antioxidant

capability is limited at high temperatures because of its high volatility (Gursul et al., 2019) which can explain the lower antioxidant activity of 0.5% thymol at 50 °C.

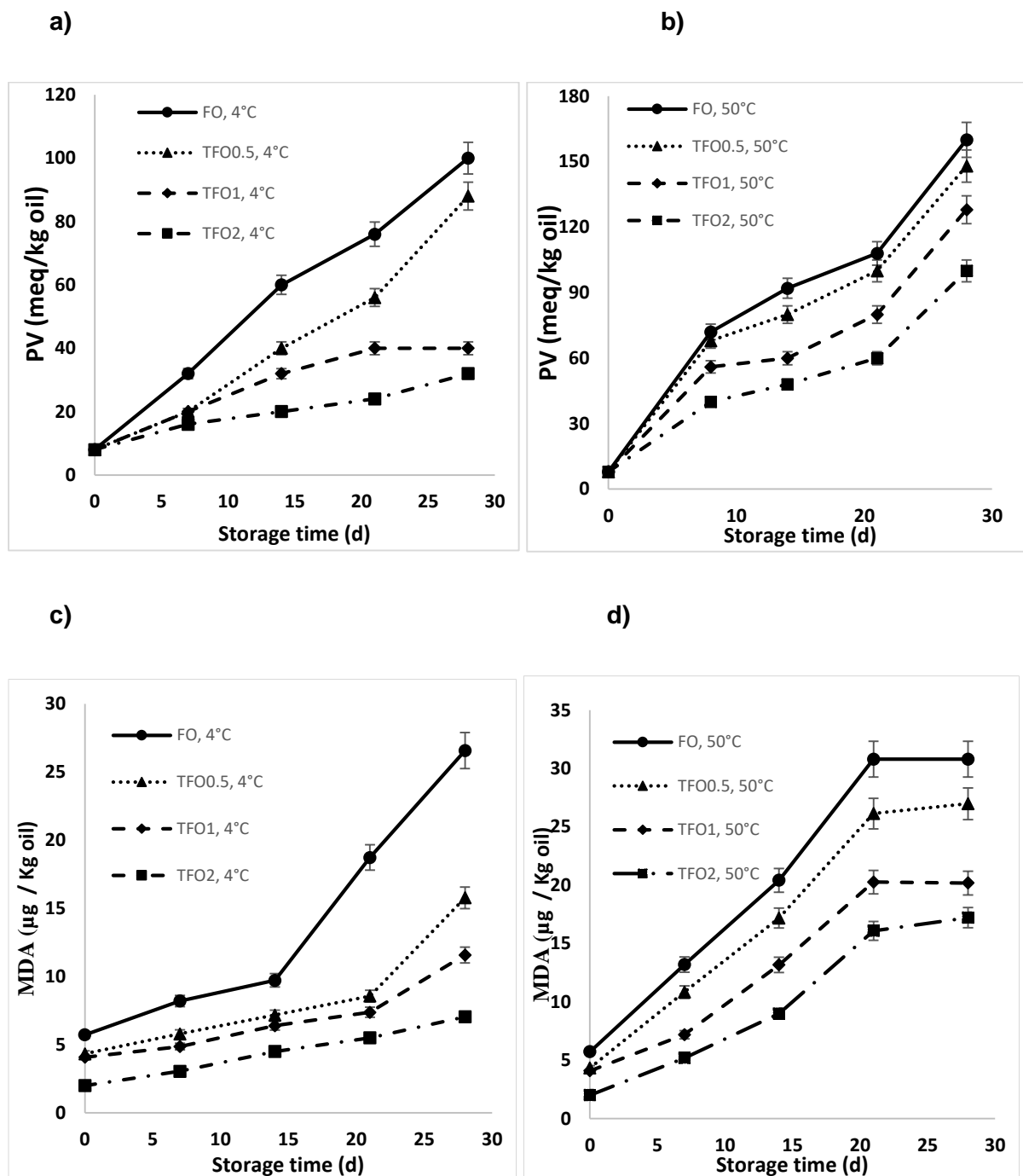


Figure 4.3. Influence of thymol content and storage temperature on the peroxide values (PV, mEq of O<sub>2</sub> per kg of sample) of FO over 28 days of storage at a) 4°C and b) 50°C, and on the TBA values (µg malonaldehyde (MDA) per kg oil) of FO over 28 days of storage at c) 4°C and d) 50°C.

The analysis of the PV and TBARS results evidenced that Pickering stabilization was successful to depress the oxidation of FO at both of the studied temperatures (Figure

4.4). The amount of LH in FO particle-stabilized emulsions was significantly lower than that in bulk FO and even lower than in bulk TFO (0.5%) at 4 °C (Figure 4.4a) and 50 °C (Figure 4.4c) during 28 days of storage. Since the lipid oxidation in emulsions starts at the oil-water interface due to the presence and exposure of unsaturated lipids and pro-oxidants, the composition and thickness of the interface could be an important factor in controlling the lipid oxidation (Berton-Carabin et al., 2014, Salminen et al., 2017). Thus, the thicker assembled interfacial layer of particles can perform better in protecting the oil phase against oxidation in comparison to small molecule surfactants which is in agreement with the results of Kargar et al. (2011), (2012). Their results suggested that particle-stabilized emulsions due to the thicker interfacial layer around the oil droplets were more effective in preventing oil oxidation in comparison to conventional emulsions. For further depression of oxidation in emulsions, thymol was added to the oil phase of the Pickering FO emulsions. In the presence of thymol dissolved in the oil phase, the LH and MDA content in FO Pickering emulsions decreased further with an increase in the thymol level even at accelerated conditions (Figure 4.4). By comparing the results presented in Figure 4.3&4.4, it can be suggested that the antioxidant effectiveness of thymol at high temperatures increased in the Pickering stabilized FOE in comparison to the free form. This could be due to the ability of Pickering encapsulation to prevent or decrease the volatility of thymol as an essential oil. These results are in agreement with the results of Gursul et al. (2019) who reported that microencapsulation with sodium caseinate-lactose was able to prevent the volatilization of thymol and carvacrol and improved their ability to protect fortified walnut oil against oxidation. Therefore, the combination of Pickering stabilization and using thymol as a hydrophobic and plant-based antioxidant in the oil phase is a promising approach to protect FO.

According to the droplet size and oxidation measurements, the 2.5 wt % FO Pickering emulsion containing 2 wt% thymol was selected for the rest of the experiments since it had the smallest droplet size with a long-term stability and it was the most successful one in depressing the FO oxidation.

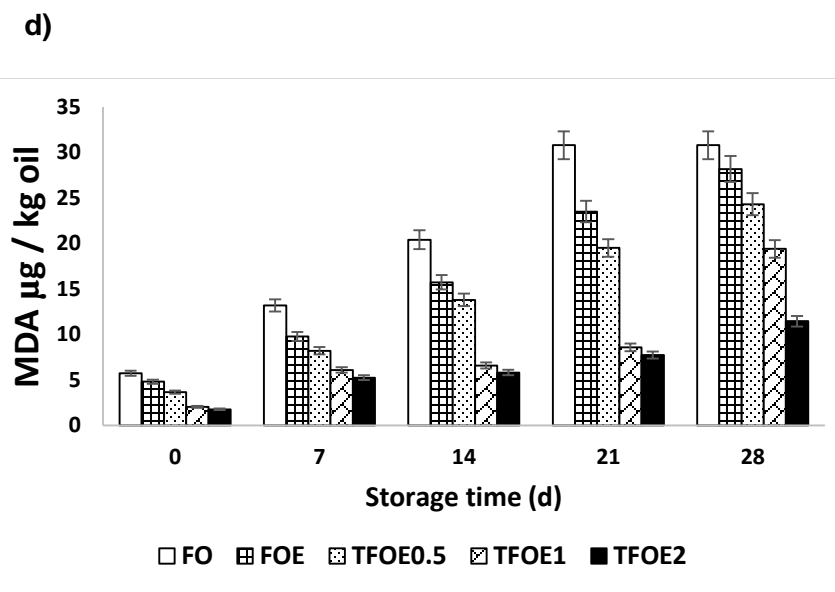
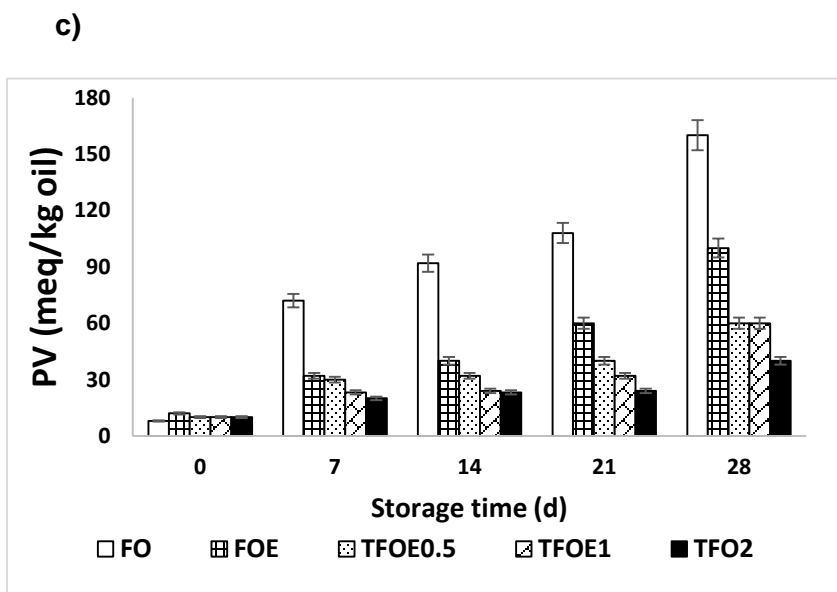
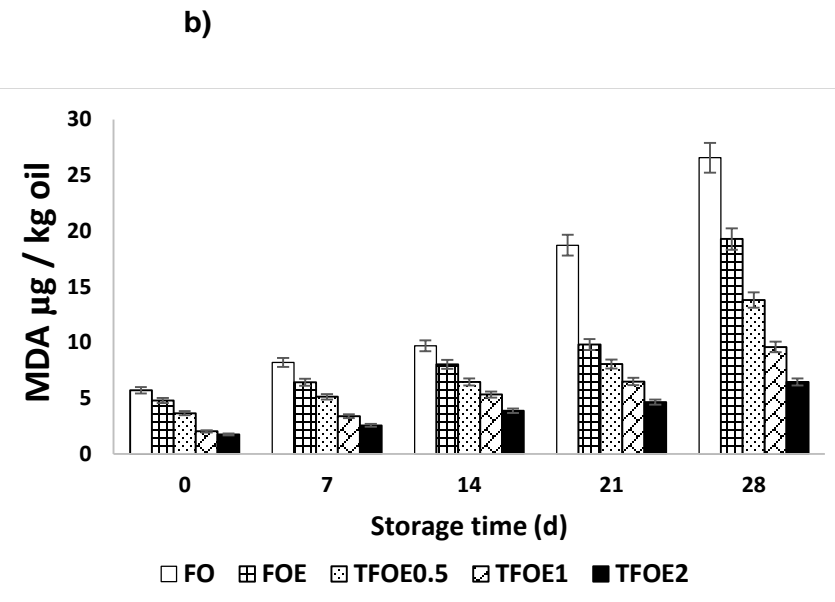
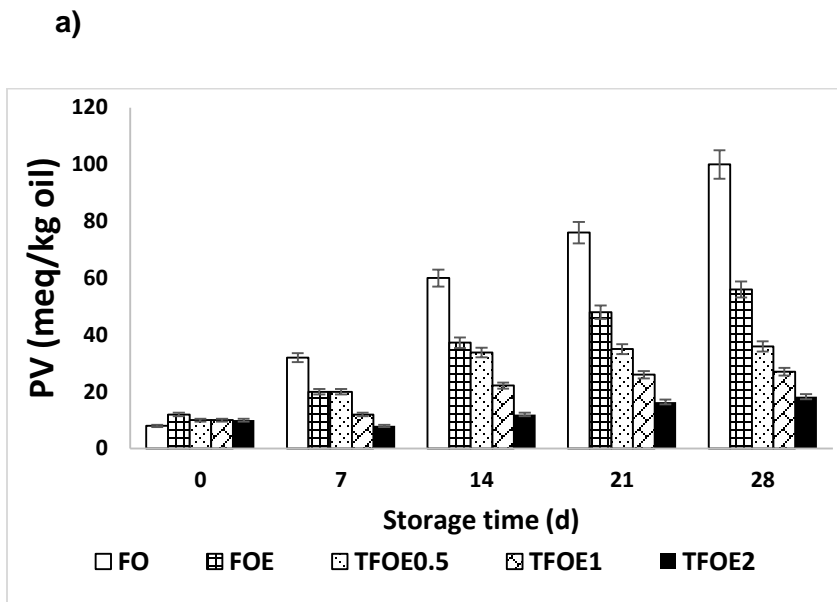


Figure 4.4. Effect of Pickering stabilization and thymol content on PV and TBA values during 28 days of storage at 4°C (a, b) and 50°C (c, d).

#### **4.3.3. Digestion fate and bioaccessibility assessment of thymol**

Lipid digestion is a bio-interfacial process which is dependent on the attachment of the lipase enzyme-colipase-biosurfactant (bile salts) complex at the O/W interface. For this reason, designing O/W interfaces that prevent competitive displacement by bile salts and/or delay the

transportation of lipases to the lipid substrate can be an effective approach to modulate lipolysis in human physiology (Sarkar et al., 2019, Anal et al., 2019).

In order to investigate the effect of FP-SFM complexes at the FO emulsions interface on the FO lipid digestion and the stability of emulsions against the digestion conditions as well as the bioaccessibility of thymol, the FO, TFO, FOE, TFOE (FOE containing 2 wt% thymol), FPFOE, TFPFOE, PS80, and TPS80 were subjected to the upper GI conditions. For excluding any decrease in pH value due to other factors than FFA release, dodecane was used instead of FO in FOE as a control. As presented in Figure 4.5, PS80 had the sharpest FFA release profile, which shows the fastest rate of the lipid digestion. The bulk oil showed the largest extent of lipid digestion after the PS80 due to its bare interface, but with a smaller rate. These results are consistent with the reported results by Xiao et al. (2015), who suggested that soybean oil Pickering emulsions stabilized with kafirin nanoparticles were more stable against lipid digestion in comparison to polysorbate 80 stabilized emulsions. This was attributed to the smaller droplet size and higher surface area for anchoring lipase as well as the thinner interfacial layer which resulted in the faster FFA generation rate. Figure 4.5 clearly shows that the protein stabilized FO emulsion also displayed very rapid FFA release. Conventional emulsions which are stabilized with surfactants and proteins can be digested fast through the easy displacement of these surfactants with the bile salts.

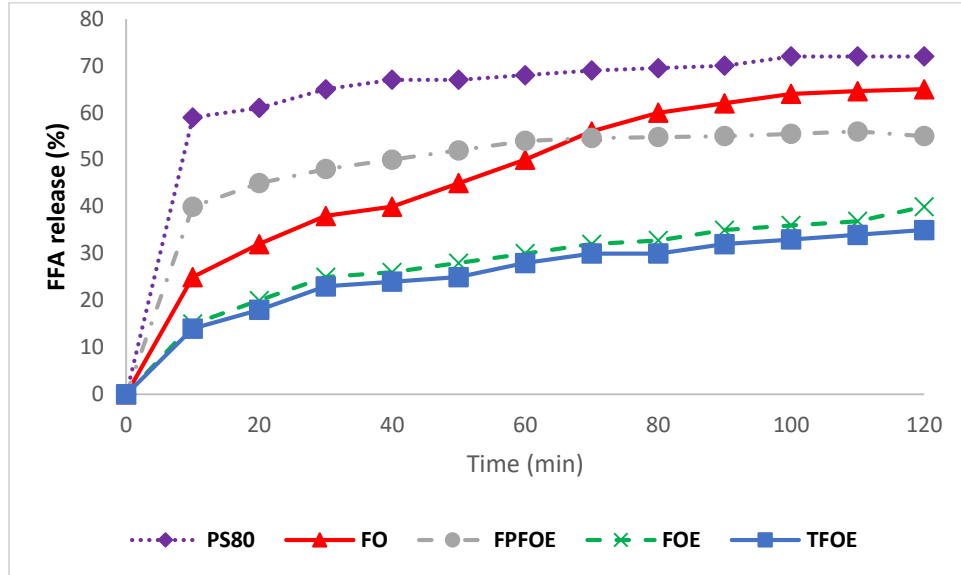


Figure 4.5. Percentage of free fatty acid (FFA) released during the *in vitro* digestion

In the case of particle-stabilized emulsions (i.e. FOE and TFOE), the displacement of the particles by bile salts requires much more energy for the desorption of the attached particles at the interface. This high required energy and the thicker interfacial layer in Pickering emulsions make them resistant to coalescence (Dickinson, 2017, Berton-Carabin and Schroën, 2015) and lipid digestion (Tzoumaki et al., 2013, Sarkar et al., 2016). It can be concluded that the FP-SFM particles by their irreversible adsorption onto the interface and providing a thick protective layer were able to disturb the pancreatic lipase activity which contributes to the control of the lipid digestibility. Thus, the access of the lipase to the inner oil core is limited and it is only possible for the lipase/co-lipase complex to attach to the interface via the available gaps between the anchored particles. Moreover, according to the results of chapter 2, FP-FSM particles were negatively charged so the assembled interfacial architecture may have the ability to act as an electrostatic barrier against negatively-charged bile salts. In terms of protein-stabilized emulsions, the proteolysis of the interfacial layer by pepsin and/or trypsin in addition to

protein displacement with bile salt makes them susceptible to the digestion due to the possible access of lipase to the oil phase. However, Sarkar et al. (2018) suggested that the protein resistance to digestion can be improved through electrostatic interaction of nanoparticles with inulin. Complexation of a protein with an enzyme-unresponsive polysaccharide provides a complex interfacial architecture leading to the gastric stability of the protein. Shimoni et al. (2013) and Meshulam and Lesmes (2014) also previously reported that electrostatic complexation of lactoferrin nanoparticles with carrageenan or alginate decreased the rate of gastric proteolysis. Sarkar et al. (2017) also reported the modulated gastric digestion of whey protein Pickering emulsions through electrostatic binding with cellulose nanocrystals at the O/W interface at pH 3. Their results revealed that the complexation increased the resistance of the protein interfacial layer to pepsin breakage. Therefore, it can be concluded that the presence of SFM which electrostatically interacted with the FP, modulated the in vitro digestion of FO emulsions and delayed the lipid digestion and FFA generation. This could be due to the increased resistance of the interfacial layer against pepsin rupturing. It can be seen from Figure 4.5 that the FFA release profiles of FOE and TFOE were fairly similar which indicated that thymol incorporation in FO did not affect the lipid digestion. Thymol loaded PS80 and FPFOE also did not have a significant difference in lipolysis with their thymol-free counterparts (data not shown).

The volume-weighted average droplet size ( $D_{4,3}$ ) of the emulsions before and after exposure to in vitro GI conditions was measured to investigate the stability of the emulsions against SGF and SIF. Table 4.1. shows that after 2 h digestion under SGF condition, the size of all the studied emulsions increased. This could be due to the fact



that the complexation with SFM could depress the FP susceptibility against destabilization along with the loss of emulsion surface charge and proteolysis under SGF conditions as discussed above. These results are in line with the results of FFA release. Shimoni et al. (2013) reported that electrostatic association of lactoferrin nanoparticles with alginate or carrageenan increased their stability against coalescence under gastric conditions. Zhou et al. (2018a) also reported that after incubation of emulsions in SGF for 10 min due to the acidic pH and the high-ionic conditions, the gliadin stabilized Pickering emulsions had extensive droplet coalescence, while the complexation of gliadin protein with proanthocyanidins improved its resistance against SGF acidic conditions and the ions present, and prevented its pepsin-induced instability. There are also similar reports in the literature about the flocculation and coalescence of oil droplets stabilized by protein particles such as kafirin (Xiao et al., 2015), gliadin (Zhou et al., 2018b) and whey protein (Winuprasith et al., 2018).

*Table 4.1. Volume-weighted average droplet size ( $D_{4,3}$ ,  $\mu\text{m}$ ) and specific surface area (SSA,  $\text{m}^2/\text{kg}$ ) before and after SGF and SIF incubation and the percent of thymol bioaccessability. Data are reported as the means and standard deviations ( $n=3$ ).*

Sample	$D_{4,3}(\mu\text{m})$			SSA ( $\text{m}^2/\text{kg}$ )			Bioaccessability (%)
	Initial	After SGF	After SIF	Initial	After SGF	After SIF	After SIF
	TFO						
TFOE	$5.0 \pm 0.0$	$12.2 \pm 0.2$	$7.5 \pm 0.1$	$2833 \pm 21$	$2452 \pm 20$	$3426 \pm 24$	$21.8 \pm 0.2$
TFFPFOE	$21.0 \pm 0.4$	$52.8 \pm 0.5$	$15.3 \pm 0.3$	$954 \pm 20$	$895 \pm 11$	$1988 \pm 1$	$15.5 \pm 0.4$
TPS80	$4.6 \pm 0.1$	$6.8 \pm 0.3$	$8.0 \pm 0.0$	$5081 \pm 28$	$4980 \pm 26$	$4875 \pm 22$	$32.5 \pm 0.5$

As can be seen in Table 4.1., PS80 was most stable against the SGF with only a limited increase in the droplet size. Polysorbate 80 is a non-ionic surfactant which makes

emulsions quite stable against low pH and high ionic strength (Sedaghat Doost et al., 2017). Shah et al. (2016) reported the greater stability of curcumin-loaded nanoemulsions stabilized with polysorbate 80 and span 80 against SGF in comparison to Pickering emulsions stabilized by chitosan-tripolyphosphate nanoparticles. They explained this good stability to the strong steric repulsion as a result of the neutral hydrophilic head groups of these non-ionic surfactants. Xiao et al. (2015) observed similar results when comparing the droplet size of the collected emulsions stabilized with polysorbate 80 and kafirin nanoparticles after SGF.

After exposing to SIF, the average droplet size of all the studied emulsions except from PS80 decreased for some reasons. First, the lipid digestion which led to some extent of oil phase being removed resulted in a smaller droplet size. Second, larger oil droplets formed through coalescence after SGF lost their integrity completely resulting in oiling-off. Therefore, these larger droplets did not exist anymore after their complete breakage. However, the droplet size results displayed that PS80 was stable against SGF and maintained its integrity until the end of the SIF with a slight increase in droplet size due to coalescence which is consistent with the results of Xiao et al. (2015). Third, after SIF incubation, small micelles and vesicles are formed due to the presence of surface-active components including bile salts and phospholipids as well as the generated products by lipase digestion (released FFA, monoacylglycerols and diacylglycerols) (Winuprasith et al., 2018, Anal et al., 2019). This can be evidenced by investigating the SSA which is also given in Table . The higher SSA after SIF is associated with the higher number of small particles, such as droplets. These formed micelles play a key role for the transportation

of hydrophobic molecules to epithelium cells for absorption and hence increase their bioavailability (Anal et al., 2019).

The bioaccessability of thymol was also evaluated after passing through the in-vitro simulated GI digestion. The results displayed in Table 4.1. suggested that the thymol bioaccessability in bulk FO was very low ( $5.0 \pm 0.7$  %). Pickering stabilization was successful to reach  $21.7 \pm 0.1$  %. However, the PS80 was more successful to enhance the thymol bioavailability ( $32.5 \pm 0.5$  %) due to its smaller droplet size (Table ) and faster lipolysis (Figure 4.5). The slower and lower extent of lipolysis of Pickering emulsions resulted in the thymol remaining trapped within the non-digested oil droplets. These results are in agreement with the results reported by Xiao et al. (2015) who found that the bioaccessability of curcumin loaded in Pickering emulsions stabilized by kafirin particles was between those of a conventional emulsion stabilized by polysorbate 80 and bulk oil. Shah et al. (2016) also reported that conventional nanoemulsions had a higher curcumin bioaccessability due to their smaller mean droplet diameter in comparison to Pickering emulsions stabilized with chitosan-tripolyphosphate nanoparticles.

#### **4.4. Conclusions**

Plant biopolymers are preferred alternatives to animal-based ingredients due to consumer and environmental concerns. FP-SFM plant-derived particles were used for Pickering stabilization of FO which is susceptible to oxidation. The oxidation stability of FO was increased in Pickering emulsions in comparison to the bulk oil. Through the addition of thymol to the oil phase the oxidation was further depressed. The evaluation of the digestion fate in an in-vitro GI model revealed that the particle stabilized emulsions retarded the oil digestion in comparison to bulk oil and to conventional emulsions stabilized with PS80 due to the ability of particles to depress the lipolysis as a result of the irreversible adsorption of particles at the interface. Moreover, it was found that the complex particles were more successful in retarding the lipid digestion in comparison to plain FP which is due to the complexation with a human enzyme-unresponsive polysaccharide. The bioaccessibility of thymol increased when it was incorporated into FO Pickering emulsions in comparison to bulk oil. Hence, Pickering stabilized thymol containing FO emulsions are a powerful formulation tool to increase the triglyceride oxidation stability. This study also opens a promising pathway for producing animal- and synthetic-free emulsions to encapsulate labile lipophilic bioactive components through Pickering stabilization using plant-based biopolymer particles. Furthermore, these findings can be used for designing functional foods with controlled lipid digestion to enhance satiety and hence to reduce the incidence of obesity.



## Chapter 5: Conclusions and future research

Proteins are natural polymers that are widely used as functional ingredients in food products. These biopolymers are capable of stabilizing emulsions and foams, thickening solutions, and forming gels. Plant-based proteins have some advantages over their animal counterparts, such as a lower risk of infection and contamination, no limitations in terms of cultural food habits and vegetarian consumers, and being more economic, sustainable and versatile compared to animal-based ingredients. The majority of the plant-based proteins have limited applications due to their low water solubility especially at and around their isoelectric point. Moreover, they are susceptible to environmental stress conditions including pH, ionic strength and thermal treatment. As a solution, the association of a polysaccharide with these plant proteins can modulate their functional properties. Electrostatic interaction can be used as a straightforward and simple way to prepare non-covalent complexes between a polysaccharide and a protein with opposite net charge. In this study, flaxseed was used as a sustainable source for the protein and polysaccharide biopolymers. The electrostatic interaction between FP and soluble portion of flaxseed mucilage (SFM) was evaluated in order to modulate the functional properties of this protein as a Pickering stabilizer. Based on our results, the formation of complex nanoparticle consisting of FP and SFM is possible at a wide pH range with no precipitation. It was shown that the electrostatic interaction between FP and SFM can prevent the aggregation and further precipitation of the protein at and around its isoelectric pH, and improve its solubility and functional properties. The anionic SFM binding to cationic patches on the protein increases FP negative surface charge which ensures the electrostatic repulsion between its molecules. These complexes can be used

as Pickering stabilizers by providing an electrostatic repulsion in addition to the creation of a steric protective layer around the oil droplets. Considering the fact that emulsions cannot be stabilized properly with FP around its pI, it can be concluded that adsorbing FP-SFM complex nanoparticles onto the interface introduces a protecting coating resisting flocculation and coalescence. The results suggest that FP-SFM complex nanoparticles show a good potential as food-grade and plant based Pickering stabilizers for surfactant-free oil-in-water emulsions even at acidic pH conditions.

Pickering emulsions with their superior stability against coalescence and Ostwald ripening can be used as a delivery system for hydrophobic bioactive compounds. Flaxseed oil is one of the functional lipids that can be used to produce healthy foods since it has about 57% alpha linolenic acid (ALA). ALA is a precursor for essential fatty acids and provides numerous beneficial effects on the consumer's health including reducing blood cholesterol (decreases LDL and increases HDL), coronary heart diseases risk, the prevention of breast and prostate cancers and improving neurological and hormonal systems. This bioactive oil is highly susceptible to oxidation due to its high degree of unsaturation, which leads to produce off-flavor, off-odor and reduced nutritional value in flaxseed oil. Also, the oil has poor solubility in aqueous food systems, which limits its application in the food industry. In this study, Pickering emulsions based on FP-SFM complex nanoparticles which are also active agents in addition to being excipients, were used as a delivery system for flaxseed oil. FP and SFM have also health beneficial effects and can be used as functional ingredients. These complex particles as Pickering emulsifiers were successful to depress flaxseed oil oxidation. It was also shown that Pickering emulsions remained stable during 28 days of storage with good stability against

environmental stress conditions with only a slight increase in droplet size, but with no sign of oiling-off and breakage. They also exhibited improved thermal stability compared to FP-stabilized emulsions. Therefore, these surfactant-free emulsions stabilized with complex FP-SFM nanoparticles can be used for fortification purposes of acidic beverages with hydrophobic bioactive lipids such as flaxseed oil.

Thymol as a natural and plant-originated antioxidant and a bioactive component was added to the flaxseed oil core of the Pickering emulsions and its effect on depressing the oxidation of the oil and also on its bioaccessibility was evaluated. The digestion fate of these Pickering emulsions was also determined and compared to conventional protein (FP)-stabilized and surfactant (polysorbate 80, PS80)-stabilized emulsions. Applying Pickering stabilization and thymol antioxidant simultaneously was a successful approach to retard the FO oxidation. The Pickering emulsions retarded the oil digestion compared to conventional emulsions stabilized with PS80 and bulk FO due to the ability of particles to decrease the lipolysis as a result of their irreversible adsorption at the interface which prevents the displacement of particles by bile salt and lipase. The bioaccessibility of thymol increased when it was incorporated into FO Pickering emulsions in comparison to bulk oil. The results revealed that the combination of Pickering stabilization and using dispersed thymol antioxidant in the core oil phase can be used as a promising way of protecting highly unsaturated oils such as FO which are susceptible to oxidation. This study also opens a promising pathway for fabricating natural and surfactant-free labeled antioxidant emulsions via Pickering stabilization using plant-based complex particles. Furthermore, these findings can be used for designing functional foods with controlled lipid digestion to increase satiety and reduce the incidence of obesity.



The present study uncovered findings that result in more unanswered questions and thus future research opportunities. More studies are required for the commercialization of this concept. Future researches should focus on the challenges for the commercial applications. A more detailed characterization and sensory evaluation should be conducted for the food applications of the FO-loaded Pickering emulsions stabilized with FP-SFM particles. A number of new alternative plant-based proteins and polysaccharides can also be used for the assembly of the complex particles. More research is also required to explore the prospects of using different lipophilic bioactive compounds in the formulation for the purpose of encapsulation and delivery. Relatively limited studies have been carried out on the release kinetics from Pickering emulsions. Therefore, more emphasis should be placed on quantitative description of the release performance of these emulsions which is necessary for designing a sophisticated delivery system. By addressing the abovementioned limitations and gaps, using Pickering emulsions as a novel delivery system in a variety of food applications can be possible.

## References

- AKHTAR, M. & DING, R. 2017. Covalently cross-linked proteins & polysaccharides: Formation, characterisation and potential applications. *Current Opinion in Colloid & Interface Science*, 28, 31-36.
- ALARGOVA, R. G., WARHADPANDE, D. S., PAUNOV, V. N. & VELEV, O. D. 2004. Foam superstabilization by polymer microrods. *Langmuir*, 20, 10371-10374.
- ALU'DATT, M. H., RABABAH, T., JOHARGY, A., GAMMOH, S., EREIFEJ, K., ALHAMAD, M. N., BREWER, M. S., SAATI, A. A., KUBOW, S. & RAWSHDEH, M. 2016. Extraction, optimisation and characterisation of phenolics from *Thymus vulgaris* L.: phenolic content and profiles in relation to antioxidant, antidiabetic and antihypertensive properties. *International Journal of Food Science & Technology*, 51, 720-730.
- ANAL, A. K., SHRESTHA, S. & SADIQ, M. B. 2019. Biopolymeric-based emulsions and their effects during processing, digestibility and bioaccessibility of bioactive compounds in food systems. *Food Hydrocolloids*, 87, 691-702.
- AOAC 2003. Official Methods of Analysis of AOAC International. 2nd ed. *Association of Official Analytical Chemists*.
- ARAVENA, G., GARCÍA, O., MUÑOZ, O., PEREZ-CORREA, J. R. & PARADA, J. 2016. The impact of cooking and delivery modes of thymol and carvacrol on retention and bioaccessibility in starchy foods. *Food Chemistry*, 196, 848-852.
- ATARES, L., MARSHALL, L. J., AKHTAR, M. & MURRAY, B. S. 2012. Structure and oxidative stability of oil in water emulsions as affected by rutin and homogenization procedure. *Food Chemistry*, 134, 1418-1424.
- BEKHIT, A. E.-D. A., SHAVANDI, A., JODJAJA, T., BIRCH, J., TEH, S., MOHAMED

- AHMED, I. A., AL-JUHAIMI, F. Y., SAEEDI, P. & BEKHIT, A. A. 2018. Flaxseed: Composition, detoxification, utilization, and opportunities. *Biocatalysis and Agricultural Biotechnology*, 13, 129-152.
- BENETTI, J. V. M., DO PRADO SILVA, J. T. & NICOLETTI, V. R. 2019. SPI microgels applied to Pickering stabilization of O/W emulsions by ultrasound and high-pressure homogenization: rheology and spray drying. *Food Research International*, 122, 383-391.
- BENGOECHEA, C., JONES, O. G., GUERRERO, A. & MCCLEMENTS, D. J. 2011. Formation and characterization of lactoferrin/pectin electrostatic complexes: Impact of composition, pH and thermal treatment. *Food Hydrocolloids*, 25, 1227-1232.
- BERTON-CARABIN, C. C., ROPERS, M.-H. & GENOT, C. 2014. Lipid oxidation in oil-in-water emulsions: involvement of the interfacial layer. *Comprehensive Reviews in Food Science and Food Safety*, 13, 945-977.
- BERTON-CARABIN, C. C. & SCHROEN, K. 2015. Pickering emulsions for food applications: background, trends, and challenges. *Annual review of food science and technology*, 6, 263-297.
- BERTON-CARABIN, C. C., ROPERS, M. H. & GENOT, C. 2014. Lipid oxidation in oil-in-water emulsions: Involvement of the interfacial layer. *Comprehensive Reviews in Food Science and Food Safety*, 13, 945-977.
- BILENLER, T., GOKBULUT, I., SISLIOGLU, K. & KARABULUT, I. 2015. Antioxidant and antimicrobial properties of thyme essential oil encapsulated in zein particles. *Flavour and Fragrance Journal*, 30, 392-398.

- BOUAZIZ, F., KOUBAA, M., BARBA, F. J., ROOHINEJAD, S. & CHAABOUNI, S. E. 2016. Antioxidant properties of water-soluble gum from flaxseed hulls. *Antioxidants*, 5, 26.
- BOWEN, K. J., HARRIS, W. S. & KRIS-ETHERTON, P. M. 2016. Omega-3 fatty acids and cardiovascular disease: are there benefits? *Current treatment options in cardiovascular medicine*, 18, 69.
- CARNEIRO, H. C. F., TONON, R. V., GROSSO, C. R. F. & HUBINGER, M. D. 2013. Encapsulation efficiency and oxidative stability of flaxseed oil microencapsulated by spray drying using different combinations of wall materials. *Journal of Food Engineering*, 115, 443-451.
- CHANG, H. W., TAN, T. B., TAN, P. Y., ABAS, F., LAI, O. M., WANG, Y., WANG, Y., NEHDI, I. A. & TAN, C. P. 2018. Physical properties and stability evaluation of fish oil-in-water emulsions stabilized using thiol-modified  $\beta$ -lactoglobulin fibrils-chitosan complex. *Food Research International*, 105, 482-491.
- CHENG, Y., XIONG, Y. L. & CHEN, J. 2010. Antioxidant and emulsifying properties of potato protein hydrolysate in soybean oil-in-water emulsions. *Food Chemistry*, 120, 101-108.
- CHUNG, M., LEI, B. & LI-CHAN, E. 2005. Isolation and structural characterization of the major protein fraction from NorMan flaxseed (*Linum usitatissimum* L.). *Food chemistry*, 90, 271-279.
- CUI, W., ESKIN, N. & BILIADERIS, C. 1995. NMR characterization of a water-soluble 1, 4-linked  $\beta$ -d-glucan having ether groups from yellow mustard (*Sinapis alba* L.) mucilage. *Carbohydrate polymers*, 27, 117-122.

- CUI, W. & MAZZA, G. 1996. Physicochemical characteristics of flaxseed gum. *Food Research International*, 29, 397-402.
- CUI, W., MAZZA, G., OOMAH, B. & BILIADERIS, C. 1994. Optimization of an aqueous extraction process for flaxseed gum by response surface methodology. *LWT-Food Science and Technology*, 27, 363-369.
- DAI, L., SUN, C., WEI, Y., MAO, L. & GAO, Y. 2018. Characterization of Pickering emulsion gels stabilized by zein/gum arabic complex colloidal nanoparticles. *Food Hydrocolloids*, 74, 239-248.
- DÁTILO, M. N., SANT'ANA, M. R., FORMIGARI, G. P., RODRIGUES, P. B., DE MOURA, L. P., DA SILVA, A. S. R., ROPELLE, E. R., PAULI, J. R. & CINTRA, D. E. 2018. Omega-3 from flaxseed oil protects obese mice against diabetic retinopathy through GPR120 receptor. *Scientific reports*, 8, 14318.
- DICKINSON, E. 2008. Interfacial structure and stability of food emulsions as affected by protein-polysaccharide interactions. *Soft Matter*, 4, 932-942.
- DICKINSON, E. 2010. Food emulsions and foams: stabilization by particles. *Current Opinion in Colloid & Interface Science*, 15, 40-49.
- DICKINSON, E. 2017. Biopolymer-based particles as stabilizing agents for emulsions and foams. *Food Hydrocolloids*, 68, 219-231.
- DING, H. H., CUI, S. W., GOFF, H. D., CHEN, J., WANG, Q. & HAN, N. F. 2015. Arabinan-rich rhamnogalacturonan-I from flaxseed kernel cell wall. *Food Hydrocolloids*, 47, 158-167.
- DUFFUS, L. J., NORTON, J. E., SMITH, P., NORTON, I. T. & SPYROPOULOS, F. 2016. A comparative study on the capacity of a range of food-grade particles to form

- stable O/W and W/O Pickering emulsions. *Journal of Colloid and Interface Science*, 473, 9-21.
- ESPINOSA-ANDREWS, H., SANDOVAL-CASTILLA, O., VÁZQUEZ-TORRES, H., VERNON-CARTER, E. J. & LOBATO-CALLEROS, C. 2010. Determination of the gum Arabic–chitosan interactions by Fourier Transform Infrared Spectroscopy and characterization of the microstructure and rheological features of their coacervates. *Carbohydrate Polymers*, 79, 541-546.
- ESTRADA-FERNÁNDEZ, A., ROMÁN-GUERRERO, A., JIMENEZ-ALVARADO, R., LOBATO-CALLEROS, C., ALVAREZ-RAMIREZ, J. & VERNON-CARTER, E. 2018. Stabilization of oil-in-water-in-oil (O1/W/O2) Pickering double emulsions by soluble and insoluble whey protein concentrate-gum Arabic complexes used as inner and outer interfaces. *Journal of Food Engineering*, 221, 35-44.
- FU, D., DENG, S., MCCLEMENTS, D. J., ZHOU, L., ZOU, L., YI, J., LIU, C. & LIU, W. 2019. Encapsulation of  $\beta$ -carotene in wheat gluten nanoparticle-xanthan gum-stabilized Pickering emulsions: Enhancement of carotenoid stability and bioaccessibility. *Food Hydrocolloids*, 89, 80-89.
- GALLARDO, G., GUIDA, L., MARTINEZ, V., LÓPEZ, M. C., BERNHARDT, D., BLASCO, R., PEDROZA-ISLAS, R. & HERMIDA, L. G. 2013. Microencapsulation of linseed oil by spray drying for functional food application. *Food Research International*, 52, 473-482.
- GONZÁLEZ-PEREZ, S. & ARELLANO, J. B. 2009. 15 - Vegetable protein isolates. *In: PHILLIPS, G. O. & WILLIAMS, P. A. (eds.) Handbook of Hydrocolloids (Second Edition)*. Woodhead Publishing.

- GURSUL, S., KARABULUT, I. & DURMAZ, G. 2019. Antioxidant efficacy of thymol and carvacrol in microencapsulated walnut oil triacylglycerols. *Food Chemistry*, 278, 805-810.
- HARMAN, C. L. G., PATEL, M. A., GULDIN, S. & DAVIES, G.-L. 2019. Recent developments in Pickering emulsions for biomedical applications. *Current Opinion in Colloid & Interface Science*, 39, 173-189.
- HU, Y.-Q., YIN, S.-W., ZHU, J.-H., QI, J.-R., GUO, J., WU, L.-Y., TANG, C.-H. & YANG, X.-Q. 2016. Fabrication and characterization of novel Pickering emulsions and Pickering high internal emulsions stabilized by gliadin colloidal particles. *Food Hydrocolloids*, 61, 300-310.
- HUMBLET-HUA, N.-P. K., VAN DER LINDEN, E. & SAGIS, L. M. 2013. Surface rheological properties of liquid–liquid interfaces stabilized by protein fibrillar aggregates and protein–polysaccharide complexes. *Soft Matter*, 9, 2154-2165.
- ISLAM, M. T., KHALIPHA, A. B. R., BAGCHI, R., MONDAL, M., SMRITY, S. Z., UDDIN, S. J., SHILPI, J. A. & ROUF, R. 2019. Anticancer activity of thymol: A literature-based review and docking study with Emphasis on its anticancer mechanisms. *IUBMB Life*, 71, 9-19.
- JAIN, A., THAKUR, D., GHOSHAL, G., KATARE, O. & SHIVHARE, U. 2015. Microencapsulation by complex coacervation using whey protein isolates and gum acacia: an approach to preserve the functionality and controlled release of  $\beta$ -carotene. *Food and bioprocess technology*, 8, 1635-1644.
- JAIN, A., THAKUR, D., GHOSHAL, G., KATARE, O., SINGH, B. & SHIVHARE, U. 2016. Formation and functional attributes of electrostatic complexes involving casein and

- anionic polysaccharides: An approach to enhance oral absorption of lycopene in rats in vivo. *International Journal of Biological Macromolecules*, 93, 746-756.
- JIAO, B., SHI, A., QIANG, W. & BINKS, B. 2018a. High Internal Phase Pickering Emulsions Stabilized Solely by Peanut Protein Microgel Particles with Multiple Potential Applications. *Angewandte Chemie International Edition*.
- JIAO, B., SHI, A., WANG, Q. & BINKS, B. P. 2018b. High-Internal-Phase Pickering Emulsions Stabilized Solely by Peanut-Protein-Isolate Microgel Particles with Multiple Potential Applications. *Angewandte Chemie International Edition*, 57, 9274-9278.
- JONES, O. G., LESMES, U., DUBIN, P. & MCCLEMENTS, D. J. 2010. Effect of polysaccharide charge on formation and properties of biopolymer nanoparticles created by heat treatment of  $\beta$ -lactoglobulin-pectin complexes. *Food Hydrocolloids*, 24, 374-383.
- JOYE, I. J. & MCCLEMENTS, D. J. 2014. Biopolymer-based nanoparticles and microparticles: Fabrication, characterization, and application. *Current Opinion in Colloid & Interface Science*, 19, 417-427.
- KAEWMANEE, T., BAGNASCO, L., BENJAKUL, S., LANTERI, S., MORELLI, C. F., SPERANZA, G. & COSULICH, M. E. 2014. Characterisation of mucilages extracted from seven Italian cultivars of flax. *Food chemistry*, 148, 60-69.
- KARACA, A. C., LOW, N. & NICKERSON, M. 2011. Emulsifying properties of canola and flaxseed protein isolates produced by isoelectric precipitation and salt extraction. *Food Research International*, 44, 2991-2998.
- KARGAR, M., FAYAZMANESH, K., ALAVI, M., SPYROPOULOS, F. & NORTON, I. T.



2012. Investigation into the potential ability of Pickering emulsions (food-grade particles) to enhance the oxidative stability of oil-in-water emulsions. *Journal of Colloid and Interface Science*, 366, 209-215.
- KARGAR, M., SPYROPOULOS, F. & NORTON, I. T. 2011. The effect of interfacial microstructure on the lipid oxidation stability of oil-in-water emulsions. *Journal of Colloid and Interface Science*, 357, 527-533.
- KAUSHIK, P., DOWLING, K., ADHIKARI, R., BARROW, C. J. & ADHIKARI, B. 2017. Effect of extraction temperature on composition, structure and functional properties of flaxseed gum. *Food chemistry*, 215, 333-340.
- KAUSHIK, P., DOWLING, K., BARROW, C. J. & ADHIKARI, B. 2015. Complex coacervation between flaxseed protein isolate and flaxseed gum. *Food Research International*, 72, 91-97.
- KAUSHIK, P., DOWLING, K., MCKNIGHT, S., BARROW, C. J. & ADHIKARI, B. 2016a. Microencapsulation of flaxseed oil in flaxseed protein and flaxseed gum complex coacervates. *Food research international*, 86, 1-8.
- KAUSHIK, P., DOWLING, K., MCKNIGHT, S., BARROW, C. J., WANG, B. & ADHIKARI, B. 2016b. Preparation, characterization and functional properties of flax seed protein isolate. *Food chemistry*, 197, 212-220.
- KHALLOUFI, S., CORREDIG, M. & ALEXANDER, M. 2009. Interactions between flaxseed gums and WPI-stabilized emulsion droplets assessed insitu using diffusing wave spectroscopy. *Colloids and Surfaces B: Biointerfaces*, 68, 145-153.
- KOLANOWSKI, W., ZIOLKOWSKI, M., WEIßBRODT, J., KUNZ, B. & LAUFENBERG, G. 2006. Microencapsulation of fish oil by spray drying--impact on oxidative stability.

Part 1. *European Food Research and Technology*, 222, 336-342.

KONG, X., JIA, C., ZHANG, C., HUA, Y. & CHEN, Y. 2017. Characteristics of soy protein isolate/gum arabic-stabilized oil-in-water emulsions: influence of different preparation routes and pH. *RSC Advances*, 7, 31875-31885.

LADJAL-ETTOUMI, Y., BOUDRIES, H., CHIBANE, M. & ROMERO, A. 2016. Pea, Chickpea and Lentil Protein Isolates: Physicochemical Characterization and Emulsifying Properties. *Food Biophysics*, 11, 43-51.

LADJAL ETTOUMI, Y., CHIBANE, M. & ROMERO, A. 2016. Emulsifying properties of legume proteins at acidic conditions: Effect of protein concentration and ionic strength. *LWT - Food Science and Technology*, 66, 260-266.

LAM, S., VELIKOV, K. P. & VELEV, O. D. 2014. Pickering stabilization of foams and emulsions with particles of biological origin. *Current Opinion in Colloid & Interface Science*, 19, 490-500.

LE, X. T. & TURGEON, S. L. 2013. Rheological and structural study of electrostatic cross-linked xanthan gum hydrogels induced by  $\beta$ -lactoglobulin. *Soft Matter*, 9, 3063-3073.

LEMAHIEU, C., BRUNEEL, C., RYCKEBOSCH, E., MUylaERT, K., BUYSE, J. & FOUBERT, I. 2015. Impact of different omega-3 polyunsaturated fatty acid (n-3 PUFA) sources (flaxseed, *Isochrysis galbana*, fish oil and DHA Gold) on n-3 LC-PUFA enrichment (efficiency) in the egg yolk. *Journal of Functional Foods*, 19, 821-827.

LI, J., XU, X., CHEN, Z., WANG, T., LU, Z., HU, W. & WANG, L. 2018. Zein/gum Arabic nanoparticle-stabilized Pickering emulsion with thymol as an antibacterial delivery

- system. *Carbohydrate Polymers*, 200, 416-426.
- LI, X. & DE VRIES, R. 2018. Interfacial stabilization using complexes of plant proteins and polysaccharides. *Current Opinion in Food Science*, 21, 51-56.
- LIANG, H.-N. & TANG, C.-H. 2013. pH-dependent emulsifying properties of pea [*Pisum sativum* (L.)] proteins. *Food Hydrocolloids*, 33, 309-319.
- LIANG, H.-N. & TANG, C.-H. 2014. Pea protein exhibits a novel Pickering stabilization for oil-in-water emulsions at pH 3.0. *LWT-Food Science and Technology*, 58, 463-469.
- LIANG, L., CHEN, F., WANG, X., JIN, Q., DECKER, E. A. & MCCLEMENTS, D. J. 2017a. Physical and Oxidative Stability of Flaxseed Oil-in-Water Emulsions Fabricated from Sunflower Lecithins: Impact of Blending Lecithins with Different Phospholipid Profiles. *Journal of agricultural and food chemistry*, 65, 4755-4765.
- LIANG, S., LIAO, W., MA, X., LI, X. & WANG, Y. 2017b. H<sub>2</sub>O<sub>2</sub> oxidative preparation, characterization and antiradical activity of a novel oligosaccharide derived from flaxseed gum. *Food chemistry*, 230, 135-144.
- LIU, B., ZHU, Y., TIAN, J., GUAN, T., LI, D., BAO, C., NORDE, W., WEN, P. & LI, Y. 2019. Inhibition of oil digestion in Pickering emulsions stabilized by oxidized cellulose nanofibrils for low-calorie food design. *RSC Advances*, 9, 14966-14973.
- LIU, F. & TANG, C.-H. 2016. Soy glycinin as food-grade Pickering stabilizers: Part. I. Structural characteristics, emulsifying properties and adsorption/arrangement at interface. *Food Hydrocolloids*, 60, 606-619.
- LIU, J., SHEN, J., SHIM, Y. Y. & REANEY, M. J. 2016a. Carboxymethyl derivatives of flaxseed (*Linum usitatissimum* L.) gum: Characterisation and solution rheology.

- International journal of food science & technology*, 51, 530-541.
- LIU, J., SHIM, Y. Y., POTH, A. G. & REANEY, M. J. 2016b. Conlinin in flaxseed (*Linum usitatissimum* L.) gum and its contribution to emulsification properties. *Food Hydrocolloids*, 52, 963-971.
- LIU, J., SHIM, Y. Y., POTH, A. G. & REANEY, M. J. T. 2016c. Conlinin in flaxseed (*Linum usitatissimum* L.) gum and its contribution to emulsification properties. *Food Hydrocolloids*, 52, 963-971.
- LIU, J., SHIM, Y. Y., TSE, T., WANG, Y. & REANEY, M. J. 2018a. Flaxseed gum a versatile natural hydrocolloid for food and non-food applications. *Trends in Food Science & Technology*.
- LIU, J., SHIM, Y. Y., TSE, T. J., WANG, Y. & REANEY, M. J. T. 2018b. Flaxseed gum a versatile natural hydrocolloid for food and non-food applications. *Trends in Food Science & Technology*, 75, 146-157.
- LIU, J., SHIM, Y. Y., WANG, Y. & REANEY, M. J. 2015. Intermolecular interaction and complex coacervation between bovine serum albumin and gum from whole flaxseed (*Linum usitatissimum* L.). *Food Hydrocolloids*, 49, 95-103.
- LIU, S., ELMER, C., LOW, N. & NICKERSON, M. 2010. Effect of pH on the functional behaviour of pea protein isolate–gum Arabic complexes. *Food Research International*, 43, 489-495.
- LUO, J., LI, Y., MAI, Y., GAO, L., OU, S., WANG, Y., LIU, L. & PENG, X. 2018. Flaxseed gum reduces body weight by regulating gut microbiota. *Journal of Functional Foods*, 47, 136-142.
- LV, Y., YANG, F., LI, X., ZHANG, X. & ABBAS, S. 2014. Formation of heat-resistant

- nanocapsules of jasmine essential oil via gelatin/gum arabic based complex coacervation. *Food Hydrocolloids*, 35, 305-314.
- MADADLOU, A., RAKHSHI, E. & ABBASPOURRAD, A. 2016. Engineered emulsions for obesity treatment. *Trends in Food Science & Technology*, 52, 90-97.
- MADIVALA, B., VANDEBRIL, S., FRANSAER, J. & VERMANT, J. 2009. Exploiting particle shape in solid stabilized emulsions. *Soft Matter*, 5, 1717-1727.
- MARCHESE, A., ORHAN, I. E., DAGLIA, M., BARBIERI, R., DI LORENZO, A., NABAVI, S. F., GORTZI, O., IZADI, M. & NABAVI, S. M. 2016. Antibacterial and antifungal activities of thymol: A brief review of the literature. *Food Chemistry*, 210, 402-414.
- MESHULAM, D. & LESMES, U. 2014. Responsiveness of emulsions stabilized by lactoferrin nano-particles to simulated intestinal conditions. *Food & function*, 5, 65-73.
- MIKSHINA, P. V., GURJANOV, O. P., MUKHITOVA, F. K., PETROVA, A. A., SHASHKOV, A. S. & GORSHKOVA, T. A. 2012. Structural details of pectic galactan from the secondary cell walls of flax (*Linum usitatissimum* L.) phloem fibres. *Carbohydrate polymers*, 87, 853-861.
- MINEKUS, M., ALMINGER, M., ALVITO, P., BALLANCE, S., BOHN, T., BOURLIEU, C., CARRIERE, F., BOUTROU, R., CORREDIG, M. & DUPONT, D. 2014. A standardised static in vitro digestion method suitable for food—an international consensus. *Food & function*, 5, 1113-1124.
- MOURA-ASSIS, A., AFONSO, M. S., DE OLIVEIRA, V., MORARI, J., DOS SANTOS, G. A., KOIKE, M., LOTTENBERG, A. M., RAMOS CATHARINO, R., VELLOSO, L. A., SANCHEZ RAMOS DA SILVA, A., DE MOURA, L. P., ROPELLE, E. R., PAULI, J.

- R. & CINTRA, D. E. C. 2018. Flaxseed oil rich in omega-3 protects aorta against inflammation and endoplasmic reticulum stress partially mediated by GPR120 receptor in obese, diabetic and dyslipidemic mice models. *The Journal of Nutritional Biochemistry*, 53, 9-19.
- MUIR, A. D. & WESTCOTT, N. D. 2003. 12 Flaxseed constituents and human health. *Flax: the genus Linum*, 243.
- NIKBAKHT NASRABADI, M., GOLI, S. A. H., SEDAGHAT DOOST, A., ROMAN, B., DEWETTINCK, K., STEVENS, C. V. & VAN DER MEEREN, P. 2019. Plant based Pickering stabilization of emulsions using soluble flaxseed protein and mucilage nano-assemblies. *Colloids and Surfaces A: Physicochemical and Engineering Aspects*, 563, 170-182.
- NWACHUKWU, D. I., GIRGIH, T. A., MALOMO, A. S., ONUH, O. J. & ALUKO, E. R. 2014. Thermoase-Derived Flaxseed Protein Hydrolysates and Membrane Ultrafiltration Peptide Fractions Have Systolic Blood Pressure-Lowering Effects in Spontaneously Hypertensive Rats. *International Journal of Molecular Sciences*, 15.
- NWACHUKWU, I. D. & ALUKO, R. E. 2018. Physicochemical and emulsification properties of flaxseed (*Linum usitatissimum*) albumin and globulin fractions. *Food Chemistry*, 255, 216-225.
- OOMAH, B. D. & MAZZA, G. 1998. Compositional changes during commercial processing of flaxseed. *Industrial Crops and Products*, 9, 29-37.
- PAN, A., O'REILLY, E. J., MIRZAEI, F., KAWACHI, I., KOENEN, K., LUCAS, M., WILLETT, W. C. & ASCHERIO, A. 2011. Dietary intake of n-3 and n-6 fatty acids

- and the risk of clinical depression in women: a 10-y prospective follow-up study. *The American Journal of Clinical Nutrition*, 93, 1337-1343.
- PAN, K., CHEN, H., DAVIDSON, P. M. & ZHONG, Q. 2014. Thymol Nanoencapsulated by Sodium Caseinate: Physical and Antilisterial Properties. *Journal of Agricultural and Food Chemistry*, 62, 1649-1657.
- PHAM, L. B., WANG, B., ZISU, B. & ADHIKARI, B. 2019. Complexation between flaxseed protein isolate and phenolic compounds: Effects on interfacial, emulsifying and antioxidant properties of emulsions. *Food Hydrocolloids*, 94, 20-29.
- PICKERING, S. U. 1907a. CXCVI.—Emulsions. *Journal of the Chemical Society, Transactions*, 91, 2001-2021.
- PICKERING, S. U. 1907b. Emulsions. *Journal of the Chemical Society, Transactions*, 91, 2001-2021.
- PIVETTA, T. P., SIMÕES, S., ARAÚJO, M. M., CARVALHO, T., ARRUDA, C. & MARCATO, P. D. 2018. Development of nanoparticles from natural lipids for topical delivery of thymol: Investigation of its anti-inflammatory properties. *Colloids and Surfaces B: Biointerfaces*, 164, 281-290.
- QIAN, K.-Y., CUI, S. W., NIKIFORUK, J. & GOFF, H. D. 2012a. Structural elucidation of rhamnogalacturonans from flaxseed hulls. *Carbohydrate research*, 362, 47-55.
- QIAN, K. Y., CUI, S. W., WU, Y. & GOFF, H. D. 2012b. Flaxseed gum from flaxseed hulls: Extraction, fractionation, and characterization. *Food Hydrocolloids*, 28, 275-283.
- RAMSDEN, W. 1903. Separation of solids in the surface-layers of solutions and suspensions (observations on surface-membranes, bubbles, emulsions, and mechanical coagulation). *Proceedings of the royal Society of London*, 72, 156-164.

- RAYNER, M., MARKU, D., ERIKSSON, M., SJÖÖ, M., DEJMEK, P. & WAHLGREN, M. 2014. Biomass-based particles for the formulation of Pickering type emulsions in food and topical applications. *Colloids and Surfaces A: Physicochemical and Engineering Aspects*, 458, 48-62.
- ROUSSEAU, D. 2013. Trends in structuring edible emulsions with Pickering fat crystals. *Current Opinion in Colloid & Interface Science*, 18, 283-291.
- SALMINEN, H., HELGASON, T., KRISTINSSON, B., KRISTBERGSSON, K. & WEISS, J. 2017. Tuning of shell thickness of solid lipid particles impacts the chemical stability of encapsulated  $\omega$ -3 fish oil. *Journal of Colloid and Interface Science*, 490, 207-216.
- SARKAR, A., ADEMUYIWA, V., STUBLEY, S., ESA, N. H., GOYCOOLEA, F. M., QIN, X., GONZALEZ, F. & OLVERA, C. 2018. Pickering emulsions co-stabilized by composite protein/ polysaccharide particle-particle interfaces: Impact on in vitro gastric stability. *Food Hydrocolloids*, 84, 282-291.
- SARKAR, A., MURRAY, B., HOLMES, M., ETTELAIE, R., ABDALLA, A. & YANG, X. 2016. In vitro digestion of Pickering emulsions stabilized by soft whey protein microgel particles: influence of thermal treatment. *Soft Matter*, 12, 3558-3569.
- SARKAR, A., ZHANG, S., HOLMES, M. & ETTELAIE, R. 2019. Colloidal aspects of digestion of Pickering emulsions: Experiments and theoretical models of lipid digestion kinetics. *Advances in Colloid and Interface Science*, 263, 195-211.
- SARKAR, A., ZHANG, S., MURRAY, B., RUSSELL, J. A. & BOXAL, S. 2017. Modulating in vitro gastric digestion of emulsions using composite whey protein-cellulose nanocrystal interfaces. *Colloids and Surfaces B: Biointerfaces*, 158, 137-146.



- SCHMITT, C., KOLODZIEJCZYK, E. & LESER, M. E. 2005. Interfacial and foam stabilization properties of b-lactoglobulin e Acacia gum electrostatic complexes. *Food colloids: Interactions, microstructure and processing*, 289e300.
- SCHMITT, V. & RAVAINÉ, V. 2013. Surface compaction versus stretching in Pickering emulsions stabilised by microgels. *Current Opinion in Colloid & Interface Science*, 18, 532-541.
- SCHRÖDER, A., CORSTENS, M. N., HO, K. K. H. Y., SCHROEN, K. & BERTON-CARABIN, C. C. 2018a. Pickering Emulsions. *Emulsion-based Systems for Delivery of Food Active Compounds*.
- SCHRÖDER, A., SPRAKEL, J., SCHROEN, K., SPAEN, J. N. & BERTON-CARABIN, C. C. 2018b. Coalescence stability of Pickering emulsions produced with lipid particles: A microfluidic study. *Journal of Food Engineering*, 234, 63-72.
- SEDAGHAT DOOST, A., DEVLIEGHERE, F., DIRCKX, A. & VAN DER MEEREN, P. 2018a. Fabrication of Origanum compactum essential oil nanoemulsions stabilized using Quillaja Saponin biosurfactant. *Journal of Food Processing and Preservation*, 42, e13668.
- SEDAGHAT DOOST, A., DEWETTINCK, K., DEVLIEGHERE, F. & VAN DER MEEREN, P. 2018b. Influence of non-ionic emulsifier type on the stability of cinnamaldehyde nanoemulsions: A comparison of polysorbate 80 and hydrophobically modified inulin. *Food Chemistry*, 258, 237-244.
- SEDAGHAT DOOST, A., KASSOZI, V., GROOTAERT, C., CLAEYS, M., DEWETTINCK, K., VAN CAMP, J. & VAN DER MEEREN, P. 2019a. Self-assembly, functionality, and in-vitro properties of quercetin loaded nanoparticles based on shellac-almond

- gum biological macromolecules. *International Journal of Biological Macromolecules*, 129, 1024-1033.
- SEDAGHAT DOOST, A., MUHAMMAD, D. R. A., STEVENS, C. V., DEWETTINCK, K. & VAN DER MEEREN, P. 2018c. Fabrication and characterization of quercetin loaded almond gum-shellac nanoparticles prepared by antisolvent precipitation. *Food Hydrocolloids*, 83, 190-201.
- SEDAGHAT DOOST, A., NIKBAKHT NASRABADI, M., KASSOZI, V., DEWETTINCK, K., STEVENS, C. V. & VAN DER MEEREN, P. 2019b. Pickering stabilization of thymol through green emulsification using soluble fraction of almond gum – Whey protein isolate nano-complexes. *Food Hydrocolloids*, 88, 218-227.
- SEDAGHAT DOOST, A., SINNAEVE, D., DE NEVE, L. & VAN DER MEEREN, P. 2017. Influence of non-ionic surfactant type on the salt sensitivity of oregano oil-in-water emulsions. *Colloids and Surfaces A: Physicochemical and Engineering Aspects*, 525, 38-48.
- SEDAGHAT DOOST, A., VAN CAMP, J., DEWETTINCK, K. & VAN DER MEEREN, P. 2019c. Production of thymol nanoemulsions stabilized using Quillaja Saponin as a biosurfactant: Antioxidant activity enhancement. *Food Chemistry*, 293, 134-143.
- SHAH, B. R., ZHANG, C., LI, Y. & LI, B. 2016. Bioaccessibility and antioxidant activity of curcumin after encapsulated by nano and Pickering emulsion based on chitosan-tripolyphosphate nanoparticles. *Food Research International*, 89, 399-407.
- SHARMA, T., KUMAR, G. S., CHON, B. H. & SANGWAI, J. S. 2015. Thermal stability of oil-in-water Pickering emulsion in the presence of nanoparticle, surfactant, and polymer. *Journal of Industrial and Engineering Chemistry*, 22, 324-334.

- SHIM, Y. Y., GUI, B., ARNISON, P. G., WANG, Y. & REANEY, M. J. T. 2014. Flaxseed (*Linum usitatissimum* L.) bioactive compounds and peptide nomenclature: A review. *Trends in Food Science & Technology*, 38, 5-20.
- SHIMONI, G., SHANI LEVI, C., LEVI TAL, S. & LESMES, U. 2013. Emulsions stabilization by lactoferrin nano-particles under in vitro digestion conditions. *Food Hydrocolloids*, 33, 264-272.
- SILMORE, K. S., GUPTA, C. & WASHBURN, N. R. 2016. Tunable Pickering emulsions with polymer-grafted lignin nanoparticles (PGLNs). *Journal of colloid and interface science*, 466, 91-100.
- SILVA, F. G. D., O'CALLAGAHAN, Y., O'BRIEN, N. M. & NETTO, F. M. 2013. Antioxidant Capacity of Flaxseed Products: The Effect of In vitro Digestion. *Plant Foods for Human Nutrition*, 68, 24-30.
- SONG, X., PEI, Y., QIAO, M., MA, F., REN, H. & ZHAO, Q. 2015. Preparation and characterizations of Pickering emulsions stabilized by hydrophobic starch particles. *Food Hydrocolloids*, 45, 256-263.
- SPEICIENE, V., GUILMINEAU, F., KULOZIK, U. & LESKAUSKAITE, D. 2007. The effect of chitosan on the properties of emulsions stabilized by whey proteins. *Food chemistry*, 102, 1048-1054.
- SUFI-MARAGHEH, P., NIKFARJAM, N., DENG, Y. & TAHERI-QAZVINI, N. 2019. Pickering emulsion stabilized by amphiphilic pH-sensitive starch nanoparticles as therapeutic Containers. *Colloids and Surfaces B: Biointerfaces*.
- SUN, C., DAI, L. & GAO, Y. 2017. Formation and characterization of the binary complex between zein and propylene glycol alginate at neutral pH. *Food Hydrocolloids*, 64,

36-47.

TAMAYO TENORIO, A., GIETELING, J., NIKIFORIDIS, C. V., BOOM, R. M. & VAN DER GOOT, A. J. 2017. Interfacial properties of green leaf cellulosic particles. *Food Hydrocolloids*, 71, 8-16.

TAVERNIER, I., WIJAYA, W., VAN DER MEEREN, P., DEWETTINCK, K. & PATEL, A. R. 2016. Food-grade particles for emulsion stabilization. *Trends in Food Science & Technology*, 50, 159-174.

TENORIO, A. T., GIETELING, J., NIKIFORIDIS, C., BOOM, R. & VAN DER GOOT, A. 2017. Interfacial properties of green leaf cellulosic particles. *Food Hydrocolloids*, 71, 8-16.

THAKUR, G., MITRA, A., PAL, K. & ROUSSEAU, D. 2009. Effect of flaxseed gum on reduction of blood glucose and cholesterol in type 2 diabetic patients. *International Journal of Food Sciences and Nutrition*, 60, 126-136.

TIMGREN, A., RAYNER, M., SJÖÖ, M. & DEJMEK, P. 2011. Starch particles for food based Pickering emulsions. *Procedia Food Science*, 1, 95-103.

TIRGAR, M., SILCOCK, P., CARNE, A. & BIRCH, E. J. 2017. Effect of extraction method on functional properties of flaxseed protein concentrates. *Food Chemistry*, 215, 417-424.

TONON, R. V., GROSSO, C. R. F. & HUBINGER, M. D. 2011. Influence of emulsion composition and inlet air temperature on the microencapsulation of flaxseed oil by spray drying. *Food Research International*, 44, 282-289.

TRUJILLO-RAMÍREZ, D., LOBATO-CALLEROS, C., ROMÁN-GUERRERO, A., HERNÁNDEZ-RODRÍGUEZ, L., ALVAREZ-RAMIREZ, J. & VERNON-CARTER,

- E. J. 2018. Complexation with whey protein hydrolysate improves cacao pods husk pectin surface active and emulsifying properties. *Reactive and Functional Polymers*, 123, 61-69.
- TURGEON, S., BEAULIEU, M., SCHMITT, C. & SANCHEZ, C. 2003. Protein–polysaccharide interactions: phase-ordering kinetics, thermodynamic and structural aspects. *Current opinion in colloid & interface science*, 8, 401-414.
- TZOUMAKI, M. V., MOSCHAKIS, T., SCHOLTEN, E. & BILIADERIS, C. G. 2013. In vitro lipid digestion of chitin nanocrystal stabilized o/w emulsions. *Food & Function*, 4, 121-129.
- WANG, B., LI, D., WANG, L.-J. & ÖZKAN, N. 2010. Effect of concentrated flaxseed protein on the stability and rheological properties of soybean oil-in-water emulsions. *Journal of Food Engineering*, 96, 555-561.
- WANG, L.-J., HU, Y.-Q., YIN, S.-W., YANG, X.-Q., LAI, F.-R. & WANG, S.-Q. 2015. Fabrication and Characterization of Antioxidant Pickering Emulsions Stabilized by Zein/Chitosan Complex Particles (ZCPs). *Journal of Agricultural and Food Chemistry*, 63, 2514-2524.
- WANG, Y., WANG, W., JIA, H., GAO, G., WANG, X., ZHANG, X. & WANG, Y. 2018. Using Cellulose Nanofibers and Its Palm Oil Pickering Emulsion as Fat Substitutes in Emulsified Sausage. *Journal of Food Science*, 83, 1740-1747.
- WARR, J., MICHAUD, P., PICTON, L., MULLER, G., COURTOIS, B., RALAINIRINA, R. & COURTOIS, J. 2003. Large-scale purification of water-soluble polysaccharides from flaxseed mucilage, and isolation of a new anionic polymer. *Chromatographia*, 58, 331-335.

- WARRANT, J., MICHAUD, P., PICTON, L., MULLER, G., COURTOIS, B., RALAINIRINA, R. & COURTOIS, J. 2005a. Structural investigations of the neutral polysaccharide of *Linum usitatissimum* L. seeds mucilage. *International Journal of Biological Macromolecules*, 35, 121-125.
- WARRANT, J., MICHAUD, P., PICTON, L., MULLER, G., COURTOIS, B., RALAINIRINA, R. & COURTOIS, J. 2005b. Structural investigations of the neutral polysaccharide of *Linum usitatissimum* L. seeds mucilage. *International Journal of Biological Macromolecules*, 35, 121-125.
- WESTERN, T. L. 2012. The sticky tale of seed coat mucilages: production, genetics, and role in seed germination and dispersal. *Seed Science Research*, 22, 1-25.
- WINUPRASITH, T., KHOMEIN, P., MITBUMRUNG, W., SUPHANTHARIKA, M., NITITHAMYONG, A. & MCCLEMENTS, D. J. 2018. Encapsulation of vitamin D3 in Pickering emulsions stabilized by nanofibrillated mangosteen cellulose: Impact on in vitro digestion and bioaccessibility. *Food Hydrocolloids*, 83, 153-164.
- WU, J., SHI, M., LI, W., ZHAO, L., WANG, Z., YAN, X., NORDE, W. & LI, Y. 2015. Pickering emulsions stabilized by whey protein nanoparticles prepared by thermal cross-linking. *Colloids and Surfaces B: Biointerfaces*, 127, 96-104.
- XIAO, J., LI, C. & HUANG, Q. 2015. Kafirin nanoparticle-stabilized Pickering emulsions as oral delivery vehicles: Physicochemical stability and in vitro digestion profile. *Journal of agricultural and food chemistry*, 63, 10263-10270.
- XIAO, J., LI, Y. & HUANG, Q. 2016a. Recent advances on food-grade particles stabilized Pickering emulsions: fabrication, characterization and research trends. *Trends in Food Science & Technology*, 55, 48-60.

- XIAO, J., WANG, X. A., GONZALEZ, A. J. P. & HUANG, Q. 2016b. Kafirin nanoparticles-stabilized Pickering emulsions: Microstructure and rheological behavior. *Food Hydrocolloids*, 54, 30-39.
- XIONG, W., REN, C., LI, J. & LI, B. 2018. Characterization and interfacial rheological properties of nanoparticles prepared by heat treatment of ovalbumin-carboxymethylcellulose complexes. *Food Hydrocolloids*, 82, 355-362.
- XU, W., JIN, W., LI, Z., LIANG, H., WANG, Y., SHAH, B. R., LI, Y. & LI, B. 2015. Synthesis and characterization of nanoparticles based on negatively charged xanthan gum and lysozyme. *Food Research International*, 71, 83-90.
- YANG, Y., CUI, S. W., GONG, J., GUO, Q., WANG, Q. & HUA, Y. 2015. A soy protein-polysaccharides Maillard reaction product enhanced the physical stability of oil-in-water emulsions containing citral. *Food Hydrocolloids*, 48, 155-164.
- YANO, H., FUKUI, A., KAJIWARA, K., KOBAYASHI, I., YOZA, K.-I., SATAKE, A. & VILLENEUVE, M. 2017. Development of gluten-free rice bread: Pickering stabilization as a possible batter-swelling mechanism. *LWT - Food Science and Technology*, 79, 632-639.
- YAO, X., XIANG, S., NIE, K., GAO, Z., ZHANG, W., FANG, Y., NISHINARI, K., PHILLIPS, G. O. & JIANG, F. 2016. Whey protein isolate/gum arabic intramolecular soluble complexes improving the physical and oxidative stabilities of conjugated linoleic acid emulsions. *RSC Advances*, 6, 14635-14642.
- YI, J., NING, J., ZHU, Z., CUI, L., DECKER, E. A. & MCCLEMENTS, D. J. 2019. Impact of interfacial composition on co-oxidation of lipids and proteins in oil-in-water emulsions: Competitive displacement of casein by surfactants. *Food*

*Hydrocolloids*, 87, 20-28.

- YILDIZ, G., DING, J., ANDRADE, J., ENGESETH, N. J. & FENG, H. 2018. Effect of plant protein-polysaccharide complexes produced by mano-thermo-sonication and pH-shifting on the structure and stability of oil-in-water emulsions. *Innovative Food Science & Emerging Technologies*, 47, 317-325.
- ZENG, T., WU, Z.-L., ZHU, J.-Y., YIN, S.-W., TANG, C.-H., WU, L.-Y. & YANG, X.-Q. 2017. Development of antioxidant Pickering high internal phase emulsions (HIPEs) stabilized by protein/polysaccharide hybrid particles as potential alternative for PHOs. *Food Chemistry*, 231, 122-130.
- ZHANG, Y., NIU, Y., LUO, Y., GE, M., YANG, T., YU, L. & WANG, Q. 2014. Fabrication, characterization and antimicrobial activities of thymol-loaded zein nanoparticles stabilized by sodium caseinate–chitosan hydrochloride double layers. *Food Chemistry*, 142, 269-275.
- ZHOU, F.-Z., YAN, L., YIN, S.-W., TANG, C.-H. & YANG, X.-Q. 2018a. Development of Pickering emulsions stabilized by gliadin/proanthocyanidins hybrid particles (GPHPs) and the fate of lipid oxidation and digestion. *Journal of Agricultural and Food Chemistry*, 66, 1461-1471.
- ZHOU, F. Z., ZENG, T., YIN, S. W., TANG, C. H., YUAN, D. B. & YANG, X. Q. 2018b. Development of antioxidant gliadin particle stabilized Pickering high internal phase emulsions (HIPEs) as oral delivery systems and the in vitro digestion fate. *Food & Function*, 9, 959-970.
- ZHU, Q., LU, H., ZHU, J., ZHANG, M. & YIN, L. 2019a. Development and characterization of pickering emulsion stabilized by zein/corn fiber gum (CFG) complex colloidal



- particles. *Food Hydrocolloids*, 91, 204-213.
- ZHU, Z., WEN, Y., YI, J., CAO, Y., LIU, F. & MCCLEMENTS, D. J. 2019b. Comparison of natural and synthetic surfactants at forming and stabilizing nanoemulsions: Tea saponin, Quillaja saponin, and Tween 80. *Journal of Colloid and Interface Science*, 536, 80-87.
- ZOU, Y., BAALEN, C. V., YANG, X. & SCHOLTEN, E. 2018. Tuning hydrophobicity of zein nanoparticles to control rheological behavior of Pickering emulsions. *Food Hydrocolloids*, 80, 130-140.
- ZOU, Y., GUO, J., YIN, S.-W., WANG, J.-M. & YANG, X.-Q. 2015. Pickering emulsion gels prepared by hydrogen-bonded zein/tannic acid complex colloidal particles. *Journal of agricultural and food chemistry*, 63, 7405-7414.
- ZOU, Y., WAN, Z., GUO, J., WANG, J., YIN, S. & YANG, X. 2017. Tunable assembly of hydrophobic protein nanoparticle at fluid interfaces with tannic acid. *Food Hydrocolloids*, 63, 364-371.

# CURRICULUM VITAE

## Personal information

**Name** Maryam Nikbakht Nasrabadi

**Address** No.158, Khaghani St., Isfahan, Iran

**Email:** [Maryam.nikbakhtnasrabadi@ugent.be](mailto:Maryam.nikbakhtnasrabadi@ugent.be)  
[m.nikbakht@ag.iut.ac.ir](mailto:m.nikbakht@ag.iut.ac.ir)

**Place of birth:** Isfahan, Iran

**Nationality:** Iranian

**Marital status:** Single

## Education

- 2014-2019, Joint PhD student, University of Ghent (UGent) and Isfahan University of Technology (IUT)

**Thesis: Fabrication and physicochemical investigation of plant based flaxseed oil-in-water Pickering emulsion stabilized by flaxseed protein-mucilage complex particles**

- 2011-2013, Master of Food Technology, Isfahan University of Technology (IUT)

**Thesis: Evaluation of Production of Functional Beverage Emulsion Containing Conjugated Linoleic Acid (CLA)**

- 2007-2011, Bachelor in Food Science and Technology, Shiraz university

## Publications

### Selected papers published in peer-reviewed journals

1. **NIKBAKHT NASRABADI, M.**, SEDAGHAT DOOST, A., AMIR HOSSEIN GOLI, S. & VAN DER MEEREN, P. 2019c. Effect of thymol and Pickering stabilization on in-vitro digestion fate and oxidation stability of plant-derived flaxseed oil emulsions. *Food Chemistry*, 125872.
2. SEDAGHAT DOOST, A., **NIKBAKHT NASRABADI, M.**, AMIR HOSSEIN GOLI, S., VAN TROYS, M., DUBRUEL, P., DE NEVE, N. & VAN DER MEEREN, P. 2019a. Maillard conjugation of whey protein isolate with water-soluble fraction of almond gum or flaxseed mucilage by dry heat treatment. *Food Research International*, 108779

3. **NIKBAKHT NASRABADI, M.**, GOLI, S. A. H., SEDAGHAT DOOST, A., DEWETTINCK, K. & VAN DER MEEREN, P. 2019a. Bioparticles of flaxseed protein and mucilage enhance the physical and oxidative stability of flaxseed oil emulsions as a potential natural alternative for synthetic surfactants. *Colloids and Surfaces B: Biointerfaces*, 184, 110489
4. SEDAGHAT DOOST, A., **NIKBAKHT NASRABADI, M.**, WU, J., A'YUN, Q. & VAN DER MEEREN, P. 2019c. Maillard conjugation as an approach to improve whey proteins functionality: A review of conventional and novel preparation techniques. *Trends in Food Science & Technology*, 91, 1-11.
5. **NIKBAKHT NASRABADI, M.**, GOLI, S. A. H., SEDAGHAT DOOST, A., ROMAN, B., DEWETTINCK, K., STEVENS, C. V. & VAN DER MEEREN, P. 2019b. Plant based Pickering stabilization of emulsions using soluble flaxseed protein and mucilage nano-assemblies. *Colloids and Surfaces A: Physicochemical and Engineering Aspects*, 563, 170-182.
6. SEDAGHAT DOOST, A., **NIKBAKHT NASRABADI, M.**, KASSOZI, V., DEWETTINCK, K., STEVENS, C. V. & VAN DER MEEREN, P. 2019b. Pickering stabilization of thymol through green emulsification using soluble fraction of almond gum – Whey protein isolate nano-complexes. *Food Hydrocolloids*, 88, 218-227

#### **Other Journal Publications**

7. FATHI, M., **NIKBAKHT NASRABADI, M. N.** & VARSHOSAZ, J. 2017. Characteristics of vitamin E-loaded nanofibres from dextran. *International journal of food properties*, 20, 2665-2674.
8. KHATIBI AGHDA, S., NASIRPOUR, A. & **NIKBAKHT NASRABADI, M.** 2017. Effect

- of acidification rate, acidification temperature, final pH, and stabilizer content on colloidal stability of whey-based pomegranate beverage. *Journal of Dispersion Science and Technology*, 38, 58-64.
9. **NIKBAKHT NASRABADI, M.**, GOLI, S. A. H. & NASIRPOUR, A. 2016. Stability assessment of conjugated linoleic acid (CLA) oil-in-water beverage emulsion formulated with acacia and xanthan gums. *Food Chemistry*, 199, 258-264.
  10. **NIKBAKHT NASRABADI, M.**, GOLI, S. A. H. & NASIRPOUR, A. 2015. Evaluation of biopolymer-based emulsion for delivering conjugated linoleic acid (CLA) as a functional ingredient in beverages. *Journal of Dispersion Science and Technology*, 36, 778-788.

#### **Presentations at conferences**

- 1) 16<sup>th</sup> Conference of the International Association of Colloid and Interface Scientists (IACIS), May 2018, Rotterdam, Netherlands. (Poster presentations). Complexation of flaxseed mucilage and protein through electrostatic interaction, Maryam Nikbakht Nasrabadi, Sayed Amir Hossein Goli, Ali Sedaghat Doost and Paul Van der Meeren.
- 2) Self-Assembly of Colloidal Systems (SACS), September 2018, Bordeaux, France. (Oral and Poster presentation). Self-assembly and characterization of biopolymer particles via electrostatic interaction between flaxseed mucilage and protein, Maryam Nikbakht Nasrabadi, Sayed Amir Hossein Goli, Ali Sedaghat Doost and Paul Van der Meeren.
- 3) 17<sup>th</sup> European Student Colloid Conference (ESC), June 2019, Varna, Bulgaria. (Poster presentations). Plant-based flaxseed oil-in-water emulsion:

Physicochemical stability and in-vitro digestion, Maryam Nikbakht Nasrabadi,  
Sayed Amir Hossein Goli, Ali Sedaghat Doost and Paul Van der Meeren.

- 4) 32<sup>nd</sup> Conference of the European Colloid and Interface Society (ECIS),  
September 2018, Ljubliana, Slovenia. (Poster presentations)